

**From Host to Pathogen:
Caenorhabditis elegans as a model
host system to study Basic Innate
Immunity and Antimicrobial Drug
Discovery**

Iliana E Escobar

BA, Brown University 2013

A Dissertation Submitted in Partial Fulfillment of the Requirements for the Degree of
Doctor of Philosophy In the Division of Biology and Medicine at Brown University

Providence, RI

October 2021

© Copyright 2021 by Iliana E Escobar

Signature Page

This dissertation by Iliana E Escobar is accepted in its present form by the Pathobiology Graduate Program as satisfying the dissertation requirement for the degree of Doctor of Philosophy.

Date: _____

Dr. Eleftherios Mylonakis (Advisor)

Recommended to the Graduate Council

Date: _____

Dr. Peter Belenky (Reader)

Date: _____

Dr. Craig Lefort (Reader)

Date: _____

Dr. Jennifer Sanders (Reader)

Date: _____

Dr. Frederick Ausubel (Outside
Reader)

Approved by the Graduate Council

Date: _____

Dr. Andrew Campbell

Dean of the Graduate School

Curriculum Vitae

ILIANA E ESCOBAR

EDUCATION

Brown University, Providence, RI
Ph.D. in Pathobiology

Aug 2021

Brown University, Providence, RI
BA Biology

Class of 2013

RESEARCH EXPERIENCE

Brown University, *Pathobiology Graduate Program*, Providence, RI

Graduate Researcher – Dr. Eleftherios Mylonakis MD, Ph.D. **Sept 2017-Aug 2021**

- Lead a project examining the potential of the *C. elegans* as a whole-animal infectious model to study drug repurposing as a means to aid antimicrobial discovery against methicillin-resistant *Staphylococcus aureus* (MRSA). This work led to two first author publications.
- Significantly contributed to work studying lipid transporter S1P, which we postulate is able to modulate *C. elegans* innate immune response to infection. Additional contributions to this project included extensive manuscript writing and editing. These work lead to a first co-author publication.

Brown University, *Department of Mol. Pharm. Physis., BioT. (MPPB)*, Providence, RI

Research Assistant- Dr. Elena Oancea Ph.D.

March 2013-Aug 2017

- Projects
 - Spearhead experiments to identify the amino acid transporter that supplies L-tyrosine to melanosomes for melanin production.
 - Co-lead research on two pore channel 2 (TPC2) proteins as a hypothesized melanosomal ion channel.
 - Investigated hypothesis that oculocutaneous albinism II (OCA2) protein is a Cl⁻ ion channel on the melanosomal membrane.
- Accountable for ordering and tracking of all chemicals and consumables for daily lab use and support for a 9 person lab of 5 graduate students and 2 undergraduates.

Lizard Island Research Station, Lizard Island, Australia

Nov 2012-Dec 2012

Research Assistant Intern

- Investigated fish species recruitment on degraded coral reef environments via snorkeling.
- Learned research methodology needed to conduct a field based marine research project.

NSF REU Research Intern

- Investigated how chemical cues affect fiddler crab habitat settlement via daily collections and harvesting of fiddler crabs larvae.
- Helped design and build chemical-cue-releasing megalopae collectors, trained in chelex DNA extraction and multiplex PCR.

PUBLICATIONS

1. **Escobar IE**, Possamai Rossatto FC, Kim SM, Kang MH, Kim W, Mylonakis E. Repurposing Kinase Inhibitor Bay 11-7085 to Combat *Staphylococcus aureus* and *Candida albicans* Biofilms. *Front. Pharmco.* 2021 May 4,12:1021. doi: 10.3389/fphar.2021.67530.
2. Lee K*, **Escobar I***, Jang Y, Kim W, Ausubel FM, Mylonakis E. In the Model Host *Caenorhabditis elegans*, Sphingosine-1-Phosphate-Mediated Signaling Increases Immunity toward Human Opportunistic Bacteria. *Int J Mol Sci.* 2020 Oct 22;21(21):7813. doi: 10.3390/ijms21217813.
3. **Escobar IE**, White A, Kim W, Mylonakis E. New Antimicrobial Bioactivity against Multidrug-Resistant Gram-Positive Bacteria of Kinase Inhibitor IMD0354. *Antibiotics (Basel).* 2020 Oct 1;9(10):665. doi: 10.3390/antibiotics9100665.
4. Kim SM, **Escobar I**, Lee K, Fuchs BB, Mylonakis E, Kim W. Anti-MRSA agent discovery using *Caenorhabditis elegans*-based high-throughput screening. *J Microbiol.* 2020 Jun;58(6):431-444. doi: 10.1007/s12275-020-0163-8. Epub 2020 May 27. PMID: 32462486.
5. Cheng AV, Schrank CL, **Escobar IE**, Mylonakis E, Wuest WM. Addition of ethylamines to the phenols of bithionol and synthetic retinoids does not elicit activity in gram-negative bacteria. *Bioorg Med Chem Lett.* 2020;30(9):127099. doi:10.1016/j.bmcl.2020.127099
6. Cheng AV, Kim W, **Escobar IE**, Mylonakis E, Wuest WM. Structure-Activity Relationship and Anticancer Profile of Second-Generation Anti-MRSA Synthetic Retinoids. *ACS Med Chem Lett.* 2019;11(3):393-397. Published 2019 Jul 17. doi:10.1021/acsmchemlett.9b00159
7. Kim W, **Escobar IE**, Fuchs BB, Mylonakis E. Antimicrobial Drug Discovery Against Persisters. In: Kim Lewis, eds. *Persister Cells and Infectious Disease*. Cham, Switzerland: Springer Link; 2019: 273-295. <https://doi.org/10.1007/978-3-030-25241-0>
8. Bellono NW, **Escobar IE**, Lefkovith AJ, Marks MS, Oancea E. An intracellular anion channel critical for pigmentation. *elife* 3, e04543, doi:10.7554/eLife.04543 (2014).

9. Bellono NW*, **Escobar IE***, Oancea E. A melanosomal two-pore sodium channel regulates pigmentation. *Scientific Reports*. *Scientific Reports* 6, 26570, doi:10.1038/srep26570 (2016).

***Co-First Authorship**

Abstracts and Conferences Attended

SACNAS National Diversity in STEM Conference 2019, Honolulu, Hawaii, Attended.

Biomedical Science Careers Program Student Conference 2016, Boston, MA, Attended.

SACNAS National Diversity in STEM Conference 2014, Los Angeles, CA
Determining the Function of the oculocutaneous albinism 2 gene in Pigmentation. **Iliana E. Escobar**, Nicholas W. Bellono, and Elena V Oancea.

Meeting of The Society of General Physiologist: Sensory Transduction 2014, Wood Hole, MA
Direct Patch-Clamp Recordings from Melanosomes Reveal a Chloride Channel Required for Pigmentation. Nicholas W. Bellono, **Iliana E. Escobar**, Michael S. Marks, and Elena V Oancea.

OTHER SKILLS

Languages: Spanish (Fluent) **Computers:** GraphPad, ImageJ , Photoshop, Excel-Data Analysis, Powerpoint

*This Thesis is dedicated to my beloved mother – Carmen E Escobar
1955-2020*

'Till we meet again in the golden streets of heaven

Acknowledgements

God said, “*And who do you think made the human mouth? And who makes some mute, some deaf, some sighted, some blind? Isn't it I, God? So, get going. I'll be right there with you—with your mouth! I'll be right there to teach you what to say.*”

Exodus 4: 11-12 MSG

It might seem strange for a biologist to hold so firmly to their faith, but I have seen many miracles in my life. Therefore, my first acknowledgment goes to the big Guy upstairs.

To my mother, who I lost just shy of a year ago, thank you for always believing in me. Thank you for never allowing me to dream small and sheltering me from any stigma of what a first-generation Latina woman “should” be. I am 50% you. All your teachings and lessons I will hold close to my heart forever. I have overcome because of you.

To my sister Claudia, brother Steve, and my father Tony, thank you for calling, even when I keep forgetting to call back. Thank you.

To my mother- and father-in-law, Thelma and Rodolfo Franco thank you for loving me like a daughter. For feeding me when I was too busy to cook and praying for me when I felt I would never make my goals.

To my brother- and sister-in-law, Randall and Debbie Franco. You are good family, and I am lucky to have you in my life.

To Guisela, thank you for helping me empower my mind. Always a listening ear through the ups and the downs.

To my husband, Anthony Franco. Thank you for being my number one cheerleader. You are the pillar on which I lean-on. You have kept me steady for so many years, making sure I have what I need without me even asking. You are a selfless person, and I am blessed to have you as my husband. Thank you for reading all those emails and “first drafts.” Thank you for listening to all my practice presentations. You are one of the most intelligent people I know. Without your help, this would not be possible.

Thank you to all my academic advisors through this process. Thank you to everyone on my committee, my outside reader Dr. Frederick Ausubel, and my PI, Dr. Mylonakis. Thank you, Dr. Wooseong Kim and Dr. Kiho Lee, for all the hands-on training and answering endless questions and a big thank you to all the members of the Mylonakis Lab.

Preface

The work presented in this thesis was performed in the laboratory of Dr. Eleftherios Mylonakis at Rhode Island Hospital. I performed all of the experiments reported with the following exceptions:

Chapter 2: *C. elegans* killing assays (Figure 1-3, 5, 7, and S2) were performed by Dr. Kiho Lee.

Chapter 3: *C. elegans*-MRSA screening was originally done by Dr. Wooseong Kim (Figure 1B)

Chapter 3: Two replicates of MRSA MW2 time-kill assay (Figure 2) were performed by Alexis White.

Chapter 4: *C. elegans*-MRSA screening was originally done by Dr. Wooseong Kim (Figure 1)

Chapter 4: *Candida* time-kill (Figure 2B) and biofilm assays (Figure 5 & 6) were done by Fernanda Cristina Possamai Rossatto.

List of Tables and Figures

Chapter 1

Figure 1. <i>C. elegans</i> High-throughput Screening.....	15
--	----

Chapter 2

Figure 1. Sphingosine kinase and S1P transporters are related to the immune response in <i>C. elegans</i> on <i>P. aeruginosa</i> PA14.....	43
Figure 2. Sphingosine kinase and S1P transporters control the immune response toward <i>E. faecalis</i> MMH594 in <i>C. elegans</i>	44
Figure 3. External supplementation of S1P stimulates the immune response to <i>P. aeruginosa</i> PA14 in <i>C. elegans</i>	45
Figure 4. Spingosine-1-phosphate has limited antibiotic activity on <i>E. faecalis</i> MMH594 but not on Gram (-) bacteria.....	46
Figure 5. Increased immune response by S1P in <i>C. elegans</i> is dependent on p38 mitogen-activated protein kinase (MAPK) pathway and partially on <i>hlh-30</i>	47
Figure 6. Transcriptional activation of immune response genes, <i>lys-2</i> , was diminished in the <i>spin-2</i> mutant worm.	48
Figure 7. Select S1P transporters affect <i>C. elegans</i> lifespan while S1P supplementation has no affect.	49
Figure 8. Model of S1P transporters directionality in <i>C. elegans</i>	50
Table 1. qPCR primer list.....	51
Figure S1. Amino acid alignment of <i>C. elegans</i> S1P transporters with human SNPS1 and SNPS2.	53
Figure S2. S1P stimulates immune response to <i>E. faecalis</i> MMH594 in <i>C. elegans</i>	54
Figure S3. Relative expression of immune response genes.....	55

Chapter 3

Figure 1. IMD0354 rescues <i>C. elegans</i> from MRSA infection.	85
Figure 2. Time-killing curve shows IMD0354 is bacteriostatic against vancomycin-resistant strain VRS1.	86
Figure 3. Dose toxicity studies show IMD0354 has cytotoxicity activity above MIC levels.....	87
Figure 4. IMD0354 shows minimal toxicity toward <i>C. elegans</i>	88
Figure 5. IMD0354 does not show hemolytic activity.	89
Figure 6. IMD0354 induces membrane permeabilization at high concentrations.....	90
Figure 7. IMD0354 shows dose-dependent inhibition of initial cell attachment and complete inhibition of biofilm formation.	91
Table 1. Minimum inhibitory concentration ($\mu\text{g}/\text{mL}$) of IMD0354 to selected ESKAPE pathogens.	92
Table 2. Minimum inhibitory concentration and Minimum Bactericidal Concentration (MBC) ($\mu\text{g}/\text{mL}$) of NF- κ B inhibitors IMD0354 against vancomycin-resistant <i>Staphylococcus aureus</i> (VISA) and vancomycin-intermediate <i>Staphylococcus aureus</i> (VISA) clinical strains.....	93

Table 3. Minimum inhibitory concentration and Minimum Bactericidal Concentration (MBC) ($\mu\text{g}/\text{mL}$) of NF- κB inhibitors IMD0354 against vancomycin-resistant enterococci (VRE) clinical strains.....	94
Supplementary Figure 1. IMD0354 does not kill VRS1 antibiotic-tolerant cells.....	95
Supplementary Table 1. Fractional Inhibitory Concentration Index of IMD0354 paired in combination with various antibiotics.	96

Chapter 4

Figure 1. Bay 11-7085 rescues <i>C. elegans</i> from a MRSA infection and shows low antibiotic resistance to <i>S. aureus</i> strain MW2.	137
Figure 2. Bay 11-7085 is bactericidal toward MRSA and fungistatic toward <i>C. albicans</i>	139
Figure 3. Bay 11-7085 shows varied toxicity to <i>C. elegans</i> , human red blood cells, and mammalian cells.	140
Figure 4. Bay 11-7085 shows anti-biofilm activity toward three phases of <i>S. aureus</i> strain VRS1 biofilm maturation.	141
Figure 5. Bay 11-7085 shows anti-biofilm activity toward <i>C. albicans</i> and <i>C. auris</i> biofilm formation and maturation biofilm.	142
Figure 6. Bay 11-7085 shows anti-biofilm activity against <i>C. albicans</i> and <i>C. auris</i> initial cell attachment.....	144
Figure 7. Bay 11-7085 shows anti-biofilm activity towards three phases of <i>S. aureus-C. albicans</i> polymicrobial biofilm maturation.	145
Figure 8. Bay 11-7085 inhibits <i>C. albicans</i> but not <i>S. aureus</i> growth in a multispecies Lubbock chronic wound model.	147
Figure 9. Bay 11-7085 prolongs <i>C. elegans</i> survival after <i>C. albicans</i> infection.	148
Table 1. Minimum inhibitory concentrations ($\mu\text{g}/\text{mL}$) of Bay 11-7085 and conventional antibiotics against various pathogenic strains.....	149
Table S1. Microbial strains used in this study.....	150
Table S2. Minimum inhibitory concentration ($\mu\text{g}/\text{ml}$) of Bay 11-7085 against <i>Candida auris</i> antifungal resistant clinical isolates.....	154
Figure S1. Bay 11-7085 inhibits <i>C. albicans</i> and <i>C. auris</i> initial cell attachment through direct killing of yeast cells.	155

Table of Contents

Signature Page.....	iii
Curriculum Vitae.....	iv
Acknowledgements.....	viii
Preface.....	ix
List of Tables and Figures.....	x
CHAPTER 1: INTRODUCTION.....	4
<i>C. elegans</i> as a whole-animal infection model.....	5
Antibiotic-resistance and antimicrobial discovery.....	9
<i>C. elegans</i> high-throughput screening.....	11
Thesis Overview & Summary of Findings.....	13
Figures and Tables.....	15
References.....	17
CHAPTER 2: IN THE MODEL HOST CAENORHABDITIS ELEGANS, SPHINGOSINE-1-PHOSPHATE-MEDIATED SIGNALING INCREASES IMMUNITY TOWARD HUMAN OPPORTUNISTIC BACTERIA.....	20
Abstract.....	22
Introduction.....	24
Results.....	26
Sphingosine Kinase and S1P Transporters Affect the <i>C. elegans</i> Immune Response.....	26
External Supplementation of S1P Extends Worm Survival.....	27
S1P Has No or Nominal Antimicrobial Activity.....	29
S1P Signaling Depends on p38 MAPK Pathway and the Transcription Factor h1h-30.....	30
S1P Signaling Affects <i>C. elegans</i> Immune Effect Gene <i>Lys-2</i>	31
S1P Signaling Has a Modest Effect on <i>C. elegans</i> Lifespan in a Normal Food Source.....	31
Discussion.....	33
Materials and Methods.....	38
Nematode Strains.....	38
Bacterial Strains and Maintenance.....	38
Reagents and Media Preparation.....	38
<i>C. elegans</i> Lifespan and Killing Assay.....	39
Measuring Minimum Inhibitory Concentration.....	40
Sequence Alignment.....	40
RNA Preparation, cDNA Synthesis, and Quantitative PCR.....	40
Abbreviations.....	42
Acknowledgments.....	42

Author Contributions	42
Conflicts of Interest.....	42
Figures and Tables	43
References.....	56
CHAPTER 3: NEW ANTIMICROBIAL BIOACTIVITY AGAINST MULTIDRUG-RESISTANT GRAM-POSITIVE BACTERIA OF KINASE INHIBITOR IMD0354.....	60
Abstract.....	62
Introduction	63
Results.....	66
IMD0354 Exhibits Anti-Staphylococcal Activity In Vitro & in a Whole Animal C. elegans Infection Model	66
IMD0354 Shows Antimicrobial Activity against Multidrug-Resistant Gram-Positive Pathogens	66
Cytotoxicity of IMD0354 on Human Cells and C. elegans	68
IMD0354 Causes Bacterial Membrane Permeability at High Concentrations	69
IMD0354 Inhibits Initial Cell Attachment in a Dose-Dependent Manner and Fully Inhibits Biofilm Formation	69
IMD0354 does not Affect the Viability of Antibiotic-Tolerant Cells or Synergize with Conventional Antibiotics	70
Discussion.....	72
Conclusion	76
Materials and Methods.....	77
Bacterial Strains and Growth Conditions	77
Drugs and Antibiotics.....	77
Minimum Inhibitory Concentration Assay	77
C. elegans Infection Assay for Compound Screening	78
C. elegans dose-Dependent Toxicity Assay	79
Bacterial Time-Course Killing Assay.....	79
Human Blood Hemolysis.....	80
Antibiotic-Tolerant Cell Killing	80
SYTOX Green Membrane Permeability Assay	81
Cell Attachment Assay	81
Biofilm Inhibition Assay	82
Mammalian Cancer Cell Viability Assay.....	83
Acknowledgements.....	84
Author Contributions	84
Conflicts of Interest.....	84
Figures and Tables	85
Supplementary Figures and Tables	95
References.....	97
CHAPTER 4: REPURPOSING KINASE INHIBITOR BAY 11-7085 TO COMBAT STAPHYLOCOCCUS AUREUS AND CANDIDA ALBICANS BIOFILMS.....	101
Abstract.....	103
Introduction	104

Material and Methods	108
Pathogenic Strains and Growth Conditions	108
Drugs and Antibiotics.....	108
Minimum Inhibitory Concentration	108
C. elegans Infection Assay for Compound Screening	109
C. elegans Dose-Dependent Toxicity Assay	111
Bacterial and Fungal Time-Course Killing Assay	111
Human Blood Hemolysis	112
Mammalian Cell Viability Assay.....	113
Biofilm Initial Cell Attachment Assay.....	113
Biofilm Inhibition and Eradication Assay	116
In vitro Multispecies Lubbock Chronic Wound Biofilm Model.....	118
C. elegans-Candida spp. Infection Assay	119
Results	121
Bay 11-7085 Shows Anti-Staphylococcal Activity in vitro and in a Whole Animal C. elegans Infection Model	121
Bay 11-7085 Shows Antimicrobial Activity to S. aureus and Fungal Candida spp.	121
Cytotoxicity of Bay 11-7085 on Human Cells and C. elegans	123
Bay 11-7085 has Anti-Biofilm Activity Toward Three Phases of S. aureus Biofilm Maturation	123
Bay 11-7085 has Anti-Biofilm Activity Toward Three Phases of C. albicans and C. auris Biofilm Maturation	125
Bay 11-7085 has Anti-Biofilm Activity Toward Staphylococcal-Candida Polymicrobial Biofilm	127
Bay 11-7085 Shows Activity Against C. albicans in an In Vitro Multispecies Lubbock Chronic Wound Model	128
Bay 11-7085 Shows Activity in a C. elegans-C. albicans Infection Model	129
Discussion	130
Figures and Tables	137
Supplementary Figures and Tables	150
References.....	156
CHAPTER 5: SUMMARY AND FUTURE DIRECTIONS	161
References.....	171

CHAPTER 1: INTRODUCTION

Host-microbe interactions heavily influence both fitness and disease [1–3]. Understanding the mechanism of microbial pathogenesis and the subsequent host immune response is essential information that aids drug discovery and treatment [1,4]. Traditionally, research on host-microbe interactions focused on the concept that microbes contribute to pathogenesis [5]. However, recent studies have begun to elucidate the positive influence microorganisms can have on human immunity and development [6,7]. These findings broaden the scope of host-microbe interactions and highlight the need for novel and multidisciplinary approaches for research [1–5,7,8]. In this thesis, I focus on the study of basic innate immunity and antimicrobial discovery using *Caenorhabditis elegans* as a whole-animal infection model. Throughout this introduction, I will lay out the benefits and utility of *C. elegans* as a whole-animal infection model system, exemplified by *C. elegans* evolutionarily conserved innate immune signaling pathways. I will also discuss the ongoing antibiotic-resistance crisis and why antimicrobial discovery is in desperate need of novel approaches. I will then explain how *C. elegans* can be used to perform high-throughput screening to assist in drug discovery. The Introduction will conclude with a summary of my findings.

***C. elegans* as a whole-animal infection model**

C. elegans is a free-living nematode worm initially established as a model to study developmental and neurobiology [9,10]. *C. elegans* possess an abundance of features that make them an any extremely useful organism for basic research. For instance, *C. elegans* adults are small, ~ 1 mm long, and typically hermaphroditic, although males appear at about 0.2 % [11]. Due to their small size, they are easy to

manipulate, and culture in the lab, and their transparent bodies facilitate intracellular imaging using fluorescent probes and dyes. *C. elegans* has a 3-day life cycle from egg to adult and lays about 300 eggs per cycle [11] making them ideal candidates to study longevity [12]. They possess a basic innate immune system that is evolutionarily conserved in higher organisms. Additionally, all 302 neurons of the *C. elegans* neuronal network are mapped. Given all these qualities, *C. elegans* has become a staple whole-animal organism used in research from neurobiology to immunity, aging and developmental biology.

C. elegans are microbivores that live in the soil and rotting fruits that eat bacteria as a primary food source in the wild [11]. As a result, *C. elegans* quickly became a widely used model organism to study host-microbe interactions. In 1999 the Ausubel group became the first to characterize a human pathogen (*Pseudomonas aeruginosa*) infection in *C. elegans* [13]. Since then, *C. elegans* has been successfully infected with various pathogens including *Staphylococcus aureus*, *Enterococcus faecalis*, and *Enterococcus faecium* [14,15] and has become an influential model to study the evolution of innate immunity [16–18].

To survive in their natural microbe-rich environment, *C. elegans* need a robust immune response. To date, there are three main immune signaling pathways that have been described. These include the p38 mitogen-activated protein kinase (MAPK) pathway [19,20], the insulin-like signaling pathway (DAF-2, DAF-16) [21], and the transforming growth factor- β (TGF- β) pathway [22]. All three pathways exhibit homology with corresponding mammalian cellular pathways.

The **p38 MAPK pathway** is important in metabolism, development, and homeostasis of many metazoans. In *C. elegans*, this signaling cascade contains neuronal symmetry family member 1 (*nsy-1*), SAPK/ERK kinase 1 (*sek-1*), and p38 MAPK family member 1 (*pmk-1*), which encode the *C. elegans* orthologs of human ASK1 (a MAPK kinase kinase, also known as MAP3K5), MKK3 and MKK6 (MAPK kinases) and p38 (a MAPK), respectively [16]. NSY-1, SEK-1 and PMK-1 are believed to work in a linear phosphotransferase cascade [20,23]. It has also been shown that *tir-1*, a homolog of human *SARM-1*, found within the toll-like receptor signaling cascade in mammals, works upstream of the p38 MAPK kinases in *C. elegans*. Knockdown of *tir-1* blocks phosphorylation of PMK-1 [23]. In humans, TOL(L)-like receptors are upstream of the phosphorylation cascade and SARM-1. *C. elegans* have one TOL(L)-like receptor gene, *tol-1*; however, there is no evidence to suggest that *tol-1* plays a significant role in *C. elegans* immunity [24]. Mutations in the p38 MAPK pathway show increased susceptibility to many pathogens making this pathway an integral part of *C. elegans* immunity [20].

The **insulin-like signaling pathway (DAF-2, DAF-16)** was initially shown to be involved in longevity, metabolism, and stress resistance. In *C. elegans*, the receptor DAF-2 is activated by Insulin Growth Factor I (IGF1). Through a signaling cascade (including the phosphoinositide 3-kinase AGE-1), the phosphoinositide-dependent kinase PDK-1, AKT-1, AKT-2, and serum/glucocorticoid-regulated kinase 1 (SGK-1), block the translocation of the DAF-16 transcription factor into the nucleus. *Daf-16* is responsible for the upregulation of various effector genes involved in longevity, metabolism, and stress resistance. Interestingly, *daf-2* mutant worms are resistant to

several bacterial pathogens [21], and *daf-16* is able to regulate antimicrobial gene expression [25–27]. Given these findings, the insulin/*daf-2* pathway is believed to play an important part in *C. elegans* immunity. However, it has also been reported that *daf-16* mutants are not defective in the induction of host response genes during infection with *P. aeruginosa* or *S. aureus* [19,28,29], nor do they have an increased survival rate. In addition, *daf-2* mutant resistance to pathogens is PMK-1 dependent [19], suggesting *pmk-1* works downstream of *daf-2*, or works in separate but parallel pathways. Whether the role of *daf-2/daf-16* in survival is secondary to the initial innate immune responses is up for debate, and further research is needed to address this discrepancy.

Another major immunity pathway conserved in *C. elegans* is the **transforming growth factor- β (TGF- β) pathway**. In *C. elegans*, the TGF- β homolog DBL-1 regulates a number of immune response factors such as lectins and lysozymes via the TGF- β receptor subunits SMA-6 and DAF-4, as well as the downstream signaling component SMA-3 [22,30]. In addition, knock-down of *dbl-1* results in heightened susceptibility to *Serratia marcescens* and *P. aeruginosa* infection [22,31]. However, there are still many gaps in the exact mechanism by which DBL-1 mediates the activation of immune effectors.

Thus far, I have discussed how *C. elegans* provides utility as a model organism for the study of various cellular and genetic immune response processes. I have described how *C. elegans* is a powerful *in vivo* infection model due to their susceptibility to various human pathogens and evolutionarily conserved basic immunity pathways [13–15]. Taken in totality, investigators have previously leveraged these qualities for research in antibiotic resistance and antimicrobial discovery. In the following two

sections, I will discuss the crisis in antibiotic resistance and how *C. elegans* high-throughput screening is aiding in that fight.

Antibiotic-resistance and antimicrobial discovery

In the year 1928, Alexander Fleming discovered the first antibiotic -penicillin [32], revolutionizing the treatment of infectious disease thereafter. By the 1940s, penicillin was FDA approved and the lives of many individuals and families were benefited via the successful treatment of previously incurable microbial afflictions [33]. Regrettably, what was not taken into serious consideration at the time, was the ability of bacteria to constantly evolve mechanisms to inhibit or evade environmental stressors, particularly host immunity [34]. Examples include the secretion of proteases that can eliminate soluble antimicrobial peptides [35], or the ability of some bacteria to modify their exterior membrane lipopolysaccharides to evade host recognition mechanisms [36]. In a similar manner, bacteria have adapted and evolved to evade and block natural or man-made antimicrobials.

Antibiotic resistance can be mediated by the acquisition of genes by horizontal gene transfer that produce proteins that modify an antibiotics' structure, by mutation of the antibiotic's target, or by enhancing the activity of efflux pumps [37]. For example, antibiotics target critical cell survival mechanisms such as protein, cell wall, DNA, or RNA synthesis [38]. The antibiotic class aminoglycosides targets protein synthesis by binding to ribosomal sites, subsequently producing translational misreading and blockage of translocation [38]. Resistance is acquired when bacteria produce aminoglycoside-modifying enzymes, acquire mutations in the ribosomal target site, or decrease efflux pump activity, diminishing cell wall penetration [38]. This is an example

of just one antibiotic class and its corresponding bacterial resistance mechanism. Each class targets different processes within the cell, thus imparting its own resistance mechanism.

In recent decades bacteria have unsurprisingly adapted to resist antibiotics of last resort such as vancomycin and daptomycin. Highly pathogenic microbes like vancomycin-resistant enterococcus strains, vancomycin-resistant *S. aureus*, and even daptomycin-resistant [39] mutants have emerged. Similar to bacterial pathogens, fungal pathogens can also quickly develop resistance to anti-fungal therapeutics. For example, antifungal resistant *Candida auris* has quickly earned a listing on the CDCs urgent threat list, being highly resistant to common antifungals such as fluconazole and amphotericin B [40].

Collectively, the emergence of antibiotic resistance points to a global health care crisis. New antimicrobial agents possessing novel mechanisms of action are required to attenuate the development of antibiotic resistance. However, traditional antimicrobial screening has been slow and ineffective. Conventional antimicrobial discovery has focused on an *in vitro* multi-well plate system. Thousands of synthetic or natural compounds have been tested to assess bacterial growth. However, this method has two main disadvantages. The first of these is the inability to readily assess host toxicity of tested compounds. Secondly, traditional screens for novel antibiotics cannot identify novel anti-infective compounds such as anti-virulence or immunomodulatory drugs. In the next section, I will discuss how the *in vivo* *C. elegans*-infection high-throughput screening model can compensate for both problems, making it an innovative system for antimicrobial discovery.

***C. elegans* high-throughput screening**

With the discovery of life-saving penicillin, the race to develop and synthesize new and improved antibiotics began. By unearthing the natural anti-infectives produced by bacteria and fungi, or through chemically modifying the scaffold of these natural antimicrobials, initial efforts were successful as new antibiotics were developed that possessed greater efficacy against a broader spectrum of infections [8]. However, as antibiotic resistance began to increase, clinicians and scientists realized that new drugs would need to be more specific and less likely to develop resistance in order to stop or hinder the proliferation of antibiotic-resistant strains. With the golden age of antibiotic discovery behind them, the rise of modern technologies such as genome sequencing, has allowed scientists to focus their efforts on target-based screening. This included the *in vitro* assessment of thousands of essential bacterial genes necessary for growth or survival in the hopes of developing a compound potent enough to block a gene's critical function. This also included the use of thousands of synthetically derived chemical compounds screened using *in vitro* methods plus target-based screening. Many of these drugs failed *in vivo* due to their inability to cross the bacterial cell membrane, off-target effects, and toxicity [8,41]. One of the few effective new antibiotics, daptomycin, has overcome such obstacles and has been the only new anti-infective agent to make it to the clinic in the last 20 years [42,43]. The current situation is grave and new methods of screening for antibiotic targets are desperately needed.

In 1999, the Ausubel laboratory at Massachusetts General Hospital was the first to show that the nematode worm, *C. elegans*, could succumb to a lethal infection by a known human pathogen, *P. aeruginosa* [13]. Thus began a new field of study using *C.*

elegans as a whole- animal infection model. In a few short years, the Ausubel lab developed a high-throughput screening method using *C. elegans* to identify potential anti-infectives against the microbe *E. faecalis* [44]. To date, there have been several screens involving pathogen-mediated killing of *C. elegans* to identify new potentially anti-microbial compounds for a variety of bacterial species.

This method leverages the use of 96-well or 384-well plates, a COPAS Biosort worm sorter, a plate washing system, and a multi-well fluorescent microscope. For example, when screening for an anti-infective against methicillin-resistant *S. aureus* (MRSA), the methods are as follows (Figure 1). First, thousands of young adult *C. elegans* are washed and sorted into individual wells of a designated microplate using a COPAS Biosort instrument (Figure 1A). Each well will contain a unique compound that is being tested for anti-infective properties. Next, MRSA is added to each well and incubated at 25°C for 5 days to let the infection take its course (Figure 1B). After 5 days of incubation MRSA and test compounds are washed out, leaving only the worms, using a 405 LS microplate washer (Figure 1C). Plates are then incubated once again with Sytox Orange for 24 h and then imaged using an Xpress Micro automated microscope to determine *C. elegans* survivability (Figure 1C). Sytox Orange is a live dead stain that will penetrate the cuticle of a dead *C. elegans*, thus causing it to fluoresce. If the worm is alive, the dye cannot penetrate the cuticle, and the worm will not fluoresce. Thus it will be denoted as alive. Through screens such as these many compounds have been identified and designated for additional study to combat deadly species like *P. aeruginosa*, *S. aureus*, and *E. faecium* [45].

C. elegans-based screening overcomes many of the issues with *in vitro* screening methods because it allows for identification of agents that can save *C. elegans* from pathogen-mediated killing, but are not toxic enough to kill the host. Due to the whole-animal nature of the *C. elegans* infection screening method, nontraditional compounds such as those that affect host immunity or pathogen virulence have also been discovered [45]. Ultimately, these qualities make *C. elegans*-infection based high-throughput screening a powerful tool in antimicrobial drug discovery.

Thesis Overview & Summary of Findings

This thesis focuses on applying the C. elegans whole-animal infection model to the study of basic innate immunity and antimicrobial discovery. In the following chapters, I begin by investigating basic mechanisms underlying *C. elegans* innate immunity. I will report how large RNA sequencing datasets led us to study cell signaling sphingolipid- Sphingosine-1-phosphate (S1P)-, which we show is important for basic innate immunity. This work uncovered an evolutionarily conserved function for S1P, but a non-canonical role for S1P transporters in the *C. elegans* immune response to Gram-negative *P. aeruginosa* and Gram-positive *E. faecalis*. This work also shows how S1P activity is dependent on the known *C. elegans* immunity pathway p38 MAPK and transcription factor *hlh-30*.

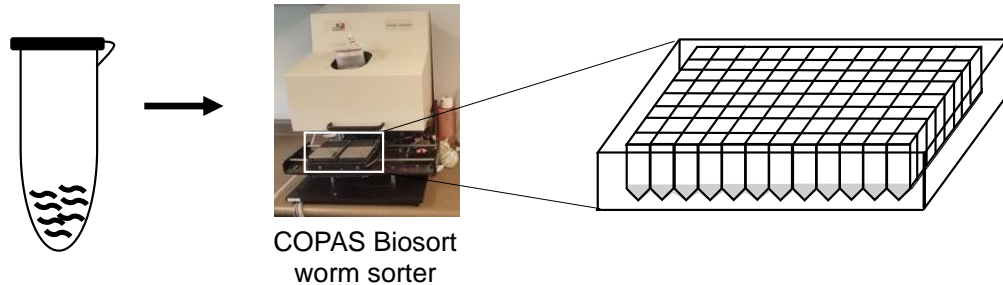
In a subsequent chapter, I focus on kinase inhibitors IMD0354 and Bay 11-7085. Through this work, I showed that IMD0354 is a potent antimicrobial against Gram-positive bacteria with an extremely low minimum inhibitory concentration (MIC) of 0.06 µg/ml. I also discovered that IMD0354 can inhibit *S. aureus* single cell attachment and

prevent biofilm formation at or above MIC concentrations. Furthermore, I found that high concentrations of IMD0354 can affect cell permeability.

In the final chapter I examine how Bay 11-7085 exhibits anti-infective activity to both *S. aureus* and *Candida* spp., at an MIC of 0.5-4 µg/ml. Importantly, I show that Bay 11-7085 inhibits three stages of biofilm maturation, both in monoculture and in a polymicrobial culture of *S. aureus* and *C. albicans*. Lastly, I detail how Bay 11-7085 possesses a low probability of antibiotic resistance and can be utilized to save worms from lethal infections by *S. aureus* and *C. albicans*.

Figures and Tables

A Dispense 15 worms per well using worm sorter



B *C. elegans* are infected with MRSA via liquid dilution for 5 days.

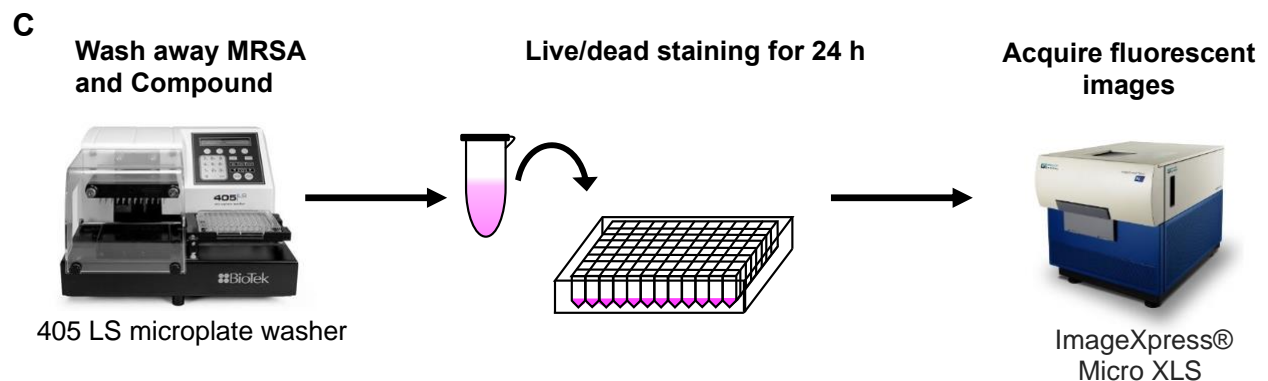
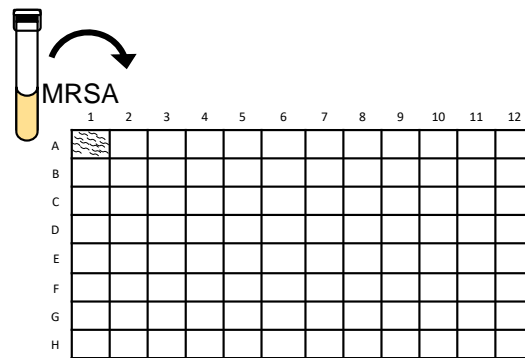


Figure 1. *C. elegans* High-throughput Screening.

(A) Fifteen *C. elegans* are dispensed in individual wells of 96-well or 384-well microplates containing one test compound per well. **(B)** A set volume and concentration of MRSA is added into each well and incubated for 5 days to facilitate infection. **(C)**

After 5 days, worms are washed and stained with Sytox Orange (live/dead stain) and imaged using an ImageXpress fluorescent microscope.

References

1. Stilling, R. M., Bordenstein, S. R., Dinan, T. G. & Cryan, J. F. Friends with social benefits: host-microbe interactions as a driver of brain evolution and development? *Front Cell Infect Mi* **4**, 147 (2014).
2. Gould, A. L. et al. Microbiome interactions shape host fitness. *Proc National Acad Sci* **115**, 201809349 (2018).
3. Chen, L., Garmaeva, S., Zhernakova, A., Fu, J. & Wijmenga, C. A system biology perspective on environment–host–microbe interactions. *Hum Mol Genet* **27**, R187–R194 (2018).
4. Malla, M. A. et al. Exploring the Human Microbiome: The Potential Future Role of Next-Generation Sequencing in Disease Diagnosis and Treatment. *Front Immunol* **9**, 2868 (2019).
5. Scott, E. A., Bruning, E., Nims, R. W., Rubino, J. R. & Ijaz, M. K. A 21st century view of infection control in everyday settings: moving from the Germ Theory of Disease to the Microbial Theory of Health. *Am J Infect Control* **48**, 1387–1392 (2020).
6. Brown, E. M., Sadarangani, M. & Finlay, B. B. The role of the immune system in governing host-microbe interactions in the intestine. *Nat Immunol* **14**, 660–667 (2013).
7. Langdon, A., Crook, N. & Dantas, G. The effects of antibiotics on the microbiome throughout development and alternative approaches for therapeutic modulation. *Genome Med* **8**, 39 (2016).
8. Brown, E. D. & Wright, G. D. Antibacterial drug discovery in the resistance era. *Nature* **529**, 336–343 (2016).
9. White, J. G., Southgate, E., Thomson, J. N. & Brenner, S. The structure of the nervous system of the nematode *Caenorhabditis elegans*. *Philosophical transactions of the Royal Society of London. Series B, Biological sciences* **314**, 1–340 (1986).
10. Sulston, J. E., Schierenberg, E., White, J. G. & Thomson, J. N. The embryonic cell lineage of the nematode *Caenorhabditis elegans*. *Developmental biology* **100**, 64–119 (1983).
11. Corsi, A. K. A Transparent window into biology: A primer on *Caenorhabditis elegans*. *WormBook* 1–31 (2015) doi:10.1895/wormbook.1.177.1.
12. Tissenbaum, H. A. Using *C. elegans* for aging research. *Invertebr Reprod Dev* **59**, 59–63 (2014).
13. Tan, M. W., Mahajan-Miklos, S. & Ausubel, F. M. Killing of *Caenorhabditis elegans* by *Pseudomonas aeruginosa* used to model mammalian bacterial pathogenesis. *Proceedings of the National Academy of Sciences* **96**, 715–720 (1999).
14. Sifri, C. D., Begun, J., Ausubel, F. M. & Calderwood, S. B. *Caenorhabditis elegans* as a model host for *Staphylococcus aureus* pathogenesis. *Infection and immunity* **71**, 2208–2217 (2003).
15. Garsin, D. A. et al. A simple model host for identifying Gram-positive virulence factors. *Proc National Acad Sci* **98**, 10892–10897 (2001).
16. Irazoqui, J. E., Urbach, J. M. & Ausubel, F. M. Evolution of host innate defence: insights from *Caenorhabditis elegans* and primitive invertebrates. *Nature reviews. Immunology* **10**, 47–58 (2010).

17. Pukkila-Worley, R. & Ausubel, F. M. Immune defense mechanisms in the *Caenorhabditis elegans* intestinal epithelium. *Current Opinion in Immunology* **24**, 3–9 (2012).
18. Ermolaeva, M. A. & Schumacher, B. Insights from the worm: the *C. elegans* model for innate immunity. *Seminars in immunology* **26**, 303–309 (2014).
19. Troemel, E. R. et al. p38 MAPK regulates expression of immune response genes and contributes to longevity in *C. elegans*. *PLoS genetics* **2**, e183 (2006).
20. Kim, D. H. et al. A Conserved p38 MAP Kinase Pathway in *Caenorhabditis elegans* Innate Immunity. *Science (New York, N.Y.)* **297**, 623–626 (2002).
21. Garsin, D. A. et al. Long-lived *C. elegans* *daf-2* mutants are resistant to bacterial pathogens. *Science (New York, N.Y.)* **300**, 1921–1921 (2003).
22. Mallo, G. V. et al. Inducible antibacterial defense system in *C. elegans*. *Current biology : CB* **12**, 1209–1214 (2002).
23. Liberati, N. T. et al. Requirement for a conserved Toll/interleukin-1 resistance domain protein in the *Caenorhabditis elegans* immune response. *Proceedings of the National Academy of Sciences* **101**, 6593–6598 (2004).
24. Pujol, N. et al. A reverse genetic analysis of components of the Toll signaling pathway in *Caenorhabditis elegans*. *Current biology : CB* **11**, 809–821 (2001).
25. McElwee, J., Bubb, K. & Thomas, J. H. Transcriptional outputs of the *Caenorhabditis elegans* forkhead protein DAF-16. *Aging Cell* **2**, 111–121 (2003).
26. Yu, R. X., Liu, J., True, N. & Wang, W. Identification of direct target genes using joint sequence and expression likelihood with application to DAF-16. *PloS one* **3**, e1821 (2008).
27. Murphy, C. T. et al. Genes that act downstream of DAF-16 to influence the lifespan of *Caenorhabditis elegans*. *Nature* **424**, 277–283 (2003).
28. Irazoqui, J. E., Ng, A., Xavier, R. J. & Ausubel, F. M. Role for beta-catenin and HOX transcription factors in *Caenorhabditis elegans* and mammalian host epithelial-pathogen interactions. *Proceedings of the National Academy of Sciences of the United States of America* **105**, 17469–17474 (2008).
29. Miyata, S., Begun, J., Troemel, E. R. & Ausubel, F. M. DAF-16-dependent suppression of immunity during reproduction in *Caenorhabditis elegans*. *Genetics* **178**, 903–918 (2008).
30. Mochii, M., Yoshida, S., Morita, K., Kohara, Y. & Ueno, N. Identification of transforming growth factor-beta- regulated genes in *caenorhabditis elegans* by differential hybridization of arrayed cDNAs. *Proceedings of the National Academy of Sciences* **96**, 15020–15025 (1999).
31. Kim, D. H. & Ewbank, J. J. Signaling in the innate immune response. *WormBook* 1–51 (2015) doi:10.1895/wormbook.1.83.2.
32. Davies, J. & Davies, D. Origins and evolution of antibiotic resistance. *Microbiology and molecular biology reviews : MMBR* **74**, 417–433 (2010).
33. Browne, K. et al. A New Era of Antibiotics: The Clinical Potential of Antimicrobial Peptides. *Int J Mol Sci* **21**, 7047 (2020).
34. Reddick, L. E. & Alto, N. M. Bacteria fighting back: how pathogens target and subvert the host innate immune system. *Molecular cell* **54**, 321–328 (2014).

35. McGillivray, S. M. et al. ClpX contributes to innate defense peptide resistance and virulence phenotypes of *Bacillus anthracis*. *Journal of innate immunity* **1**, 494–506 (2009).
36. Paciello, I. et al. Intracellular *Shigella* remodels its LPS to dampen the innate immune recognition and evade inflammasome activation. *Proceedings of the National Academy of Sciences of the United States of America* **110**, E4345-54 (2013).
37. Munita, J. M. & Arias, C. A. Mechanisms of Antibiotic Resistance. *Microbiology spectrum* **4**, (2016).
38. Ogawara, H. Comparison of Antibiotic Resistance Mechanisms in Antibiotic-Producing and Pathogenic Bacteria. *Molecules* **24**, 3430 (2019).
39. Tran, T. T., Munita, J. M. & Arias, C. A. Mechanisms of drug resistance: daptomycin resistance. *Ann Ny Acad Sci* **1354**, 32–53 (2015).
40. Chaabane, F., Graf, A., Jequier, L. & Coste, A. T. Review on Antifungal Resistance Mechanisms in the Emerging Pathogen *Candida auris*. *Front Microbiol* **10**, 2788 (2019).
41. Silver, L. L. Challenges of Antibacterial Discovery. *Clin Microbiol Rev* **24**, 71–109 (2011).
42. Hutchings, M., Truman, A. & Wilkinson, B. Antibiotics: past, present and future. *Curr Opin Microbiol* **51**, 72–80 (2019).
43. Eisenstein, B. I., Oleson, F. B. & Baltz, R. H. Daptomycin: From the Mountain to the Clinic, with Essential Help from Francis Tally, MD. *Clin Infect Dis* **50**, S10–S15 (2010).
44. Moy, T. I. et al. Identification of novel antimicrobials using a live-animal infection model. *Proceedings of the National Academy of Sciences* **103**, 10414–10419 (2006).
45. Kim, W., Hendricks, G. L., Lee, K. & Mylonakis, E. An update on the use of *C. elegans* for preclinical drug discovery: screening and identifying anti-infective drugs. *Expert Opinion on Drug Discovery* **00**, 1–9 (2017).

CHAPTER 2: IN THE MODEL HOST CAENORHABDITIS ELEGANS, SPHINGOSINE-1-PHOSPHATE-MEDIATED SIGNALING INCREASES IMMUNITY TOWARD HUMAN OPPORTUNISTIC BACTERIA

A substantially similar version of this chapter was originally published in the *International Journal of Molecular Sciences* October 20, 2020, Volume 21, Issue 21

In the Model Host *Caenorhabditis elegans*, Sphingosine-1-Phosphate-Mediated Signaling Increases Immunity Toward Human Opportunistic Bacteria

Kiho Lee^{1,†}, Iliana Escobar^{1,†}, Yeeun Jang¹, Wooseong Kim², Frederick M. Ausubel³ and Eleftherios Mylonakis^{1,*}

¹ Division of Infectious Diseases, Rhode Island Hospital, Warren Alpert Medical School of Brown University, Providence, Rhode Island 02903, USA; kiho_lee@brown.edu (K.L.), iliana_escobar@brown.edu (I.E.), christine2372@gmail.com (Y.J.)

² College of Pharmacy, Graduate School of Pharmaceutical Sciences, Ewha Womans University, Seoul, 03760, Korea; wooseong_kim@g.ewha.ac.kr

³ Department of Genetics, Harvard Medical School and Department of Molecular Biology, Massachusetts General Hospital, Boston, Massachusetts 02114, USA; ausubel@molbio.mgh.harvard.edu

* Correspondence: emylonakis@lifespan.org; Tel.: +1 401 444 7856

† These authors contributed equally to this work

Abstract

Sphingosine-1-phosphate (S1P) is a sphingolipid-derived signaling molecule that controls diverse cellular functions including cell growth, homeostasis, and stress responses. In a variety of metazoans, cytosolic S1P is transported into the extracellular space where it activates S1P receptors in a concentration-dependent manner. In the free-living nematode *Caenorhabditis elegans*, the *spin-2* gene, which encodes a S1P transporter, is activated during Gram-positive or Gram-negative bacterial infection of the intestine. However, the role during infection of *spin-2* and three additional genes in the *C. elegans* genome encoding other putative S1P transporters has not been elucidated. Here, we report an evolutionally conserved function for S1P and a non-canonical role for S1P transporters in the *C. elegans* immune response to bacterial pathogens. We found that mutations in the sphingosine kinase gene (*sphk-1*) or in the S1P transporter genes *spin-2* or *spin-3* decreased nematode survival after infection with *Pseudomonas aeruginosa* or *Enterococcus faecalis*. In contrast to *spin-2* and *spin-3*, mutating *spin-1* leads to an increase in resistance to *P. aeruginosa*. Consistent with these results, when wild-type *C. elegans* were supplemented with extracellular S1P, we found an increase in their lifespan when challenged with *P. aeruginosa* and *E. faecalis*. In comparison, *spin-2* and *spin-3* mutations suppressed the ability of S1P to rescue the worms from pathogen-mediated killing, whereas the *spin-1* mutation had no effect on the immune-enhancing activity of S1P. S1P demonstrated no antimicrobial activity toward *P. aeruginosa* and *Escherichia coli* and only minimal activity against *E. faecalis* MMH594 (40 μ M). These data suggest that *spin-2* and *spin-3*, on the one hand, and *spin-1*, on the other hand, transport S1P across cellular membranes in opposite directions. Finally, the immune modulatory effect of S1P was diminished in *C. elegans* *sek-1* and *pmk-1*

mutants, suggesting that the immunomodulatory effects of S1P are mediated by the p38 MAPK signaling pathway.

Keywords: Sphingosine-1-phosphate; S1P; S1P kinase; S1P transporters; pathogenic bacteria; immunity; *Caenorhabditis elegans*

Introduction

Studies investigating the response of *Caenorhabditis elegans* to different pathogens, including bacteria and fungi, have revealed that conserved signaling pathways, such as the p38 mitogen-activated protein kinase (p38 MAPK) pathway and conserved transcription factors such as *hlh-30* (Helix Loop Helix-30, MITF/TFEB), play important roles in *C. elegans* immune responses [1,2]. In *C. elegans*, *hlh-30* drives almost 80% of the host transcriptional immune response to a *Staphylococcus aureus* infection [1]. Furthermore, *hlh-30* mutant worms not only exhibit survival deficiencies against *S. aureus* but also Gram-negative bacteria, such as *Pseudomonas aeruginosa* [1]. Using microarray analysis, investigations have identified numerous other genes that are up-regulated or down-regulated during infection with a variety of bacterial species, including *P. aeruginosa*, *Serratia marcescens*, *S. aureus*, *Enterococcus faecalis*, and *Photobacterium luminescens* as well as during infection by fungi such as *Candida albicans*, *Drechmeria coniospora*, and *Harposporium* spp. [2–5]. These studies have identified a variety of potential target genes that may play critical roles in the response to infection. Genes activated by both Gram-negative and Gram-positive bacteria are of interest for understanding general immune responses of the host to infection and may be potential therapeutic targets for new broad-spectrum antimicrobials

An example of such a broadly activated immune-regulated *C. elegans* gene is SPINSTER-2 abbreviated as *spin-2* [3,5], which encodes a sphingosine-1-phosphate (S1P) transporter. S1P is synthesized by phosphorylation of the long chain base sphingosine by intracellular sphingosine kinase [6]. In mammals, intracellularly synthesized S1P is pumped from the inside of the cell out by S1P transporters,

maintaining a higher level of S1P in the extracellular region than the inside of the cell [7]. In mammals, S1P is an important signaling molecule that is involved in a variety of cellular signaling processes including angiogenesis and anaphylaxis [8,9]. S1P transporters are highly conserved among many metazoans including nematodes and insects [10–12].

In *C. elegans*, there are four predicted S1P transporter homologs named *spin-1*, -2, -3, and -4 [13,14]. Although there is extensive research on the role of S1P and related enzymes, to the best of our knowledge, there is yet to be any published work on the specificity and directionality of *spin-1-4* transporters. In *C. elegans*, research of S1P was initiated by looking at the expression and role of sphingosine kinase (*sphk-1*) and it was found that *sphk-1* is expressed in neuromuscular junction, muscles, neurons, hypodermal cells, the excretory canal, and intestinal cells [15]. Deficiency of *sphk-1* showed decreased lifespan caused by increased susceptibility to oxidative stress [16]. Notably, *sphk-1* promotes neurotransmitter release in neuromuscular junctions and activates the mitochondrial unfolded protein response (UPR^{mt}) in the intestine [17–19].

In *C. elegans*, the UPR^{mt} stabilizes cellular integrity by alleviating oxidative stress and by regulating metabolism during the immune response [20–22]. Therefore, we hypothesized that *sphk-1* and the four S1P transporters encoding genes *spin-1*, -2, -3, and -4 may play an important role in the *C. elegans* immune response. Here, we demonstrate that deletion mutants of *sphk-1*, *spin-1*, *spin-2*, and *spin-3* exhibit aberrant immune responses in which exogenous S1P increases *C. elegans* resistance to *P. aeruginosa* and *E. faecalis*, and the immune modulatory activity of S1P is partially dependent on the p38 MAPK signaling pathway and the transcription factor *hlh-30*.

Results

Sphingosine Kinase and S1P Transporters Affect the C. elegans Immune Response

In *C. elegans*, there are four putative S1P transporters, *spin-1*, *spin-2*, *spin-3*, and *spin-4*, which exhibit significant homology with other eukaryotic S1P transporters (Figure 1A). All four *C. elegans* S1P transporters exhibit >36.30% amino acid identity to human SPNS1 and SPNS2 (Supplementary Figure 1). Additionally, it was previously shown that *spin-2* is upregulated in *C. elegans* infected with *Serratia marcescens* [23] or *Enterococcus faecalis* [5].

To test whether the S1P signaling pathway is involved in *C. elegans* immunity, we exposed sphingosine kinase *sphk-1(ok1097)* mutant worms, which lack 90% of the sphingosine kinase coding region due to deletion of the start codon [17], to infection with the Gram-negative bacterium *P. aeruginosa* strain PA14. We found that *sphk-1* mutant animals were significantly more susceptible to *P. aeruginosa* PA14-mediated killing than wild type N2 worms (Figure 1B, $p < 0.0001$). In addition, we tested the role of S1P transporters during infection using deletion mutant animals made by the *C. elegans* Deletion Mutant Consortium [24]. We found that *spin-2(ok2121)* and *spin-3(ok2286)* mutant worms (*spin-2*, $p < 0.0001$ and *spin-3*, $p = 0.0217$) were also significantly more susceptible to *P. aeruginosa* PA14-mediated killing than wild type N2 worms. Unexpectedly, however, *spin-1(ok2087)* ($p < 0.0001$) and *spin-4(ok2620)* ($p = 0.0062$) mutant worms were more resistant to *P. aeruginosa* PA14 infection than the wild-type worms (Figures 1C–1F).

We also found that *sphk-1* ($p = 0.0086$), *spin-2* ($p < 0.0001$), and *spin-3* ($p < 0.0001$) mutant worms were significantly more susceptible to infection by *E. faecalis* strain MMH594, whereas *spin-4* ($p = 0.0222$) mutant worms were modestly more resistance than N2 (Figures 2A and C-E). However, unlike infection with *P. aeruginosa* PA14, *spin-1* ($p = 0.8920$) mutant worms did not show a difference in survival from wild-type (Figure 2B). The infection results with *P. aeruginosa* and *E. faecalis* indicate that the S1P signaling pathway plays a significant role in the *C. elegans* immune response against both Gram-negative and Gram-positive bacteria.

External Supplementation of S1P Extends Worm Survival

The S1P kinase and S1P transporter mutant data in the previous section suggested that the level of S1P in or outside of intestinal epithelial cells, which is the primary site of the *C. elegans* immune response [18,19], may be critical for its activation. To test this hypothesis, we grew pathogenic bacteria *P. aeruginosa* and *E. faecalis* on various concentrations of externally supplemented S1P and control, solvent only, agar plates, which contained equal volumes of methanol without S1P. We found that, at a higher concentration such as 100 μM S1P, the methanol-only plates showed antimicrobial activity. For this reason, we chose to use 10 μM of S1P supplementation in the medium, which showed no antimicrobial effect in the methanol-only agar plate (data not shown). From our results, we found that a minimum of 10 μM of S1P supplementation dramatically extended wild-type worm survival by approximately two days (Figure 3A, $p < 0.0001$), suggesting that S1P is important for pathogen resistance.

We also tested the lifespans of *P. aeruginosa* PA14-infected *sphk-1* and *spin-1-4* mutant worms treated with S1P given that *sphk-1* mutants cannot produce any S1P and that *spin-1-4* mutant worms, presumptively, have impaired S1P transporter activity. We found that the lifespan of S1P treated *sphk-1* mutant worms was the same as wild-type worms treated with S1P (Figure 3B, $p_{sphk-1 \text{ control vs S1P}} < 0.0001$, $p_{sphk-1 \text{ vs N2 with S1P}} = 0.2583$), which is consistent with the conclusion that S1P fully rescues the hyper-susceptibility phenotype of the *sphk-1* mutant. On the other hand, mutation of *spin-2*, *spin-3*, and *spin-4* partially blocked the ability of S1P to rescue the infected worms (Figure 3D and E, $p_{spin-2 \text{ control vs S1P}} < 0.0001$, $p_{spin-2 \text{ vs N2 with S1P}} < 0.0001$, $p_{spin-3 \text{ control vs S1P}} < 0.0001$, $p_{spin-3 \text{ vs N2 with S1P}} = 0.0285$, Figure 3F, $p_{spin-4 \text{ control vs S1P}} = 0.0012$, $p_{spin-4 \text{ vs N2 with S1P}} = 0.0010$), whereas mutation of *spin-1* had no effect on the ability of S1P to enhance lifespan (Figure 4C, $p_{spin-1 \text{ control vs S1P}} < 0.0001$, $p_{spin-1 \text{ vs N2 with S1P}} = 0.04272$).

As explained in detail in the Discussion section, we think that the simplest interpretation of these data is that S1P transport into cells is important for activating the *C. elegans* immune response and that *spin-1* and *spin-4* encode canonical S1P cellular exporters. Mutation of *spin-1* or *spin-4* could, therefore, result in an accumulation of S1P inside of cells, leading to enhanced pathogen resistance, as shown in Figures 1C and 1F. In contrast, we hypothesize the *spin-2* and *spin-3* encode non-canonical S1P importers. A mutation of *spin-2* or *spin-3* could, therefore, results in the depletion of S1P levels in cells, leading to enhanced pathogen susceptibility, as shown in Figures 1D and 1E.

To further support the S1P supplementation results, we tested *sphk-1* and S1P transporter mutant worms infected with the Gram-positive *E. faecalis* MMH594. As anticipated, we observed that 10- μ M S1P supplementation extended the lifespan of N2

worms when challenged with *E. faecalis* MMH594 ($p < 0.0001$), (Supplementary Figure 2A). *sphk-1* mutant worms, which showed reduced survivability when challenged with MMH594 ($p = 0.0086$), were fully rescued with 10 μM of exogenous S1P supplementation ($p = 0.0536$). The infection sensitive phenotype *spin-2* and *spin-3* mutant worms ($p < 0.0001$) were also fully rescued by the external supplementation of S1P, while the resistant phenotype of *spin-1* and *spin-4* mutant worms were insignificantly enhanced by extra S1P (Supplementary Figures 2C–2F). Taken in their totality, these series of studies indicated that external S1P supplementation not only rescues deficiencies of the S1P mutant worms but also independently activated the immune response in *C. elegans*.

S1P Has No or Nominal Antimicrobial Activity

C. elegans pathogen resistance can be achieved by either a robust immune response or direct antimicrobial activity by a bioactive agent. In order to eliminate the possibility that S1P has direct antimicrobial activity against bacterial pathogens, we tested the antimicrobial activity of S1P by measuring a bacterial growth rate through optical scattering at 600-nm wavelength (OD_{600}). Our results revealed no significant drop in absorbance when compared to the solvent, methanol (Figure 4A and 4B), when testing *P. aeruginosa* PA14 or *Escherichia coli* OP50 with S1P at various concentrations. When we examined *E. faecalis* MMH594, we found that S1P has antimicrobial activity at concentrations greater than 40 μM (Figure 4C, $p_{\text{S1P vs vancomycin}} = 0.001011$). However, S1P did not inhibit the growth of MMH594 at the 10 μM , which is the concentration that increases the *C. elegans* immune response to *E. faecalis* MMH594 (Supplementary Figure 2). These series of experiments imply that S1P exhibits no direct antimicrobial

activity against the Gram-negative bacteria *P. aeruginosa* PA14 and *E. coli* OP50 and minimal activity against Gram-positive bacteria *E. faecalis* MMH595. This suggests that extracellular supplementation of S1P affects *C. elegans* pathogen resistance via an immune-modulatory mode of action rather than antimicrobial activity. To circumvent the issue of antimicrobial activity S1P toward *E. faecalis*, the following experiments were only carried out with the Gram-negative bacterium *P. aeruginosa* strain PA14.

S1P Signaling Depends on p38 MAPK Pathway and the Transcription Factor hlh-30

Several immune signaling pathways have been identified in *C. elegans*, including the p38 MAPK and the insulin-like signaling pathways [25]. Key immune-related genes include *sek-1* and *pmk-1* (p38 MAPK) and the transcription factor *atf-7* (ATF2/CREB5) as well as *hlh-30* (MITF/TFEB), *zip-2* (bZIP), and *daf-16* (FOXO1/3/4) [25]. In order to examine whether S1P signaling is dependent on previously identified immunity-related signaling pathways, we challenged *C. elegans* strains with mutations in a variety of immune-related genes with *P. aeruginosa* PA14 during S1P supplementation. Mutations in all of these genes, except *zip-2*, cause a decrease in the survival rate in the absence of S1P (Figure 5). Significantly, *sek-1*, *pmk-1*, and *hlh-30* mutants exhibited decreased survival rate when challenged with *P. aeruginosa* PA14 and supplemented with S1P when compared to wild-type worms ($p < 0.0001$, $p < 0.0001$, and $p = 0.0017$, respectively, Figures 5A, 5B, and 5C). On the contrary, the *P. aeruginosa* PA14-susceptible phenotypes of *atf-7* and *daf-16* mutants were fully rescued by S1P supplementation on *P. aeruginosa* PA14 to the same levels of N2 worms supplemented with S1P (Figures 5D and 5F). Furthermore, *zip-2* mutant worms exhibited no significant difference in the

survival rate when challenged with *P. aeruginosa* PA14 ($p = 0.0738$) and supplemented with S1P compared to wild-type worms ($p = 0.1786$). These results suggest that, in *C. elegans*, the S1P-mediated immune response is partially dependent on the p38 MAPK pathway and the transcription factor *hlh-30*.

S1P Signaling Affects C. elegans Immune Effect Gene Lys-2

To investigate the transcriptional expression changes of p38 MAPK-dependent immune response genes by S1P signaling, we measured and compared the mRNA levels of seven immune response genes in *sphk-1* and S1P transporters (*spin-1-4*) mutant animals in response to exposure to *E. coli* OP50 or *P. aeruginosa* PA14 for 24 h. Among the genes tested, *lys-2*, a lysozyme encoding gene, was transcriptionally activated by the exposure to *P. aeruginosa* PA14 compared to *E. coli* OP50 in wild type N2 worms (Figure 6). In the *spin-2* mutant animals, the activation of *lys-2* after exposure to *P. aeruginosa* PA14 was inhibited ($p = 0.0183$). Other immune response genes tested were not significantly changed in the *spin-2* mutant nor did we find variable expression levels in either the *spin-1*, 3, 4 and *sphk-1* mutants among multiple genes (Supplementary Figure 3).

S1P Signaling Has a Modest Effect on C. elegans Lifespan in a Normal Food Source

In *C. elegans*, the unfolded protein response through the p38 MAPK pathways connects aging and immunity [26]. Since external supplementation of S1P enhanced longevity during *P. aeruginosa* and *E. faecalis* infections, we tested whether this increase in lifespan was a consequence of a specific effect on the immune response or a general

effect of overall increased lifespan. In these series of experiments, we fed worms with heat-killed *E. coli* OP50 supplemented with S1P in order to exclude any pathogenic traits of live *E. coli*. First, we found that, in the absence of S1P, *C. elegans sphk-1* and *spin-1* mutants exhibited similar lifespans to the wild type N2 strain (Figure 7A, $p_{sphk-1} = 0.4757$, $p_{spin-1} = 0.8768$), whereas *spin-2* and *spin-3* exhibited modestly shorter life spans than wild-type (Figure 6B, $p_{spin-2} < 0.0008$, $p_{spin-3} = 0.0054$) and *spin-4* lived modestly longer (Figure 6C, $p_{spin-4} = 0.0005$). Notably, however, external supplementation with S1P did not increase the lifespan of wild-type, *sphk-1*, *spin-2*, *spin-3*, or *spin-4* worms (Figures 7D, 7E, 7G, 7H, and 7I) and modestly decreased the lifespan of the *spin-1* mutant (Figure 6F, $p = 0.0191$). These results indicate that the effects of S1P as well as the *sphk-1* and *spin-1-4* mutants on lifespan during the course of an infection are due to immunomodulatory effects rather than a non-specific effect on worm longevity.

Discussion

The elucidation of the role of S1P signaling in immune responses in mammals led to the development of immunosuppressive agents such as Fingolimod (FTY720) [27] as well as highlighting potential novel therapies for intestinal *Salmonella* infections [28]. Here, we show that sphingosine kinase and S1P transporters are important components of the *C. elegans* immune response. Exogenous S1P supplementation not only fully compensated the immune deficiency observed in sphingosine kinase (*sphk-1*) mutants, but also dramatically increased the resistance of wild type worms to pathogenic bacteria. These results indicate that the S1P signaling pathway is involved in the *C. elegans* immune response to bacterial infections.

In mammals, S1P activates the immune response through extracellular G protein coupled S1P receptors [7] that regulate many biological processes including cell growth, apoptosis, stress responses, cell migration, and development [7]. There are more than 2,000 G protein coupled receptors (GPCRs) in the genome of *C. elegans* [29], whereas only approximately 750 GPCRs have been identified in humans [30]. However, thus far, a S1P receptor has not been identified in *C. elegans* [31]. The work reported in this paper showed that external supplementation of S1P is sufficient to activate *C. elegans* immunity. In addition to S1P transport, it is possible that S1P is directly activating *C. elegans* immunity through an uncharacterized GPCR. Identification of S1P receptor(s) in *C. elegans* will give more clues in understanding how S1P signaling is related to the immune response.

In *C. elegans*, during a stress response, increased S1P in the cytosol of intestinal epithelial cells activates genes related to the intestinal UPR^{mt} [19]. Kim et al. showed that

sphk-1 localizes to the outer membrane of mitochondria [18] and subsequent production of S1P is important for the activation of intestinal UPR^{mt} [19]. In addition, they found that this phenotype is specific to intestinal cells and not neuronal cells [19]. Their working model suggests that S1P is both produced and is active inside intestinal epithelial cells in support of our model that intracellular S1P activates *C. elegans* immunity. One UPR^{mt} gene, in particular HSP-60, physically binds to SEK-1 and activates PMK-1 during the immune response [32]. Therefore, it is possible that increased levels of S1P within the cytosol by external supplementation activates the p38 MAPK pathway through the UPR^{mt}.

Furthermore, we showed that the increased resistance elicited by S1P supplementation is at least partially dependent on the p38 MAPK signaling genes *sek-1* and *pmk-1* (Figure 5). In addition, we found that the transcriptional expression of a defense response encoding protein, LYS-2, depends on *spin-2*. *lys-2* is a marker of immune response, which is increased during *P. aeruginosa* infection [33] in a *pmk-1*-dependent manner [2]. Given previous studies by Kim et al. and our own findings, we speculate that the enhanced immune response elicited by exogenous supplementation of S1P might be related to p38 MAPK-dependent gene activation. Additional genomics studies are needed to further confirm this hypothesis.

Our results show that the pathogen susceptible phenotypes of *sphk-1*, *spin-2*, and *spin-3* mutants are similar, whereas *spin-1* and *spin-4* exhibit a resistant phenotype when fed *P. aeruginosa* (Figure 1). Since *sphk-1* mutant worms are unable to produce S1P, the level of S1P inside of the cells should be low or absent. One model (Figure 8) that is consistent with these results is *spin-1* and *spin-4* encode canonical S1P transporters that export S1P out of the cytosol, whereas *spin-2* and *spin-3* encode non-canonical S1P

transporters that import extracellular S1P. In *spin-2* and *spin-3* mutant worms, extracellular S1P transport into the cytosol may be decreased enough that *C. elegans* are unable to activate and generate resistance to pathogens. In contrast, the resistant phenotype of *spin-1* and *spin-4* may be due to the accumulation of S1P inside the cell.

If *spin-2* and *spin-3* are S1P importers, we would also expect that mutating them could decrease intracellular S1P accumulation in the presence of exogenous S1P, and, therefore, partially blocking the effect of the exogenous S1P, as shown in Figure 3. The fact that the *spin-1* mutation did not affect the ability of S1P to enhance the worm lifespan in the presence of exogenous S1P is also consistent with *spin-1* encoding a canonical S1P exporter.

The model shown in Figure 8 assumes that S1P is active in the cytosol and not extracellularly during the immune response in accordance with data published by Kim et al. and discussed above [19]. Our data are not consistent with models in which extracellular accumulation of S1P is sufficient to activate *C. elegans* immunity. For example, if extracellular S1P activates *C. elegans* immunity, we would predict that *spin-2* and *spin-3* mutants supplemented with extracellular S1P would show an increased immune response after *P. aeruginosa* infection, which is similar to wild-type worms under similar conditions. Conversely, the model in Figure 8 predicts that mutations in the S1P exporters *spin-1* and *spin-4* would also exhibit decreased survival. However, we found an extended lifespan after *P. aeruginosa* infection in *spin-1* and *spin-4* mutant worms, suggesting that extracellular S1P is not fully responsible for *C. elegans* immune activation and subsequent pathogen resistance.

The model in Figure 8 does not directly address the particular cell types in which S1P is functioning, but it is reasonable to assume that the intestinal epithelial cells are the most likely candidate since the *C. elegans* immune response to *P. aeruginosa* appears to be primarily localized to these cells based on previous reports [19] and our own results. The model also does not address in which tissues or cells S1P is being synthesized in and whether these cells are the same as those in which S1P exerts its immune-enhancing effects. An additional limitation is the impossibility to physically test intra-cellular or extra-cellular S1P levels *in vivo* or *in vitro* in *C. elegans*, which could possibly further support our model [16,34]. One possibility consistent with the model in Figure 8 is that S1P is synthesized in intestinal epithelial cells as intrinsic signaling molecules to enhance immunity. It is important to point out the other models that are consistent with our data, including models in which S1P functions intracellularly and the *spin-1/spin-4* transporters and *spin-2/spin-3* transporters, on the other hand, have the opposite polarities, as shown in Figure 8. However, in models in which the polarities of the transporters are flipped, it is also necessary to postulate that S1P functions extracellularly, which seems unlikely [19].

In any case, our data strongly suggests that SPIN-2/SPIN-3 and SPIN-1/SPIN-4 transport S1P in opposite directions. One potential discrepancy with this model, however, is the observation that *spin-4* mutants exhibit decreased longevity when compared to N2 in the presence of exogenous S1P when fed *P. aeruginosa*. In these experiments, *spin-4* exhibits the same phenotype as *spin-2* and *spin-3* mutants. However, *spin-4* mutants showed more increased longevity than N2 with external supplementation of S1P when fed with *E. faecalis* (Supplementary Figure 2F). We speculate that the different lifespans of *C. elegans spin-4* mutants to different pathogenic bacteria may be caused by the

distinctive immune gene activation profiles between Gram-positive *E. faecalis* or Gram-negative *P. aeruginosa* in *C. elegans* [2,23,33,35–37]. Moreover, microarray data also suggest that even bacterial strains within the same category (Gram-negative or Gram-positive) can also elicit different immune gene activation in *C. elegans* [36,38].

It has been previously observed that *sphk-1* strain has a decreased lifespan on live *E. coli* HB101 [16]. However, we found that *sphk-1* mutant animals (as well as the *spin-1-4* mutant animals) had the same lifespan as wild-type worms when fed heat-killed *E. coli* OP50. Since a live *E. coli* food source is pathogenic as worms mature (>9 days) [39,40], it is possible that the decreased lifespan of *sphk-1* on live *E. coli* HB101 is a consequence of *E. coli*-mediated killing.

In conclusion, although direct evidence is still needed to support the relationship between intracellular concentrations of S1P and pathogenic infection, our findings provide novel insights into the studies of sphingosine signaling and the response to infection. In addition to the immune response, understanding the molecular basis of S1P signaling in *C. elegans* may yield novel insights into conserved features of the innate immune response.

Materials and Methods

Nematode Strains

The following *C. elegans* strains were used in this study. N2 wild-type, VC916 *sphk-1(ok1097)*, RB1678 *spin-1(ok2087)*, RB1702 *spin-2(ok2121)*, RB1778 *spin-3(ok2286)*, RB1986 *spin-4(ok2620)*, KU25 *pmk-1(km25)*, KU4 *sek-1(km4)*, JIN1375 *hlh-30(tm1978)*, VC1518 *atf-7(gk715)*, VC3056 *zip-2(ok3730)*, and CF1038 *daf-16(mu86)* were obtained from *C. elegans* Genome Center (CGC).

Bacterial Strains and Maintenance

Pseudomonas aeruginosa PA14 and *Escherichia coli* OP50 were cultured in Luria Broth (LB) with shaking at 37 °C for 16 to 20 h. *Enterococcus faecalis* MMH594 was incubated in Brain Heart Infusion (BHI) media with shaking at 37 °C for 16 to 20 h. The overnight culture was measured by optical density in a 600-nm wavelength (OD_{600}) and adjusted to $OD_{600} = 1.5$ to control the number of bacteria added to each plate. Adjusted inoculum was then spread on Nematode Growth Media (NGM) or Slow Killing (SK) media agar plates that contain 50 µg/mL of 5-Fluoro-2'-deoxyuridine (FUDR, Sigma Aldrich #F0503, Saint Louis, USA). SK plates contained 0.35% of peptone while NGM plates contained 0.25% [32]. Fresh bacterial plates were regularly streaked on a weekly basis from –80 °C glycerol stocks on solid agar containing nutrient broth. Plates were stored at 4 °C.

Reagents and Media Preparation

Sphingosine-1-phosphate (Sigma Aldrich #73914, Saint Louis, MO USA) was dissolved in methanol due to S1P's poor solubility in water to a final stock concentration of 2 mM. S1P was diluted into solid agar NGM or SK after autoclaved medium was cooled down to 45 °C in order to prevent degradation of S1P. S1P-containing NGM or SK was poured onto assay plates using a serological pipette. The S1P stock solution in methanol was directly diluted into liquid LB, or BHI to desired concentrations for minimum inhibitory concentration (MIC) tests. An equivalent percentage of methanol was used as a vehicle control in all experiments.

C. elegans Lifespan and Killing Assay

Methods used were as previously described in Lee et al. 2017 [41]. Synchronized L1 *C. elegans* were grown on NGM plates containing *E. coli* OP50. After 24 h of incubation at 25 °C, worms were treated with FUDR to block self-fertilization. After an additional 24 h incubation at 25 °C, worms reached a young adult stage and were then added to assay plates. *P. aeruginosa* PA14 assay plates were prepared by adding 100 µL of adjusted *P. aeruginosa* PA14 inoculum onto FUDR (50µg/mL) containing SK plate and spread to the edge. Plates were incubated at 37 °C for 24 h, and then incubated an additional 16 h at 25 °C to maximize virulence of *P. aeruginosa* PA14. To prepare assay plates with *E. faecalis* MMH594, 100 µl of *E. faecalis* MMH594 inoculum was added onto FUDR (50 µM) containing BHI plates. Plates were incubated at 37 °C for 24 h and then cooled to room temperature before the addition of worms. More than 50 young adult worms were added onto plates containing either heat-killed *E. coli* OP50 for the lifespan assay or pathogen *P. aeruginosa* PA14 or *E. faecalis* MMH594 for the killing assay and incubated

at 25 °C. Dead worms were counted daily. Worms that presented no response to physical stimuli after gentle prodding on the anterior regions of *C. elegans* with a platinum wire were scored as dead. The log-rank (Mantel-Cox) test was used for statistical analysis of worm survival. These experiments were not conducted in a blind fashion.

Measuring Minimum Inhibitory Concentration

Minimum inhibitory concentrations were determined by the standard micro-dilution method published by the Clinical and Laboratory Standards Institute [42]. Each assay was conducted in triplicate. These experiments were not conducted in a blind fashion.

Sequence Alignment

All sequence alignments and evaluations were done using open access software Clustal Omega (<http://www.clustal.org/omega/>) [43].

RNA Preparation, cDNA Synthesis, and Quantitative PCR

Young adult worms treated for 24 h with *E. coli* OP50 or *P. aeruginosa* PA14, as done in the *C. elegans* Killing Assay protocol, were collected and washed with phosphate buffer saline (PBS). Supernatant was aspirated leaving approximately 50 µL, making sure not to disturb the *C. elegans* pellet. A total of 500 µL of Trizol (Invitrogen, Carlsbad, CA USA) was then added to each sample. Samples were frozen at –80 °C and then immediately thawed at 37 °C. This freeze-thaw cycle was repeated one additional time for a total of two freeze-thaw cycles. Next, 150 µL of additional Trizol was added to each sample and allowed to incubate for 5 min at room temperature. 140

μL of chloroform was then added to each sample, vortexed vigorously for 15 s, and then incubated for 2 min at room temperature. Samples were then centrifuged at 11,000 rpm for 15 min at 4 °C. Clear supernatant was collected into clean microtubes and 70% ethanol was added at a 1:1 ratio. Samples were mixed and run through RNeasy spin columns (Qiagen # 74104, Germantown, MD USA) and washed following manufacturer's instructions. RNA concentration and 260/280 ratios were assessed to determine RNA quality. cDNA was prepared using Verso cDNA synthesis Kit (Thermo Fisher, Waltham, MA USA). Equal concentrations of RNA were used to synthesis cDNA. Real-time PCR was performed using iTaq Universal Syber Green Supermix (BioRad, Hercules, CA USA) and CFX96 Real-time PCR machine following manufacturer's instructions. Primers used for real-time PCR can be found in Table 1.

Abbreviations

S1P	Sphingosine-1-phosphate
<i>C. elegans</i>	<i>Caenorhabditis elegans</i>
<i>P. aeruginosa</i>	<i>Pseudomonas aeruginosa</i>
<i>E. faecalis</i>	<i>Enterococcus faecalis</i>
UPR ^{mt}	Mitochondrial Unfolded Protein Response

Acknowledgments

We thank the *Caenorhabditis* Genetics Center (CGC), which is funded by the NIH Office of Research Infrastructure Programs (P40 OD010440). This study was supported by the National Institutes of Health grant P01AI083214 to F.M.A. and E.M.

Author Contributions

Conceptualization, K.L. and E.M. Investigation, K.L., I.E., Y.J., and W.K. Writing—original draft preparation, review, and editing. K.L., I.E., E.M., and F.A. Supervision and project administration, E.M. Funding acquisition, E.M. and F.A.

Conflicts of Interest

The authors declare no conflict of interest.

Figures and Tables

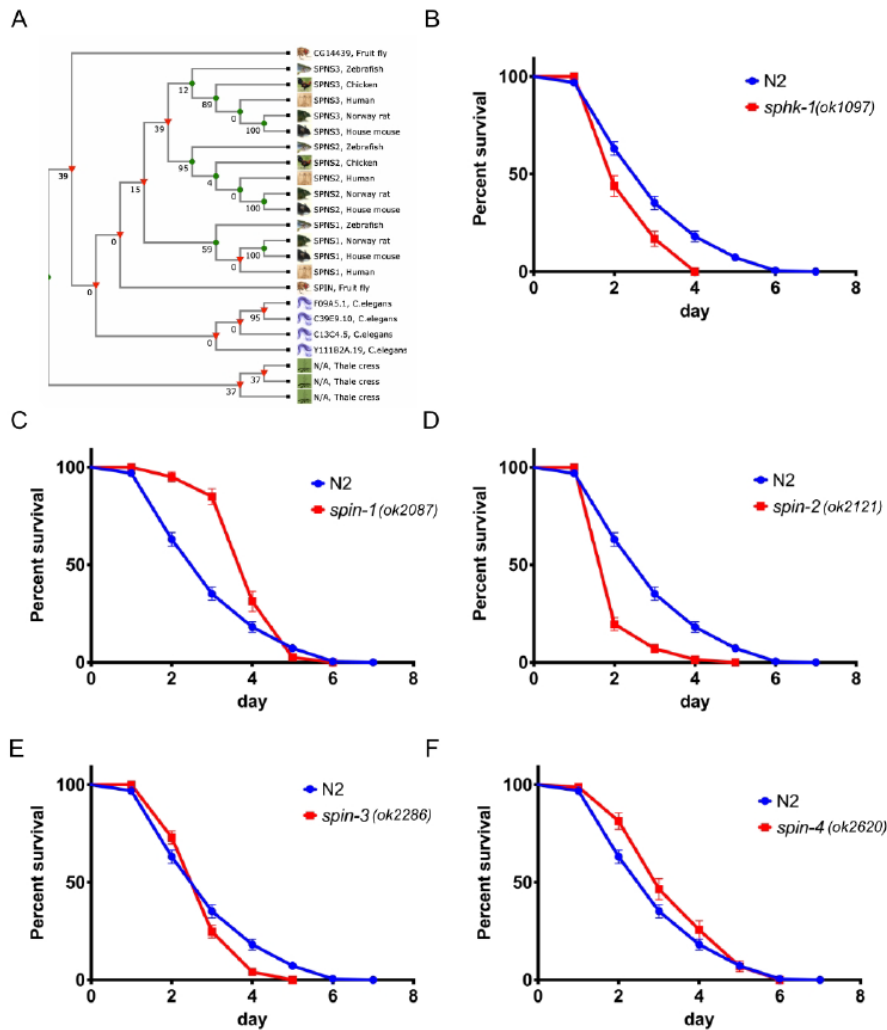


Figure 1. Sphingosine kinase and S1P transporters are related to the immune response in *C. elegans* on *P. aeruginosa* PA14.

(A) Phylogenetic tree of S1P transporters. (B) Survival of worms with mutation in sphingosine kinase, *sphk-1*, and wild type N2. Survival of worms with mutation in S1P transporters *spin-1* (C), *spin-2* (D), *spin-3* (E), and *spin-4* (F) on *P. aeruginosa* PA14.

The log-rank (Mantel-Cox) test was used for statistical analysis of worm survival. ($n > 150$ worms per condition).

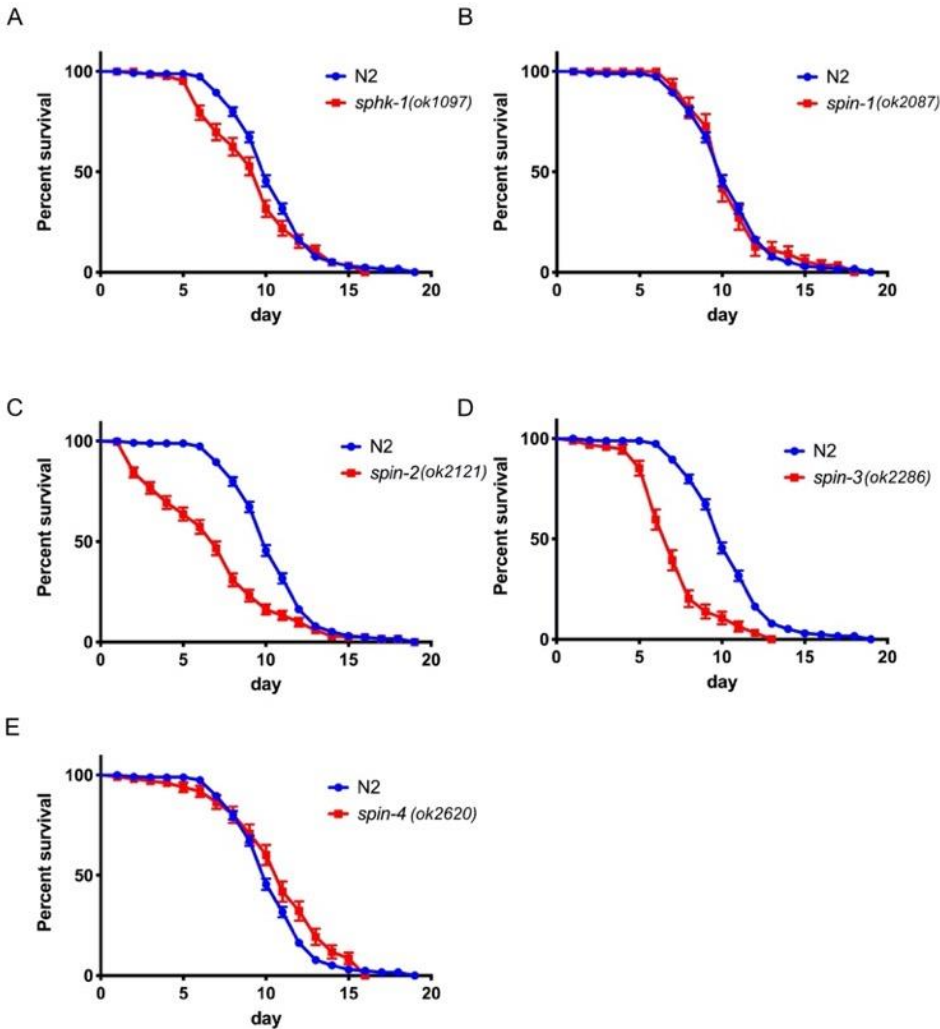


Figure 2. Sphingosine kinase and S1P transporters control the immune response toward *E. faecalis* MMH594 in *C. elegans*.

Survival of worms with mutation in sphingosine kinase, *sphk-1* (A), or S1P transporters *spin-1* (B), *spin-2* (C), *spin-3* (D), and *spin-4* (E) and wild type N2 on *E. faecalis* MMH594. The log-rank (Mantel-Cox) test was used for statistical analysis of worm survival. ($n > 150$ worms per condition).

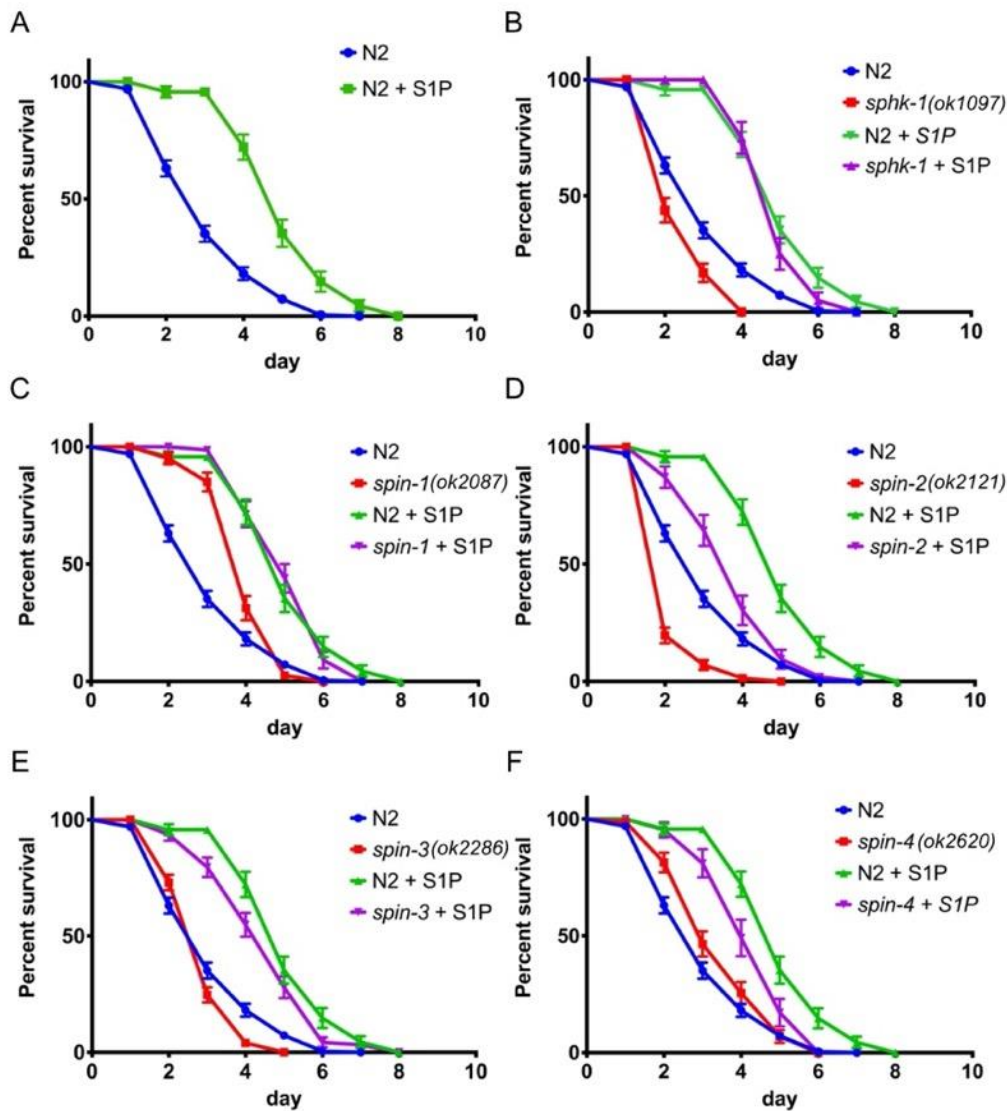


Figure 3. External supplementation of S1P stimulates the immune response to *P. aeruginosa* PA14 in *C. elegans*.

The survival of worms with or without S1P supplementation in the background of wild type N2 worms (A), *sphk-1* (B), *spin-1* (C), *spin-2* (D), *spin-3* (E), and *spin-4* (F). The log-rank (Mantel-Cox) test was used for statistical analysis of worm survival. ($n > 150$ worms per condition).

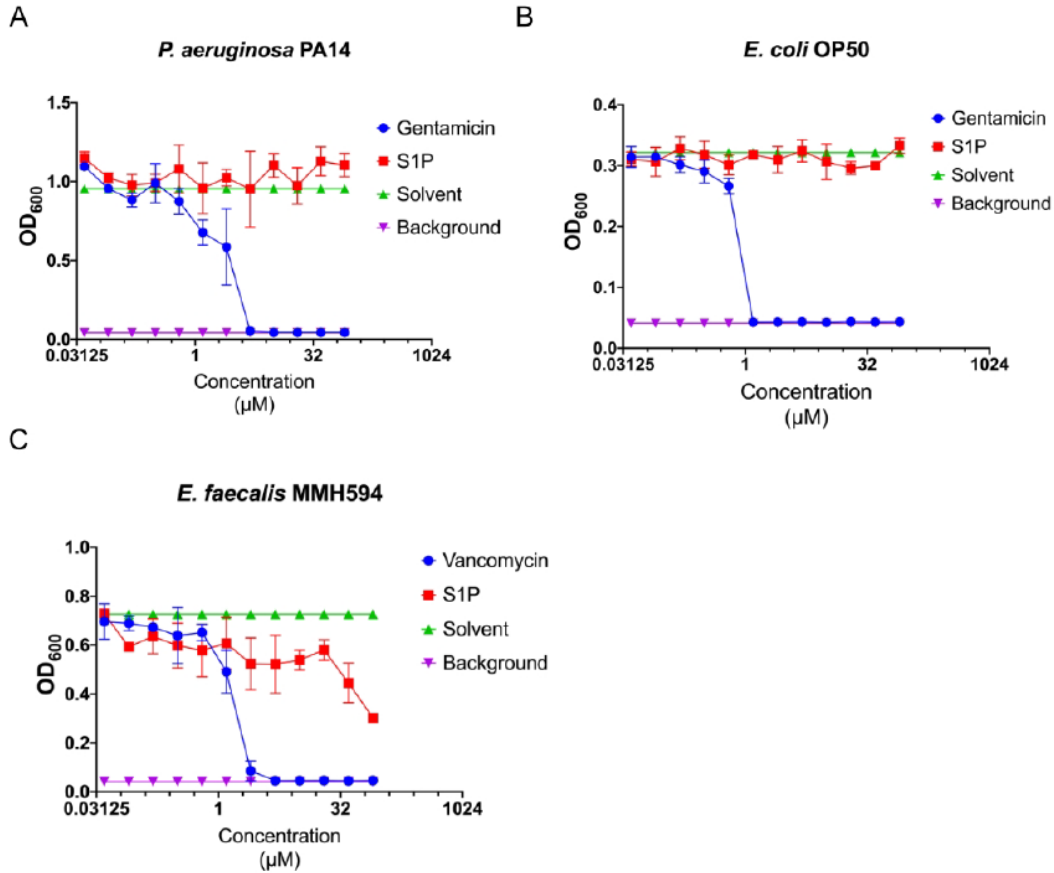


Figure 4. Spingosine-1-phosphate has limited antibiotic activity on *E. faecalis* MMH594 but not on Gram (–) bacteria.

Growth of *P. aeruginosa* PA14 (A), OP50 (B), and MMH594 (C) exposed to antibiotics, gentamycin or vancomycin, solvent (methanol), and S1P at various concentrations after 18 h in Luria Broth or Brain Heart Infusion media. OD₆₀₀, optical density at 600 nm. ($n=3$, \pm S.D.).

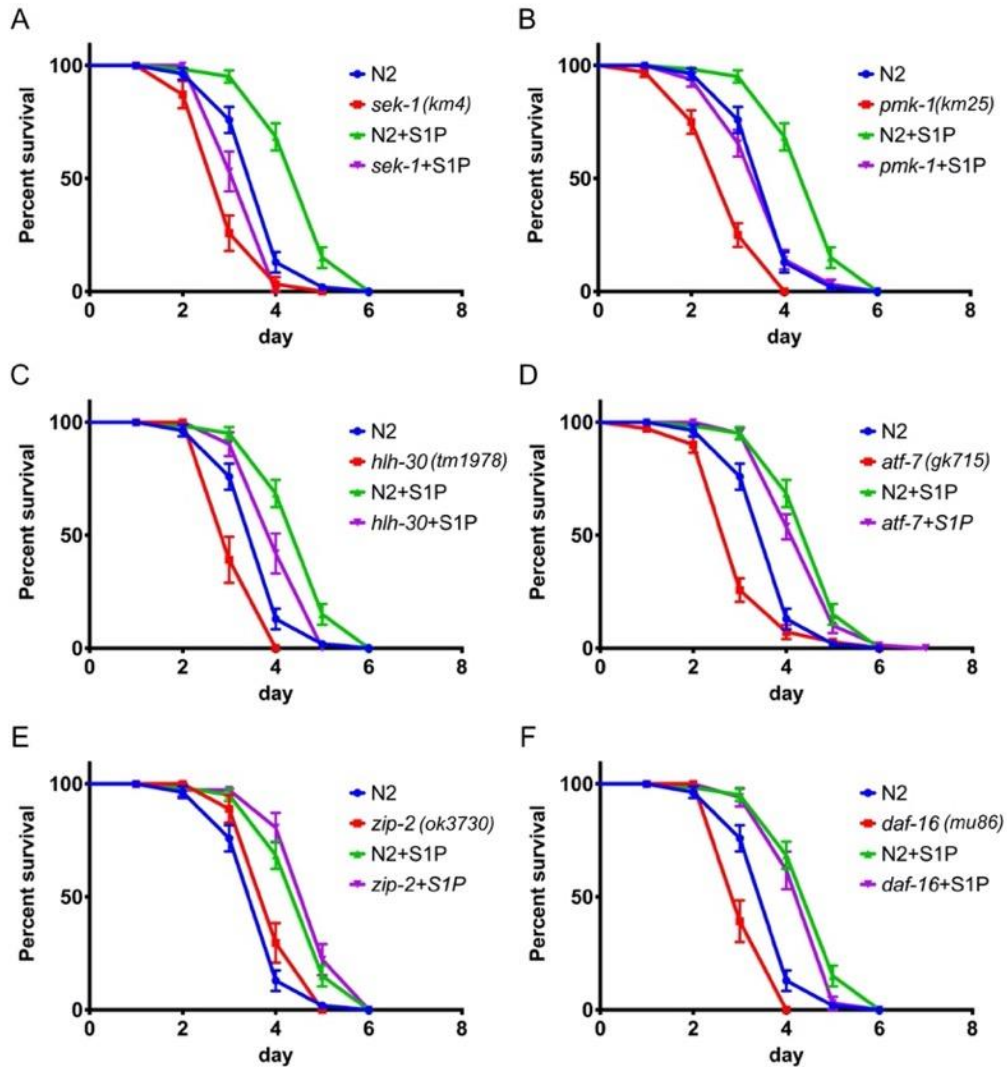


Figure 5. Increased immune response by S1P in *C. elegans* is dependent on p38 mitogen-activated protein kinase (MAPK) pathway and partially on *hlh-30*.

The survival of worms with or without S1P supplementation in the background of wild type N2 and p38 MAPK pathway, *sek-1* and *pmk-1* (A, B), transcription factors *hlh-30* (C), *atf-7* (D), *zip-2* (E), and *daf-16* (F). The log-rank (Mantel-Cox) test was used for statistical analysis of worm survival. ($n > 150$ worms per condition).

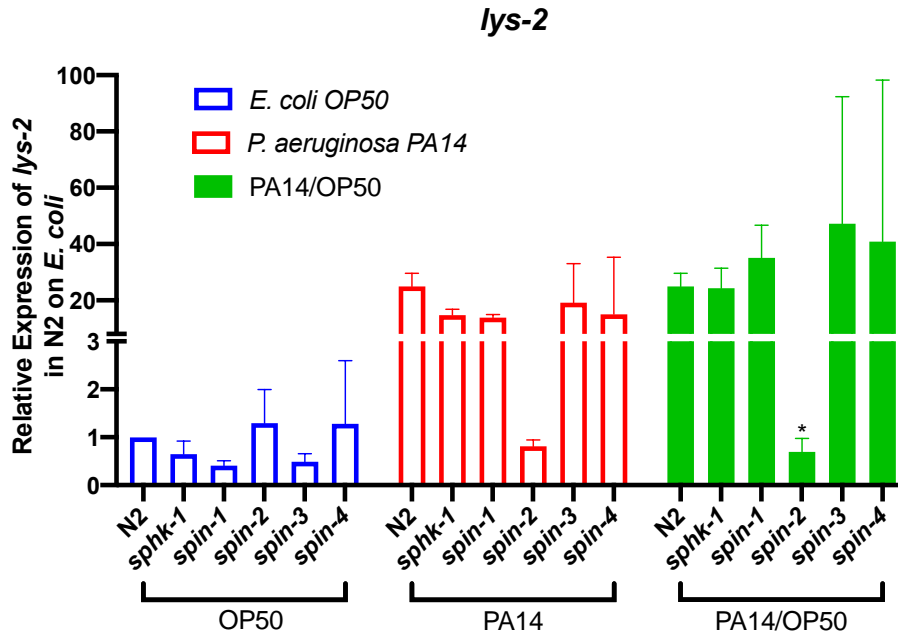


Figure 6. Transcriptional activation of immune response genes, *lys-2*, was diminished in the *spin-2* mutant worm.

The fold changes of *lys-2* in wild type, sphingosine kinase (*sphk-1*) and S1P transporters mutant (*spin-1-4*) worms were normalized to house-keeping gene, *pmp-3*, and *Y45F10D.4*. The unpaired t-test was used for statistical analysis. $p < 0.05$. ($n=2$, \pm S.D.).

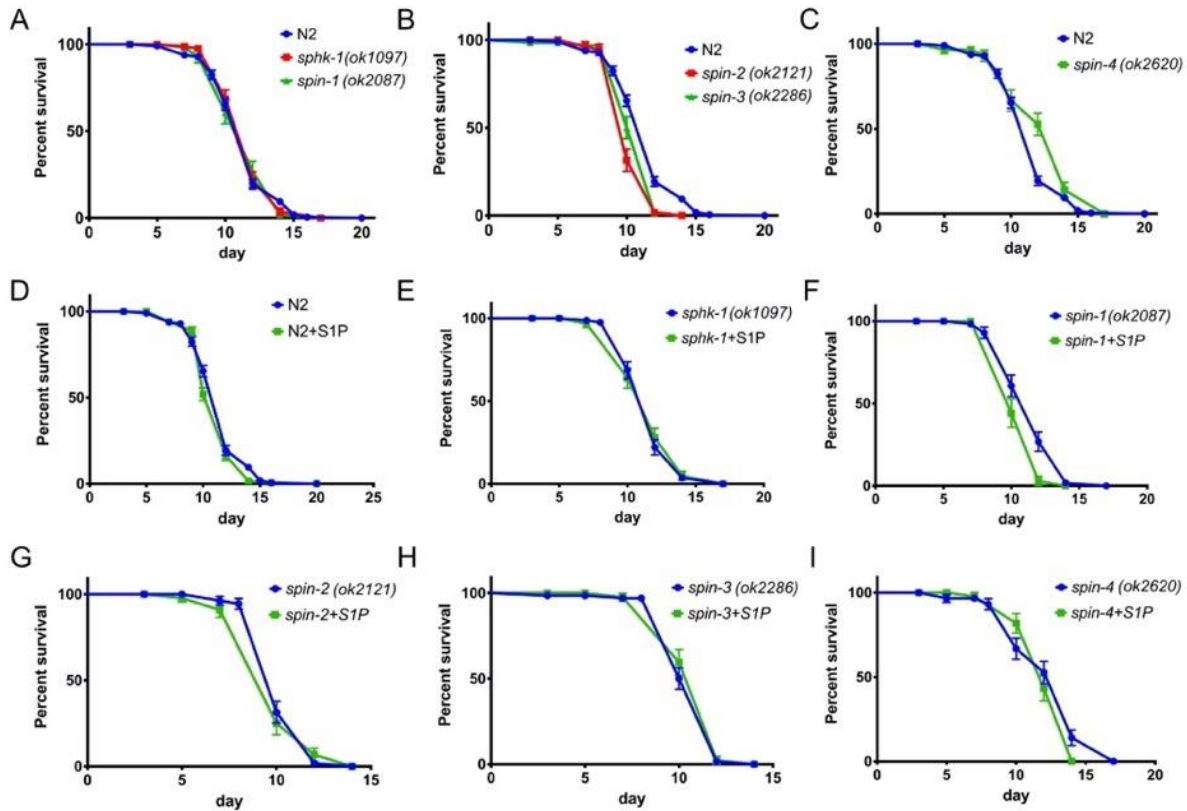


Figure 7. Select S1P transporters affect *C. elegans* lifespan while S1P supplementation has no affect.

Mutant worms showing the same lifespan (A), decreased lifespan (B), and increased lifespan (C) compared to wild type N2. Comparison of the survival with or without S1P in the background of wild type N2 (D), *sphk-1* (E), *spin-1* (F), *spin-2* (G), *spin-3* (H), and *spin-4* (I). The log-rank (Mantel-Cox) test was used for statistical analysis of worm survival. ($n > 150$ worms per condition).

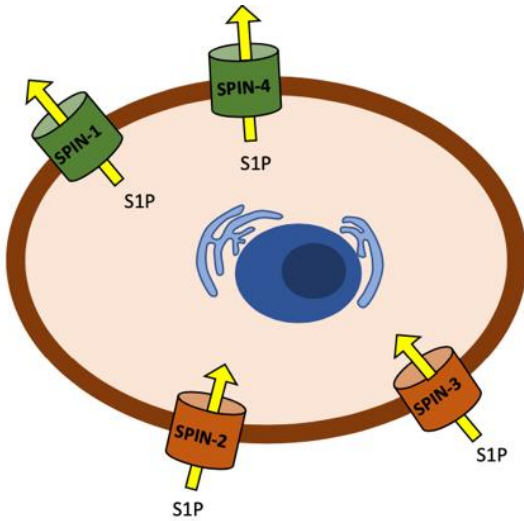


Figure 8. Model of S1P transporters directionality in *C. elegans*.

SPIN-1 and SPIN-4 show canonical directionality transporting S1P out into the extracellular space. Mutations in these transports increases cytosolic S1P. SPIN-2 and SPIN-3 pump S1P into the cytosolic space. Mutations in both these transports decreases cytosolic S1P.

Table 1. qPCR primer list.

References	Sequence Name	Gene Name	Direction	Sequence
[44]	Y22F5A.5	<i>lys-2</i>	F	GCTGGATTGGGAATTGAGAC
	Y22F5A.5	<i>lys-2</i>	R	GACGTTGGCAGTTGGATTG
[23]	F35C5.6	<i>clec-63</i>	F	AGGAGCTGCTCTTCAAACCA
	F35C5.6	<i>clec-63</i>	R	TCCAGGATGAGGAGATGGTG
[45]	T07C4.4	<i>spp-1</i>	F	TGGACTATGCTGTTGCCGTT
	T07C4.4	<i>spp-1</i>	R	ACGCCTTGTCTGGAGAATCC
[46]	K08D8.5		F	CCGGGAAGTCGAATGAACAT
	K08D8.5		R	GATGCAACACCTGCCAAAGA
[47]	F08G5.6	<i>irg-4</i>	F	CACAATGATTTCAATGCGAGA
	F08G5.6	<i>irg-4</i>	R	GTTTCGACCGAGAAATCGAG
[47]	F55G11.2		F	TGGTTCTCCAGACGTGTTCA
	F55G11.2		R	CAGCCTTGCCTTTACTGACA
[48]	C54G10.3	<i>pmp-3</i>	F	GTTCCCGTGTTCACTCAT
	C54G10.3	<i>pmp-3</i>	R	ACACCGTCGAGAAGCTGTAGA
[48]	Y45F10D.4		F	GTCGCTTCAAATCAGTTCAGC
	Y45F10D.4		R	GTTCTTGTCAAGTGATCCGACA
[23]	F56D6.2	<i>clec-67</i>	F	CGGGCTGGGAATATATCAAT
	F56D6.2	<i>clec-67</i>	R	CAATAGGTTGTGGCGTATGG

Supplementary Figures

SPNS1 1 -----MAGSDTAPF
 SPNS2 1 MMCLECASAAAGGAEEDAEERRRRRGAQRGAGGSGCCGARGAGGAGVSAAGDE-VQT
 SPIN-4 1 -----
 SPIN-1 1 -----MVRNKVAPV
 SPIN-2 1 -----
 SPIN-3 1 -----
 SPNS1 10 LSQADDDPDDGPVPGTGPGLPGSTGNPKSEEPEVPDQEGLQRITGLSPGRSALIVAVLCYIN
 SPNS2 60 LSGSVRRAPTGPPTGPTPGCAATAKGPQAQQPKPASLGR-----GRG-AAAAILSLGN
 SPIN-4 1 -----MP-----NEIEE---GS--GLDVASRLAGKKWVTCSILLLVN
 SPIN-1 10 EDGANIQRNFEPPPYTTPTDSPEDKIRS---NSTATTASQPEFQGCWTIVVVAIFFIIN
 SPIN-2 1 -----MVNSQQDYISVTALFVVN
 SPIN-3 1 -----MVNERKDYISIVILFVVN
 SPNS1 70 LLNYMDRFTVAGVLPDIEQFFNIGDSSGLIQTVFIISSYMLAPVFGYLGDRYNRKYLMLC
 SPNS2 113 VLNYLDRYTVAGVLLDIQQHFGVKDRGAGLLQSVFICSFMVAAPIFGYLGDRFNRKVIILS
 SPIN-4 34 LLNYMDRYTIVGVMSRLATFFDIDDKGQLLQTVFIVFYMFFAPLFGYLGDRYNRKMLMI
 SPIN-1 67 LLNYMDRYTIAGVLNDVQTYYNISDAWAGLIQTTFMVFIIIFSPICGFLGDRYNRKWIFV
 SPIN-2 19 LLNYVDRYTVAGVLTQVQTYYNISDSLGLIQTVFLISFMVFSVPCGYLGDRFNRKWIMI
 SPIN-3 19 LINVDRYTIAGVLPDVQSYNINDSMGGMIQTVFLISFMIGSPICGYLGDRFNRKYVML
 SPNS1 130 GGIAFWSLVTLGSSFIPGEHFWLLLLTRGLVGVGEASYSTIAPTIIADLDFVADQRSRMLS
 SPNS2 173 CGIFFWSAVTFSSSFIPQQYFWLLVLSRGLVGIGEASYSTIAPTIIGDLFTKNTRTLMLS
 SPIN-4 94 TGICIWILAVFASSFCGEGHYLLFLLCRGIVGIGEASYSTIAPTIVLSDLFSGGLRSRVLML
 SPIN-1 127 VGIAIWSAVFASTFIPSNQFWLFLFRGIVGIGEASYAIIISPTVIADMFTGVLRSRMLM
 SPIN-2 79 IGVGIWLGAVLGSSFVPANHFWLFLVLRSFVIGIGEASYSNVAPSLISDMFNGQKRSTVFM
 SPIN-3 79 VGIVIWLICVCASTFIPRNLFPFLFFRSLVGIGEASYVNICPTMISDMFTSDKRTRVYM
 SPNS1 190 IFYFAIPVGSGLGYIAGSKVKDMAGDWHWALRVTPGLGVVAVLLLFLVVREPPRGAVERH
 SPNS2 233 VFYFAIPLGSGLYITGSSVKQAAGDWHWALRVSPVLGMITGTLILILV PATKRGHADQL
 SPIN-4 154 MFYFAIPVGSGLGFISGSSISQATDSWQWVRFSPITIGIACGLMLWLLDEPVRGACDGA
 SPIN-1 187 VFYFAIPFGCGLGFVVGSAVASWTGHWQWVVRTGVLGIVCLLLIIVFVREPERGKAERE
 SPIN-2 139 IFYFAIPVGSGLGFIVGSNVATLTGHWQWIRVSAIAGLIVMIALVLFTEPERGAADKA
 SPIN-3 139 LFYLAVPVGSGLYIISNVSSLTGSWQWVVRTGIGGIVALLALLFMVHEPERGAAEKL
 SPNS1 250 SD----LPPLNPTSWWADLRALARNPSFVLSLGF TAVAFVTGSLALWAPFLLRSRVVL
 SPNS2 293 GD----Q-LKARTSWLRDMKALIRNRSYVFS SLATS AVSFATGALGMWIPLYLHRAQVVQ
 SPIN-4 214 RQNGDE-----ADLIGDIKYLMSIKTFYLSAASIASFSIGTMSWWT PQYVGF SYAVI
 SPIN-1 247 KGEI--AASTEATS YLDDMKDLLSNATYV TSSLYTATVFMVGT LAWVAPITIQYADSAR
 SPIN-2 199 MGESKDVVVTNTTYLEDLVILLKTP TLVACTWGYTALV FVSGTLSWWEPTVIQHLTAWH
 SPIN-3 199 EGK--DTTVRPS TS YWKDLKVLKCTYVVTTLAYTALIFVSGTLTWWMPTII EYSAAWT

 SPNS1 306 GETPPC-LPGDSCSSSDSLIFGLITCLTGVLGVGLGVEISRRL-----RHSNPRADP
 SPNS2 348 KTAETC--NSPPCGAKDSLIFGAITCFTGFLGVVTGAGATRWC-----RLKTQRADP
 SPIN-4 268 HN---VPKVPETELTQINLIFGIITCMAGLLGVATGSILSRWARDGSSIFRNHATEKADV
 SPIN-1 305 RN----GTITEDQKANINLVFGALTCVGGVLGVAIGTLVSNMWSRGVGFKHIQTVRADA
 SPIN-2 259 QGLNDTKDLASTDKDRVALYFGAITTAGGLIGVIFGSMLSKWLVA GWGPFRRLQTDRAQP
 SPIN-3 257 RGYKSIKELPLSFKNETGLIFGLLTTACGIIGTLLGNLLAQCFLYGWLGAW-SKTKRAHL
 SPNS1 357 LVCA TGLLGSAPFLFLSLACARGSIVATYIFIFIGETLLSMNWAIVADILLYVVIPTRRS
 SPNS2 398 LVCAVGM LGS AIFICLIFVAAKSSIVGAYICIFVGETLLFSNWAITADILMYVVIPTRRA

SPIN-4 325 YICALSMFVALPFLFFAIFIAEYSTNGCLILIIYFAIMSMCLNWSVNVVDVLMYVVVANRRA
 SPIN-1 361 LVCAIGAAICIP TLILAIQNIESNMNFAWGMLFICIVASSFNWATNVDLLLSVVVPQRRS
 SPIN-2 319 LVAGGGALLAAPFLIGMIFGDKSLVLLYIMIFFGITFMCFNWGLNIDMLTTVIHPNRRS
 SPIN-3 316 VAAGCGALISTPCLVVVFVFGHSSELLTWIMVGV SITGLCFNWSLNVEVFNQIVAPERRS
 SPNS1 417 TAEAFQIVLSHLLGDAGSPYLIGLISDRLRNWPSPFLSEFRALQFSLMLCAFV GALGGA
 SPNS2 458 TAVALQSFTSHLLGDAGSPYLIGFISDLIRQSTKDSPLWEFLSLGYALMLCPFVVVLGGM
 SPIN-4 385 TALAVQTMVAHLFGDAASPYIIGVLSDMRLRGDDA-SAVGHFFALQKALYVPTFMLVVAGA
 SPIN-1 421 SASSWQILISHMFGDASGPYIIGLISDAIRGNED-TAQAHYKSLVTSFWLCVGTLVLSVI
 SPIN-2 379 TAFSYFVLVSHLFGDASGPYLIGLISDAIRHGST-YPKDQYHSLV SATYCCVALLLLSAG
 SPIN-3 376 TAFSYVTLISHLCGDASGPYIIGAISDAIKSNHLDSP EW DYKSLAYASMLAPVMMGIS TV

 SPNS1 477 AFLGTAIFIEADRRRAQLHVQGLLHEA----GSTDDRIVVPQRGRSTRVPVAS----VLI
 SPNS2 518 FFLATALFFVSDRARAEEQQVNQLAMPP----ASVKV-----
 SPIN-4 444 FYLAATFFVEDDRKEALYQMDAPDNWHHDDPSEDLDD-LLSHENPETVEGV E EHPADMIV
 SPIN-1 480 LFGISAITVVKDKARFNEIMLAQANKD--NTSSGTL--PIEDRNTEDETGSEV--QHM--
 SPIN-2 438 LYFVSSLTLVSDRKKFRAEMGLDDLQS--KPIRTSTD-SLERIGINDDVA-SS---RL--
 SPIN-3 436 LYFVAAIIFKRDARRLVREMRNESDD--QEKSYTN-----GIWADDCLTHSS---KF--
 SPNS1 529 -----
 SPNS2 -----
 SPIN-4 503 PLAHSDGDTA
 SPIN-1 -----
 SPIN-2 -----
 SPIN-3 -----

	SPNS1	SPNS2	SPIN-4	SPIN-1	SPIN-2	SPIN-3
SPNS1	100.00	54.02	39.29	37.98	38.77	36.67
SPNS2	54.02	100.00	39.43	37.96	37.42	36.30
SPIN-4	39.29	39.43	100.00	39.43	37.58	33.62
SPIN-1	37.98	37.96	39.43	100.00	44.70	44.03
SPIN-2	38.77	37.42	37.58	44.70	100.00	50.31
SPIN-3	36.67	36.30	33.62	44.03	50.31	100.00

Figure S1. Amino acid alignment of *C. elegans* S1P transporters with human SNPS1 and SNPS2.

Percent identity matrix included below alignment.

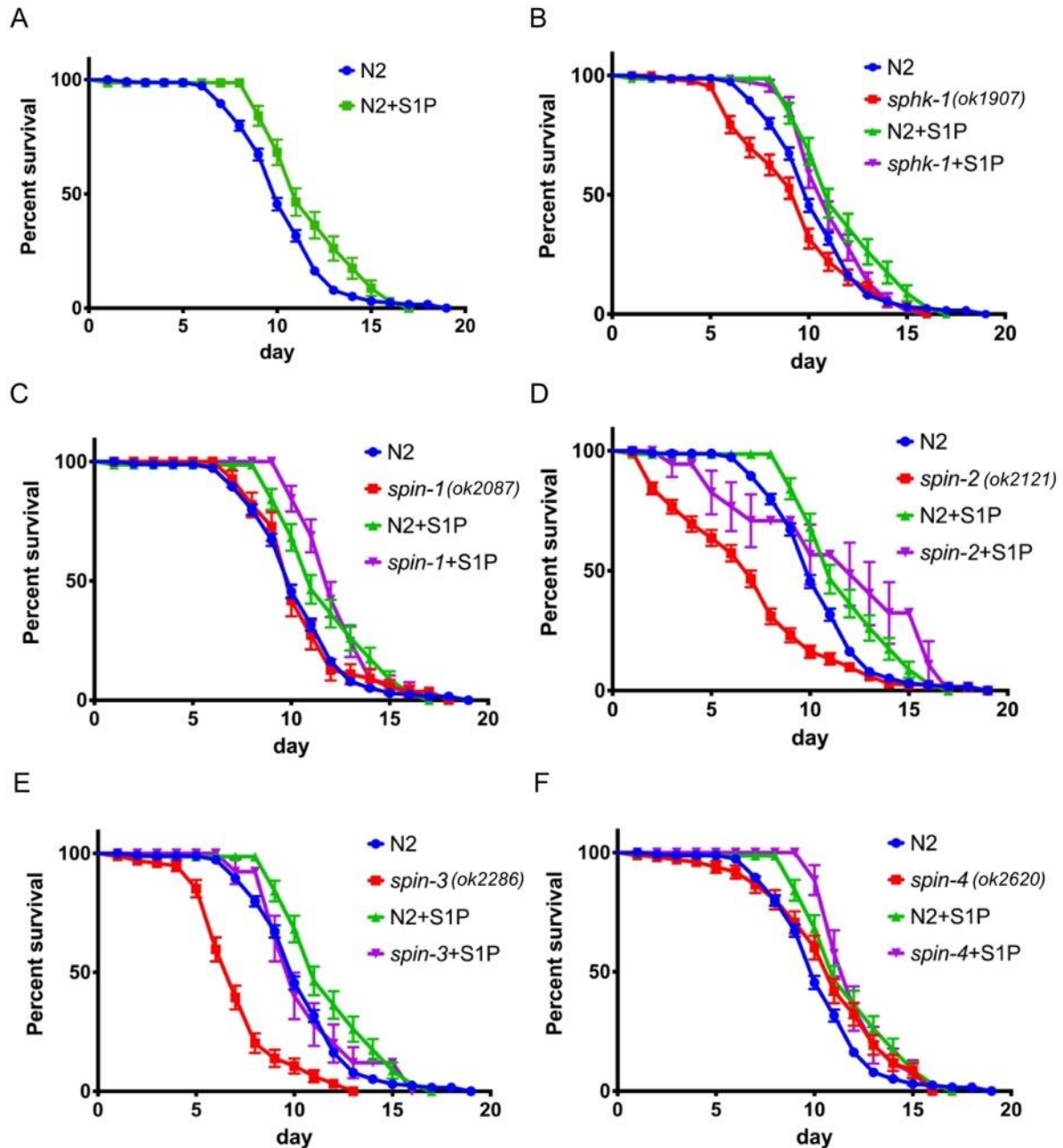


Figure S2. S1P stimulates immune response to *E. faecalis* MMH594 in *C. elegans*.

The survival of worms with or without S1P in the background of wild type N2 worms (**A**), *sphk-1* (**B**), *spin-1* (**C**), *spin-2* (**D**), *spin-3* (**E**), and *spin-4* (**F**). The log-rank (Mantel-Cox) test was used for statistical analysis of worm survival. ($n > 150$ worms per condition).

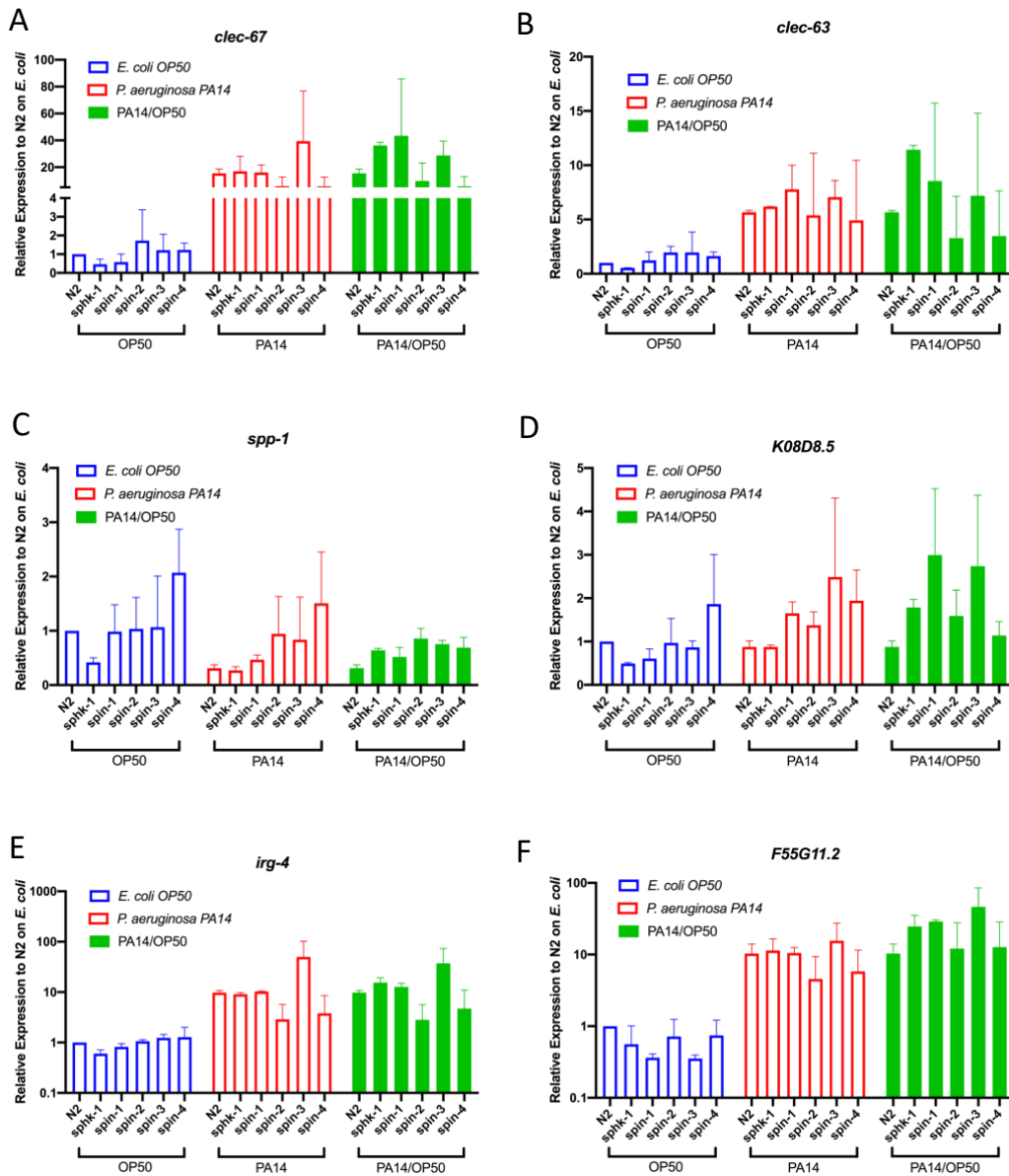


Figure S3. Relative expression of immune response genes.

The relative mRNA level immune response genes in wild type N2, *sphk-1*, *spin-1*, *spin-2*, *spin-3*, and *spin-4* was measured by quantitative PCR. The fold changes of each genes in wild type, sphingosine kinase (*sphk-1*), and S1P transporters mutant (*spin-1-4*) worms were normalized with house-keeping gene, *pmp-3*, and Y45F10D.4. ($n=2$, \pm S.D.).

References

1. Visvikis, O.; Ihuegbu, N.; Labeed, S.A.; Luhachack, L.G.; Alves, A.-M. F.; Wollenberg, A.C.; Stuart, L.M.; Stormo, G.D.; Irazoqui, J.E. Innate Host Defense Requires TFEB-Mediated Transcription of Cytoprotective and Antimicrobial Genes. *Immunity* **2014**, *40*, 896–909.
2. Troemel, E.R.; Chu, S.W.; Reinke, V.; Lee, S.S.; Ausubel, F.M.; Kim, D.H. p38 MAPK Regulates Expression of Immune Response Genes and Contributes to Longevity in *C. elegans*. *PLoS Genet.* **2006**, *2*, e183.
3. Shivers, R.P.; Pagano, D.J.; Kooistra, T.; Richardson, C.E.; Reddy, K.C.; Whitney, J.K.; Kamanzi, O.; Matsumoto, K.; Hisamoto, N.; Kim, D.H. Phosphorylation of the Conserved Transcription Factor ATF-7 by PMK-1 p38 MAPK Regulates Innate Immunity in *Caenorhabditis elegans*. *PLoS Genet.* **2010**, *6*, e1000892.
4. Irazoqui, J.E.; Urbach, J.M.; Ausubel, F.M. Evolution of host innate defence: Insights from *Caenorhabditis elegans* and primitive invertebrates. *Nat Rev Immunol* **2010**, *10*, 47–58.
5. Engelmann, I.; Griffon, A.; Tichit, L.; Montañana-Sanchis, F.; Wang, G.; Reinke, V.; Waterston, R.H.; Hillier, L.W.; Ewbank, J.J. A Comprehensive Analysis of Gene Expression Changes Provoked by Bacterial and Fungal Infection in *C. elegans*. *PLoS ONE* **2011**, *6*, e19055–13.
6. Rosen, H.; Germana Sanna, M.; Gonzalez-Cabrera, P.J.; Roberts, E. The organization of the sphingosine 1-phosphate signaling system. *Curr. Top. Microbiol. Immunol.* **2014**, *378*, 1–21.
7. Maceyka, M.; Spiegel, S. Sphingolipid metabolites in inflammatory disease. *Nature* **2014**, *510*, 58–67.
8. Wang, F.; Van Brocklyn, J.R.; Hobson, J.P.; Movafagh, S.; Zukowska-Grojec, Z.; Milstien, S.; Spiegel, S. Sphingosine 1-phosphate stimulates cell migration through a G(i)-coupled cell surface receptor. Potential involvement in angiogenesis. *J. Biol. Chem.* **1999**, *274*, 35343–35350.
9. Spiegel, S.; Milstien, S. The outs and the ins of sphingosine-1-phosphate in immunity. *Nat. Rev. Immunol.* **2011**, *11*, 403–415.
10. Pantoja, M.; Fischer, K.A.; Ieronimakis, N.; Reyes, M.; Ruohola-Baker, H. Genetic elevation of sphingosine 1-phosphate suppresses dystrophic muscle phenotypes in *Drosophila*. *Development* **2013**, *140*, 136–146.
11. Kawahara, A.; Nishi, T.; Hisano, Y.; Fukui, H.; Yamaguchi, A.; Mochizuki, N. The Sphingolipid Transporter Spns2 Functions in Migration of Zebrafish Myocardial Precursors. *Science* **2009**, *323*, 524–527.
12. Hisano, Y.; Kobayashi, N.; Yamaguchi, A.; Nishi, T. Mouse SPNS2 Functions as a Sphingosine-1-Phosphate Transporter in Vascular Endothelial Cells. *PLoS ONE* **2012**, *7*, e38941.
13. Shaye, D.D.; Greenwald, I. OrthoList: A compendium of *C. elegans* genes with human orthologs. *PLoS ONE* **2011**, *6*, e20085.
14. Kim, W.; Underwood, R.S.; Greenwald, I.; Shaye, D.D. OrthoList 2: A New Comparative Genomic Analysis of Human and *Caenorhabditis elegans* Genes. *Genetics* **2018**, *210*, 445–461.

15. Chan, J.P.; Sieburth, D. Localized sphingolipid signaling at presynaptic terminals is regulated by calcium influx and promotes recruitment of priming factors. *J. Neurosci.* **2012**, *32*, 17909–17920.
16. Chan, J.P.; Brown, J.; Hark, B.; Nolan, A.; Servello, D.; Hrobuchak, H.; Staab, T.A. Loss of Sphingosine Kinase Alters Life History Traits and Locomotor Function in *Caenorhabditis elegans*. *Front. Genet.* **2017**, *8*, 132.
17. Chan, J.P.; Hu, Z.; Sieburth, D. Recruitment of sphingosine kinase to presynaptic terminals by a conserved muscarinic signaling pathway promotes neurotransmitter release. *Genes Development* **2012**, *26*, 1070–1085.
18. Kim, S.; Sieburth, D. Sphingosine Kinase Regulates Neuropeptide Secretion During the Oxidative Stress-Response Through Intertissue Signaling. *J. Neurosci.* **2018**, *38*, 8160–8176.
19. Kim, S.; Sieburth, D. Sphingosine Kinase Activates the Mitochondrial Unfolded Protein Response and Is Targeted to Mitochondria by Stress. *Cell Reports* **2018**, *24*, 2932–2945.e4.
20. Runkel, E.D.; Liu, S.; Baumeister, R.; Schulze, E. Surveillance-Activated Defenses Block the ROS-Induced Mitochondrial Unfolded Protein Response. *PLoS Genet.* **2013**, *9*, e1003346.
21. Pellegrino, M.W.; Nargund, A.M.; Kirienko, N.V.; Gillis, R.; Fiorese, C.J.; Haynes, C.M. Mitochondrial UPR-regulated innate immunity provides resistance to pathogen infection. *Nature* **2014**, 1–15.
22. Melber, A.; Haynes, C.M. UPR mt regulation and output: A stress response mediated by mitochondrial-nuclear communication. *Cell Res* **2018**, *28*, 281–295.
23. Wong, D.; Bazopoulou, D.; Pujol, N.; Tavernarakis, N.; Ewbank, J.J. Genome-wide investigation reveals pathogen-specific and shared signatures in the response of *Caenorhabditis elegans* to infection. *Genome Biol* **2007**, *8*, R194.
24. The *C. elegans* Deletion Mutant Consortium Large-Scale Screening for Targeted Knockouts in the *Caenorhabditis elegans* Genome. *G3: Genes/Genomes/Genetics* **2012**, *2*, 1415–1425, doi:10.1534/g3.112.003830.
25. Kim, D.H. Signaling in the innate immune response. *WormBook* **2018**, *2018*, 1–35, doi:10.1895/wormbook.1.83.2.
26. Kim, D.H. Bacteria and the aging and longevity of *Caenorhabditis elegans*. *Annu. Rev. Genet.* **2013**, *47*, 233–246.
27. Takabe, K.; Paugh, S.W.; Milstien, S.; Spiegel, S. “Inside-Out” Signaling of Sphingosine-1-Phosphate: Therapeutic Targets. *Pharmacol. Rev.* **2008**, *60*, 181–195.
28. Huang, F.-C. The Role of Sphingolipids on Innate Immunity to Intestinal Salmonella Infection. *Int. J. Mol. Sci.* **2017**, *18*, 1720, doi:10.3390/ijms18081720.
29. Bargmann, C.I. Neurobiology of the *Caenorhabditis elegans* Genome. *Science* **1998**, *282*, 2028–2033.
30. Vassilatis, D.K.; Hohmann, J.G.; Zeng, H.; Li, F.; Ranchalis, J.E.; Mortrud, M.T.; Brown, A.; Rodriguez, S.S.; Weller, J.R.; Wright, A.C.; et al. The G protein-coupled receptor repertoires of human and mouse. *Proc. Natl. Acad. Sci. USA.* **2003**, *100*, 4903–4908.
31. Deng, X.; Kolesnick, R. *Caenorhabditis elegans* as a model to study sphingolipid signaling. *Biol. Chem.* **2015**, *396*, 767–773.

32. Jeong, D.-E.; Lee, D.; Hwang, S.; Lee, Y.; Lee, J.; Seo, M.; Hwang, W.; Seo, K.; Hwang, A.B.; Artan, M.; et al. Mitochondrial chaperone HSP -60 regulates anti-bacterial immunity via p38 MAP kinase signaling. *EMBO J.* **2017**, *36*, 1046–1065, doi:10.15252/embj.201694781.
33. Shapira, M.; Hamlin, B.J.; Rong, J.; Chen, K.; Ronen, M.; Tan, M.-W. A conserved role for a GATA transcription factor in regulating epithelial innate immune responses. *Proc. Natl. Acad. Sci. USA.* **2006**, *103*, 14086–14091.
34. Menuz, V.; Howell, K.S.; Gentina, S.; Epstein, S.; Riezman, I.; Fornallaz-Mulhauser, M.; Hengartner, M.O.; Gomez, M.; Riezman, H.; Martinou, J.-C. Protection of *C. elegans* from anoxia by HYL-2 ceramide synthase. *Science* **2009**, *324*, 381–384.
35. Bolz, D.D.; Tenor, J.L.; Aballay, A. A conserved PMK-1/p38 MAPK is required in *Caenorhabditis elegans* tissue-specific immune response to *Yersinia pestis* infection. *J. Biol. Chem.* **2010**, *285*, 10832–10840.
36. Dierking, K.; Yang, W.; Schulenburg, H. Antimicrobial effectors in the nematode *Caenorhabditis elegans* : An outgroup to the Arthropoda. *Philos. Trans. R. Soc. B: Biol. Sci.* **2016**, *371*, 20150299, doi:10.1098/rstb.2015.0299.
37. Fletcher, M.; Tillman, E.J.; Butty, V.L.; Levine, S.S.; Kim, D.H. Global transcriptional regulation of innate immunity by ATF-7 in *C. elegans*. *PLoS Genet.* **2019**, *15*, e1007830, doi:10.1371/journal.pgen.1007830.
38. Simonsen, K.T.; Gallego, S.F.; Færgeman, N.J.; Kallipolitis, B.H. Strength in numbers: “Omics” studies of *C. elegans* innate immunity. *Virulence* **2012**, *3*, 477–484.
39. Garigan, D.; Hsu, A.-L.; Fraser, A.G.; Kamath, R.S.; Ahringer, J.; Kenyon, C. Genetic analysis of tissue aging in *Caenorhabditis elegans*: A role for heat-shock factor and bacterial proliferation. *Genetics* **2002**, *161*, 1101–1112.
40. Youngman, M.J.; Rogers, Z.N.; Kim, D.H. A Decline in p38 MAPK Signaling Underlies Immunosenescence in *Caenorhabditis elegans*. *PLoS Genet.* **2011**, *7*, e1002082.
41. Lee, K.; Mylonakis, E. An Intestine-Derived Neuropeptide Controls Avoidance Behavior in *Caenorhabditis elegans*. *Cell Reports* **2017**, *20*, 2501–2512.
42. CLSI (Clinical and Laboratory Standards Institute) - Document CLSI M7-A7; CLSI; 2012 *Methods for dilution antimicrobial susceptibility tests for bacteria that grow aerobically; approved standard*.
43. Sievers, F.; Wilm, A.; Dineen, D.; Gibson, T. J.; Karplus, K.; Li, W.; Lopez, R.; McWilliam, H.; Remmert, M.; ding, J. S. O.; Thompson, J. D.; Higgins, D. G. Fast, scalable generation of high-quality protein multiple sequence alignments using Clustal Omega. *Mol Syst Biol* **2011**, *7*, 1–6.
44. Boehnisch, C.; Wong, D.; Habig, M.; Isermann, K.; Michiels, N.K.; Roeder, T.; May, R.C.; Schulenburg, H. Protist-type lysozymes of the nematode *Caenorhabditis elegans* contribute to resistance against pathogenic *Bacillus thuringiensis*. *PLoS ONE* **2011**, *6*, e24619.
45. Zhou, M.; Liu, X.; Yu, H.; Yin, X.; Nie, S.-P.; Xie, M.-Y.; Chen, W.; Gong, J. Cell Signaling of *Caenorhabditis elegans* in Response to Enterotoxigenic *Escherichia coli* Infection and *Lactobacillus zeae* Protection. *Front. Immunol.* **2018**, *9*, 1745.
46. Di, R.; Zhang, H.; Lawton, M.A. Transcriptome Analysis of *C. elegans* Reveals Novel Targets for DON Cytotoxicity. *Toxins (Basel)* **2018**, *10*, doi:10.20944/preprints201804.0376.v1.

47. Block, D.H.S.; Twumasi-Boateng, K.; Kang, H.S.; Carlisle, J.A.; Hanganu, A.; Lai, T.Y.-J.; Shapira, M. The Developmental Intestinal Regulator ELT-2 Controls p38-Dependent Immune Responses in Adult *C. elegans*. *PLoS Genet.* **2015**, *11*, e1005265.
48. Hoogewijs, D.; Houthoofd, K.; Matthijssens, F.; Vandesompele, J.; Vanfleteren, J.R. Selection and validation of a set of reliable reference genes for quantitative sod gene expression analysis in *C. elegans*. *BMC Mol. Biol.* **2008**, *9*, 9.

CHAPTER 3: NEW ANTIMICROBIAL BIOACTIVITY AGAINST MULTIDRUG-RESISTANT GRAM-POSITIVE BACTERIA OF KINASE INHIBITOR IMD0354

A substantially similar version of this chapter was originally published in *Antibiotics*
October 1, 2020, Volume 9, Issue 10

New Antimicrobial Bioactivity against Multidrug-Resistant Gram-Positive Bacteria of Kinase Inhibitor IMD0354

Iliana E Escobar¹, Alexis White¹, Wooseong Kim^{2,*} and Eleftherios Mylonakis^{1,*}

¹ Infectious Diseases Division, Department of Medicine, Warren Alpert Medical School of

Brown University, Rhode Island Hospital, Providence, RI 02903, USA;

iliana_escobar@brown.edu (I.E.E.); alexis_white@brown.edu (A.W.)

² College of Pharmacy, Graduate School of Pharmaceutical Sciences, Ewha Womans

University, Seoul 03760, Korea

* Correspondence: wooseong_kim@ewha.ac.kr (W.K.); emylonakis@lifespan.org

Abstract

Multidrug-resistant pathogens pose a serious threat to human health. For decades, the antibiotic vancomycin has been a potent option when treating Gram-positive multidrug-resistant infections. Nonetheless, in recent decades, we have begun to see an increase in vancomycin-resistant bacteria. Here, we show that the nuclear factor-kappa B (NF- κ B) inhibitor *N*-[3,5-Bis(trifluoromethyl)phenyl]-5-chloro-2-hydroxybenzamide (IMD0354) was identified as a positive hit through a *Caenorhabditis elegans*–methicillin-resistant *Staphylococcus aureus* (MRSA) infection screen. IMD0354 was a potent bacteriostatic drug capable of working at a minimal inhibitory concentration (MIC) as low as 0.06 μ g/mL against various vancomycin-resistant strains. Interestingly, IMD0354 showed no hemolytic activity at concentrations as high as 16 μ g/mL and is minimally toxic to *C. elegans in vivo* with 90% survival up to 64 μ g/mL. In addition, we demonstrated that IMD0354's mechanism of action at high concentrations is membrane permeabilization. Lastly, we found that IMD0354 is able to inhibit vancomycin-resistant *Staphylococcus aureus* (VRSA) initial cell attachment and biofilm formation at sub-MIC levels and above. Our work highlights that the NF- κ B inhibitor IMD0354 has promising potential as a lead compound and an antimicrobial therapeutic candidate capable of combating multidrug-resistant bacteria.

Keywords: high-throughput screening; vancomycin-resistant *Staphylococcus aureus*; vancomycin-resistant enterococci; IMD0354

Introduction

Methicillin-resistant *Staphylococcus aureus* (MRSA) is a Gram-positive pathogen that can cause skin abscess, bloodstream infections, and pneumonia [1,2]. Infections associated with MRSA are among the leading hospital-acquired infections [3]. They are associated with high mortality and increased hospital stays that result in a higher cost burden [3].

Vancomycin is a glycopeptide able to inhibit cell wall synthesis by binding to the ends of D-Ala-D-Ala moieties of un-crosslinked Lipid II molecules [4]. Vancomycin is an antibiotic effective at treating Gram-positive multidrug-resistant pathogens, including MRSA [4,5]. However, strains such as vancomycin-intermediate *Staphylococcus aureus* (VISA, minimal inhibitory concentration (MIC) = 4–8 µg/mL), vancomycin-resistant *Staphylococcus aureus* (VRSA, MIC ≥ 16 µg/mL), as well as vancomycin-resistant enterococci (VRE) have emerged [5–9].

During normal cell wall synthesis, penicillin-binding proteins (PBPs) are able to attach to terminal D-Ala-D-Ala moieties of un-crosslinked Lipid II and link them. Vancomycin is able to bind them and thus block PBPs' attachment and crosslinking. This eventually leads to osmotic stress and bursting of the cell wall making vancomycin a potent bactericidal antibiotic [4].

Initially, it had been thought that resistance to vancomycin would be minimal given that it does not target enzymatic cell processes [4]. However, we now understand that vancomycin resistance is achieved by a group of genes encoding various enzymes and regulatory proteins that alter the original structure of Gram-positive bacterial walls [4,10,11]. These groups of genes are usually referred to as resistance cassettes. For

vancomycin, the originally discovered cassette was named the “VanA”-type cassette, which is composed of the *vanHAX* cluster encoding enzymes and the *vanR* and *vanS* genes that work as a two-component regulation system [12]. Numerous other resistance cassettes to vancomycin have been discovered and described, each of which includes VanA homologs [4]. These resistance cassettes encode genes that facilitate the conversion of D-Ala to D-Lac. In addition, other cassettes exist that help replace D-Ala with D-Ser [13].

Regardless of the change in the amino acid, the basic mechanism of resistance stays the same. By altering the original composition of the Gram-positive Lipid II amino acids D-Ala-D-Ala, vancomycin is no longer able to attach to the end of these glycopeptides and thus is unable to inhibit cell wall synthesis, creating bacteria mildly susceptible or resistant to vancomycin [4]. Given this threat, vancomycin resistance in Gram-positive bacteria poses a great risk to health care systems worldwide. As a last resort, antibiotics such as linezolid and daptomycin are clinically in use [14–16]. However, resistance to both drugs has become more prevalent throughout the decades [14,17,18]. Therefore, the development of new antibiotics to combat these drug-resistant bacteria is necessary and in dire need.

We screened ~82,000 small molecules to identify anti-infective agents that block *Caenorhabditis elegans* from a MRSA infection [19]. We identified several compounds, for which biological activities have been previously determined [20], including the selective retinoic acid receptor γ (RAR γ) agonist CD437 and CD1530 [19], the selective peroxisome proliferator-activated receptor γ (PPAR γ)-agonist nTZDpa [21], the anti-parasite drug bithionol [22], and insulin-like growth factor receptor inhibitor PQ401 [23].

Each show promising antimicrobial potency against multidrug-resistant Gram-positive pathogens and their persister cells. Considering that many hit compounds are excluded for further investigation due to their *in vivo* inactivity and toxicity, previously studied bioactive compounds have a high potential to become lead compounds because their *in vivo* efficacy and *in vivo* toxicity have been previously tested in several animal models [21–23]. Therefore, we have systematically further investigated a series of bioactive compound hits.

In this study, we explore the bioactive compound hit *N*-[3,5-Bis(trifluoromethyl)phenyl]-5-chloro-2-hydroxybenzamide (IMD0354), previously described as an inhibitor of nuclear factor-kappa B (NF- κ B) that works by directly blocking I κ B phosphorylation [24]. IMD0354 is known to have multiple biological activities. For instance, it has shown anti-cancer properties by directly inhibiting cell invasion and viability as well as acting as an adjuvant with other chemotherapy drugs without showing detectable toxicity [25–27]. In addition, it has also shown anti-inflammatory properties by blocking NF- κ B and subsequent cytokine production [24,28]. Recently, it has been shown that IMD0354 potentiates colistin antimicrobial activity against colistin-resistant *Acinetobacter baumannii* [29]. However, IMD0354 has not been previously reported to have direct antimicrobial activity against Gram positive pathogens. Here, we report for the first time that IMD0354 is notably potent against the Gram-positive multidrug-resistant bacteria VRSA and VRE. We report that IMD0354 inhibits initial VRSA cell attachment and biofilm formation and is able to induce rapid membrane permeabilization at concentrations ≥ 4 μ g/mL. Furthermore, we demonstrate that IMD0354's antimicrobial activity is more potent than its anti-cancer activity.

Results

IMD0354 Exhibits Anti-Staphylococcal Activity In Vitro & in a Whole Animal C. elegans Infection Model

In a previous high-throughput screen study [19] we identified the NF- κ B inhibitor IMD0354 (Figure 1a) as a hit compound. Here we show our screen data that illustrates Bay 11-7085s ability to inhibit MRSA strain MW2 from killing *C. elegans* at 7.14 μ g/mL (Figure 1b). Upon further evaluation, we determined the protection mechanism by which IMD0354 functioned was direct antimicrobial activity against MRSA MW2 with an MIC of 0.06 μ g/mL. Although IMD0354 has been known to have multiple bioactivities, such as anti-cancer, anti-inflammatory, and anti-viral activity [25–27], its direct antimicrobial activity has not been reported. Therefore, we focused on evaluating the potential of repurposing IMD0354 as an antimicrobial agent.

IMD0354 Shows Antimicrobial Activity against Multidrug-Resistant Gram-Positive Pathogens

First, we tested the antimicrobial activity of IMD0354 against ESKAPE pathogens that often cause nosocomial infections and acquire antibiotic resistance [30,31]. ESKAPE pathogens consist of two Gram-positive bacteria, *Enterococcus faecium* and *S. aureus*, and four Gram-negative bacteria, *Klebsiella pneumoniae*, *A. baumannii*, *Pseudomonas aeruginosa*, and *Enterobacter* species [30,31]. IMD0354 displayed antimicrobial potency against *E. faecium* E004 with a MIC of 0.125 μ g/mL. In addition to *S. aureus* and *E. faecium*, IMD0354 exhibited significant antimicrobial activity against another Gram-

positive bacterium, *Enterococcus faecalis* MMH 594, with a MIC of 0.25 µg/mL. Next, we assessed its antimicrobial potency against the four Gram-negative pathogens. A previous study with IMD0354 against *A. baumannii* showed that IMD0354 can work as a potent adjuvant, enhancing the antimicrobial potency of colistin, while having no or minimal antimicrobial activity on its own [29]. In our hands, IMD0354 showed low antimicrobial activity against *A. baumannii* strain ATCC 17978 with an MIC of 16 µg/mL (Table 1). However, it was not potent against *P. aeruginosa* PA14, *K. pneumoniae* WGLW2, and *E. aerogenes* EAE 2625 (Table 1). Taken together these findings suggest that IMD0354 is effective against Gram-positive bacteria, whereas, in the absence of another agent such as colistin, it demonstrates limited antimicrobial activity against Gram-negative bacteria.

Next, we assessed the antimicrobial potency of IMD0354 against a panel of vancomycin-intermediate or -resistant strains, including the vancomycin-resistant strain VRS1 [32], 14 VISA clinical isolates acquired from the center for disease control and prevention (CDC) [33], and five VRE strains [33–36]. We found that the MIC ranged from 0.06 to 0.25 µg/mL for all vancomycin-resistant and vancomycin-intermediate *Staphylococcal* isolates (Table 2) and 0.25 µg/mL for all VRE strains (Table 3). Considering that the MICs of last-resort antibiotics, such as daptomycin and linezolid, are 1–2 µg/mL against VRSA and VRE [19,34], our results indicate that IMD0354 is a far more potent agent against these multidrug-resistant pathogens.

We then evaluated whether IMD0354 is bacteriostatic or bactericidal and found that IMD0354 is bacteriostatic to eight VISA strains (MBC/MIC ratio > 4) and bactericidal (MBC/MIC ratio ≤ 4) to six VISA strains (Table 2). Additionally, IMD0354 is bacteriostatic to the VRSA strain, VRS1, and all VRE strains tested (Tables 2 and 3). These results

were further confirmed by time-course killing kinetics of VRS1 cells treated with IMD0354 at 0.125 µg/mL (2x MIC), 0.5 µg/mL (8x MIC), 1 µg/mL (16x MIC), and 2 µg/mL (32x MIC) for up to 24 h (Figure 2). We found that IMD0354 was able to reduce colony forming units per mL (CFU/mL) of a mid-log phase culture (10^6 CFU/mL) by approximately 1 log after 24 h at a level of 8x to 16x MIC and up to 1.5 log at 32x MIC (Figure 2). However, vancomycin alone did not inhibit the bacterial growth of VRS1 [32] even at high concentrations as high as 512 µg/mL (Figure 2).

Cytotoxicity of IMD0354 on Human Cells and C. elegans

IMD0354 has been used in *in vitro* and *in vivo* studies as a potent NF-κB inhibitor and potential anti-cancer agent both dependent and independent of NF-κB inhibition [24–27]. We assessed the inhibitory activity of IMD0354 against the human liver hepatocellular carcinoma cell line (HepG2) and human kidney proximal tubular cell line (HKC-8) [39]. Consistent with previous studies, our results showed that IMD0354 has a median lethal concentration (LC_{50}) of 1.1 µg/mL and 0.94 µg/mL, respectively. Noteworthy, IMD0354's LC_{50} against cancer cells is approximately 16 times higher than its MIC to VRS1 (Figure 3). Additionally, it has been reported that IMD0354 does not exhibit detectable toxicity while showing significant efficacy in murine cancer models at concentrations as high as 30 mg/kg [26]. Consistent with this report, we found that IMD0354 did not affect *C. elegans* lifespan up to 2 µg/mL and even at 64 µg/mL, 90% worm survival was observed (Figure 4). Lastly, IMD0354 did not cause human red blood cell hemolysis up to 16 µg/mL (Figure 5). These results indicate that IMD0534 has a higher therapeutic index when used as an antimicrobial compared to when it is used as an anti-cancer agent.

IMD0354 Causes Bacterial Membrane Permeability at High Concentrations

Next, we tested whether IMD0354 affects bacterial membrane permeability using a membrane-impermeable DNA binding dye, SYTOX Green [40]. IMD0354 was not able to induce an increase in fluorescence up to 2 µg/mL. However, the VRS1 cells treated with 4 µg/mL or more IMD0354 exhibited a rapid increase in SYTOX Green fluorescence, indicating that IMD0354 is able to permeabilize VRS1 membrane at high concentration (≥ 4 µg/mL). Together with the time-killing data (Figure 2), we conclude that, at high concentrations, IMD0354 kills bacteria by disrupting the bacterial membrane integrity (Figure 6). In contrast, at low concentrations, IMD0354 inhibits VRS1 growth rather than killing VRS1 and does not induce detectable membrane permeabilization. These results demonstrate that IMD0354 may have multiple antimicrobial mechanisms of action, possibly dependent on its concentration levels.

IMD0354 Inhibits Initial Cell Attachment in a Dose-Dependent Manner and Fully Inhibits Biofilm Formation

Biofilms are resistant to antibiotic treatment and are responsible for various chronic and recalcitrant infections [41]. Cell attachment is the first stage of biofilm formation and targeting attachment is one of the principal strategies of biofilm management [42,43]. Therefore, it is clinically relevant to identify agents that inhibit biofilms during this critical step of initiation. There are already methods used to inhibit biofilm formation such as host-derived glycoproteinaceous film coating of medical implants and devices [44]. Likewise, molecular compounds such as aryl rhodanines or calcium chelators have exhibited some success at inhibiting biofilm initial cell attachment [43]. To test the inhibitory activity of IMD0354 on cell attachment, we incubated a high density of VRSA strain VRS1 cells (~

8×10^7 CFU/mL) with various concentrations of IMD0354 (Figure 7) for 1 h and measured cell attachment to polystyrene tissue culture-treated 96-well flat-bottom microplates, using XTT (2–3-bis(2-methoxy-4-nitro-5-sulfophenyl)-2H-tetrazolium-5-carboxanilide) fluorescent dye. We found that IMD0354 is indeed able to block the attachment of VRS1 cells to the plastic 96-well assay plate in a dose-dependent manner with a greater than 60% inhibition at 4x MIC (0.25 $\mu\text{g/mL}$, ($p = 0.0059$) (Figure 7a). Furthermore, we argue that the reduction in initial cell attachment is not due to antimicrobial activity given that we show that IMD0354 does not reduce cell viability after 1 h of incubation (Figure 2). To support these findings, we tested whether IMD0354 inhibits mature biofilm formation at concentrations which showed reduced initial cell attachment. As expected, we found that IMD0354 can completely inhibit biofilm formation beginning at a MIC concentration of 0.06 $\mu\text{g/mL}$ ($p = 0.0005$) with >50% inhibition at a sub-MIC concentration of 0.0313 $\mu\text{g/mL}$ ($p = 0.0077$). However, given that IMD0354 was unable to fully inhibit cell attachment but was still able to disrupt biofilm formation, we speculate that the inhibition of initial cell attachment is not the sole mechanism by which IMD0354 can hinder biofilm formation. Our working hypothesis is that the effect IMD0354 has on biofilm formation is due to the combined activity that the compound has on bacterial growth and its ability to impede initial cell attachment. Furthermore, IMD0354 is unable to eradicate fully mature biofilm once established (data not shown).

IMD0354 does not Affect the Viability of Antibiotic-Tolerant Cells or Synergize with Conventional Antibiotics

Membrane-active antimicrobial agents have been shown to exhibit antimicrobial potency against non-growing dormant antibiotic-tolerant bacteria and synergism with

other antibiotics [45]. Thus, we assessed whether IMD0354 is potent against antibiotic-tolerant *S. aureus* VRS1 and acts synergistically with conventional antibiotics. In this series of experiments, we isolated antibiotic-tolerant VRS1 cells as previously described [46] and treated them with various concentrations of IMD0354 for 4 h. IMD0354 did not kill antibiotic-tolerant cells even at concentrations as high as 4 µg/mL (64× MIC) (Supplementary Figure S1). Next, we determined whether IMD0354 worked synergistically with other antibiotics against *S. aureus* VRS1. We performed various checkerboard assays, testing vancomycin, gentamicin, ciprofloxacin, and daptomycin in conjunction with IMD0354. Unlike in the case of Gram-negative bacteria [29], we did not find any synergy or antagonism between any antibiotics tested, only additive or indifference effects (data not shown).

Discussion

Here, we report the finding that the kinase inhibitor IMD0354 is able to prolong the life of *C. elegans* during a lethal MRSA infection [19]. We show that IMD0354 inhibits MRSA growth at MIC levels as low as 0.06 $\mu\text{g}/\text{mL}$ and can inhibit growth of other multidrug-resistant Gram-positive bacteria including VRSA, VISA, and VRE. At high concentrations, IMD0354 permeabilizes Gram-positive bacterial membranes at concentrations $\geq 4 \mu\text{g}/\text{mL}$ (Figure 6), but permeabilization does not appear to be the primary mode of action at lower concentrations.

In a previous report by Barker et al., IMD0354 was found to have no antimicrobial activity on its own against Gram-negative bacteria, which is consistent with our antimicrobial susceptibility tests on Gram-negative ESKAPE pathogens (Table 1). Barker et al. demonstrated that IMD0354 enhances the potency of colistin by reversing the colistin-mediated modification of lipid A by colistin-resistant bacteria [29]. However, there is not any obvious similarity between the Gram-negative and Gram-positive modes of action of IMD0354 given that Gram-positive bacteria do not produce lipid A [47]. This may explain why we did not find any synergistic effects when we treated VRS1 with IMD0354 in combination with several traditional antibiotics, even those with cell wall- or cell membrane-targeting activity, such as vancomycin or daptomycin.

In addition to its direct antimicrobial activity, we found that IMD0354 inhibited the attachment of bacterial cells to a solid surface, the initial step in biofilm formation, in a dose-dependent manner. IMD0354 also completely inhibited biofilm formation at sub-MIC levels (Figure 7). It is possible that that antibiofilm activity is partially dependent on the antimicrobial activity of IMD0354. However, we find this unlikely given our

experimental design and supporting data. For example, killing kinetic assays showed that IMD0354 has no antibacterial effect at 1 h post drug treatment. In addition, cell attachment assays are carried out using two logs more bacteria than the killing kinetics assays. Therefore, we conclude that the reduction in initial cell attachment is independent of the antimicrobial activity of IMD0354. Biofilms pose a significant threat to public health given their high level of resistance to antibiotic therapy and their ability to form on a variety of medical devices [41,42]. Bacterial attachment to solid surfaces is controlled via various cell wall-anchoring proteins, including microbial surface components recognizing adhesive matrix molecules (MSCRAMMs) [42]. Our working hypothesis is that IMD0354 targets these associated genes or proteins and thus results in a decrease in biofilm attachment.

Another interesting finding from these studies is that IMD0354 is a more potent antimicrobial than a cell toxicity agent. Previous studies have shown that IMD0354 exhibits anti-cancer activity by inhibiting cell invasion, viability, as well as acting as an adjuvant with other chemotherapy drugs [25–27]. Our studies show that the average LC₅₀ of IMD0354 toward two cancer cell lines is 1.04 µg/mL, approximately 17× greater than its MIC of 0.06 µg/mL against VRS1. IMD0354 is known to selectively suppress the proliferation of cancer cells over normal cells [48]. For instance, in contrast to its effects on neoplastic mast cells, it did not affect the proliferation of normal human mast cells at 1 µM (0.4 µg/mL) [48]. Furthermore, various groups have used IMD0354 in murine *in vivo* models at doses ranging from 1 mg/kg up to 30 mg/kg over several weeks and have reported no detectable toxicity [24,26]. These previous *in vitro* and *in vivo* results demonstrate that IMD0354 is relatively non-toxic to normal cells. Consistently, we

observed the cytotoxic effect of IMD0354 on cancer cells at 1 $\mu\text{g}/\text{mL}$ (Figure 3), while it did not cause cytotoxicity to *C. elegans* at $\sim 7 \mu\text{g}/\text{mL}$ (Figure 1b). It is important to note that the MIC of IMD0354 against the VRSA strain VRS1 is 0.06 $\mu\text{g}/\text{mL}$ (Table 2), which is about one order of magnitude lower than its effective concentration on cancer cell lines. Given these findings, we propose that IMD0354 has greater promise in terms of being repurposed as an antimicrobial rather than it did as an anti-cancer agent.

The antibacterial activity of other anti-cancer drugs, such as mitomycin C and cisplatin, has been validated and these drugs have been proposed as antimicrobial candidates against multidrug-resistant bacteria [49,50]. For instance, mitomycin C demonstrates an LC_{50} of 27 μM (9.03 $\mu\text{g}/\text{mL}$) against HepG2 cancer cells and a MIC ranging between 0.2–15 $\mu\text{g}/\text{mL}$ to multiple Gram-negative and Gram-positive bacteria [49]. Alternatively, cisplatin shows an IC_{50} of 2 $\mu\text{g}/\text{mL}$ against HepG2 cancer cells and a MIC > 50 $\mu\text{g}/\text{mL}$ for both Gram-positive and Gram-negative bacteria [50,51]. Nonetheless, low-dose administration of cisplatin to septic mice improved bacterial clearance [52]. From these reports studies, we conclude other anti-cancer agents exhibit antimicrobial activity at concentrations similar to or greater than their anti-cancer activity. In contrast, IMD0354 has an LC_{50} of 1.1 $\mu\text{g}/\text{mL}$ to HepG2 cells and a MIC of 0.06 $\mu\text{g}/\text{mL}$ against VRS1.

Interestingly, the antimicrobial and anti-cancer mechanism of action (MOA) of mitomycin C and cisplatin appear to be similar as both compounds cross-link both mammalian and bacterial cell DNA, thus leading to cell death [49,50]. On the other hand, the anti-cancer MOA of IMD0354 has been shown to be both NF- κB dependent and independent [24–27]. Given that bacteria have no NF- κB it is reasonable to assume that

the antibacterial MOA of IMD0354 is different from its anti-cancer NF- κ B dependent activity. Importantly, this information allows us to speculate that IMD0354 could be a promising lead compound that can be structurally optimized to abate or nullify anti-cancer activity or toxicity to mammalian cells while retaining its antimicrobial properties.

In addition to anti-cancer activity, IMD0354 has other bioactivities. Onai et al. and Sugita et al. used IMD0354 to directly inhibit NF- κ B, thereby decreasing inflammation [24,28]. These *in vitro* studies showed that IMD0354 can significantly inhibit cytokine production at 1 μ M (0.4 μ g/mL) [24], nearly six times more than IMD0354's MIC (0.06 μ g/mL). Furthermore, *in vivo* data from Onai et al. showed a significant reduction in inflammation in a rat myocardial ischemia/reperfusion injury model after treatment with 5 or 10 but not 1 mg/kg IMD0354. We therefore suggest that there is therapeutic index at low concentration in which IMD0354 can be administered as an antibiotic with low cross-activation of other bioactivities.

Overall, the continued evolution of antibiotic resistance to last-resort therapeutics such as vancomycin persist as a primary threat. The *C. elegans*-M^RSA high-throughput screening system has become an invaluable tool in drug discovery research as exemplified by its ability to identify kinase inhibitors such as IMD0354 that might otherwise be neglected as potential hits due to their toxicity. Moving forward, we think that it is important to identify the specific bacterial target or targets of IMD0354 in addition to the cell envelope. Further research into analogs would be beneficial in advancing our understanding of the mechanism of action of kinase inhibitors, which can identify new antimicrobial targets against multidrug-resistant bacteria. In addition, experiments testing the efficacy of IMD0354 as an antimicrobial in a murine *in vivo* model would be insightful.

Given IMD0354's low MIC, we speculate that there may be a clinically relevant dose that is non-toxic and does not induce significant NF- κ B inhibition, but is still able to inhibit bacterial growth. However, at this time, these experiments fall outside the focus of our study.

Conclusion

In conclusion, we report that, at relatively low concentrations ($\leq 2 \mu\text{g/mL}$), IMD0354 can act either as a bactericidal or a bacteriostatic agent against VISA, VRSA, and VRE strains, depending on the strains, while, at high concentrations ($\geq 8 \mu\text{g/mL}$), IMD0354 demonstrates bactericidal activity. IMD0354 does not show any hemolytic activity at concentrations up to $16 \mu\text{g/mL}$ and shows no toxicity to *C. elegans* up to $2 \mu\text{g/mL}$ and 90% worm survival at $> 64 \mu\text{g/mL}$. Our data reveal that the antimicrobial mechanism of IMD0354 at high concentrations $\geq 4 \mu\text{g/mL}$ is membrane permeabilization. However, we are still unclear what the MOA is at low concentrations. Importantly, we find that IMD0354 is a more potent antimicrobial than anti-cancer agent. Moving forward, we believe that the further development of this compound is important. Nonetheless, further research to develop this multi-bioactive compound will require distinguishing the structural relationship between NF- κ B inhibition, anti-cancer, and antimicrobial effects in order to overcome toxicity and cross-reaction side effects.

Materials and Methods

Bacterial Strains and Growth Conditions

All strains used for these studies are listed in Table 4. All VISA and VRSA strains were grown overnight in tryptic soy broth (TSB) at 37 °C, with shaking at 180–225 rpm. All *Enterococcal* strains were grown overnight in Brain Heart Infusion broth (BHI) at 37 °C, with shaking at 180–225 rpm.

Drugs and Antibiotics

IMD0354 (Tocris 2611), gentamicin, daptomycin, and vancomycin (Sigma Aldrich) stocks were dissolved to 10 mg/mL in DMSO. Ciprofloxacin (Sigma Aldrich) was dissolved to 10 mg/mL in 0.1 N HCl.

Minimum Inhibitory Concentration Assay

Minimum Inhibitory Concentration assays were carried out as described by the Clinical and Laboratory Standard Institute [53]. In brief, bacterial strains grown overnight in appropriate media for 20–23 h were diluted to 1×10^6 CFU/mL in Mueller–Hinton Broth (MHB, BD Difco, pH: 7.3 ± 0.1). In a 96-well plate 50 μ L of diluted culture was added to 50 μ L of serial two-fold diluted drug in MHB to a final concentration of 5×10^5 CFU/mL. All assays were performed in triplicate. Experimental plates were incubated for 20–22 h at 37 °C. Optical density at 600 nm (OD_{600}) was measured using a spectrophotometer (SpectraMax M2, Molecular Devices) as a measure of bacterial growth. MIC was defined as $OD_{600} \leq 0.1$ after background subtraction.

C. elegans Infection Assay for Compound Screening

All compounds were screened as previously described in Kim et al. 2018 [19]. In brief, *glp-4(bn2);sek-1(km4)* worm embryos were synchronized by plating 2000 L1 worms on SK agar plates with HB101 bacteria as a food source at 15 °C for four days until they reached gravid adult stage. Eggs were harvested and hatched in M9 buffer at 15 °C for 48 h. L1 stage worms were then transferred onto SKHB101 plates and incubated at 25 °C for 52 h to induce sterility. Sterile young adult stage worms were harvested using M9 buffer and sorted into black, clear-bottom, 384-well plates (Corning no. 3712) containing compounds at 15 worms/well using Copa Biosort Instrument. *S. aureus* MW2 bacteria was grown overnight in TSB at 37 °C with agitation. A static culture was inoculated by seeding 100 µL of an overnight culture in 10 mL of fresh TSB, sealed to produce anaerobic conditions, and incubated at 37 °C overnight without agitation. We have found that MW2 grown anaerobically elicits a greater infection mortality rate in *C. elegans*. Furthermore, anaerobically grown MRSA MW2 cells express different virulence gene patterns [54]. Static MW2 was added to *C. elegans*-compound 384-well plates at a final concentration of OD₆₀₀ 0.04. Final well composition consisted of 70% M9 buffer, 19% Sheath solution (Union Biometrica Part no. 300-5101-000), 10% TSB, and 1% DMSO or compounds dissolved in DMSO. After a 5-day incubation at 25 °C worms were washed using a multiplate washer and incubated overnight at 37 °C with Sytox Orange dissolved in M9 at a final concentration of 0.7 µM. The following day, all plates were imaged using an Image Xpress Micro automated microscope (Molecular Devices), capturing both transmitted light and TRITC (535 nm excitation, 610 nm emission) fluorescent images using a 2x objective.

C. elegans dose-Dependent Toxicity Assay

In a black, clear-bottom, 96-well plate (Corning, no. 3690, Corning, NY, USA) IMD0354 was serially diluted to a final volume of 50 μ L using M9. N2 worms were sterilized by growing to the young adult stage fed on *E. coli* expressing *cdc 25.1* activated by 1 mM of IPTG [55] for 48 h at 25 °C. *cdc25.1* is an integral part of germ cell mitosis. Knock down of *cdc25.1* inhibits germ line cell division producing *C. elegans* incapable of laying eggs [56]. Young adult worms were washed 3 times with 50 mL of M9 and diluted to an average of 21 worms \pm 7 /25 μ L using a multichannel pipette. An additional 25 μ L of heat killed *E. coli* OP50 were added to each well to a make a final volume of 100 μ L and OD₆₀₀ of 0.5. All assays were performed in duplicate. Experimental plates were incubated for 24 h at 25 °C. Worms were then washed using a 405 LS microplate washer (BioTek) and incubated with 0.7 μ M SYTOX Orange for an additional 24 h at 25 °C. Each plate was then imaged using an Xpress Micro automated microscope (Molecular Devices) capturing both transmitted light and TRITC (535 nm excitation, 610 nm emission) fluorescent images using a 2X objective. Surviving worms were considered those with no TRITC signal relative to the control.

Bacterial Time-Course Killing Assay

Strain VRS1 [32], grown overnight in TSB medium for 20–23 h, was diluted 1:1000 (1×10^6 CFU/mL) in MHB (BD Difco, pH 7.3 \pm 0.1) in a deep 96-well plate. 250 μ L of diluted culture was added to 250 μ L of serial two-fold diluted drug in MHB to a final concentration of 5×10^5 CFU/mL. At time 0, 1 h, 2 h, 3 h, 4 h, and 24 h, 50- μ L samples were removed, serially diluted by 10-fold steps, and spot-plated on MHB agar (BD Difco) plates to

enumerate the number CFU/mL. These experiments were conducted in triplicate. Experimental plates were incubated for 20–22 h at 37 °C.

Human Blood Hemolysis

Hemolytic activity of IMD0354 on human erythrocytes was evaluated using a previously described method with modifications [57]. 10% human erythrocytes were purchased from Rockland Immunochemicals (Limerick, PA, USA). The erythrocytes were diluted to 4% with phosphate buffered saline (PBS), and 50 μ L was added to 50 μ L of two-fold serial dilutions of compounds in PBS, 0.2% DMSO (negative control), or 1% Triton-X 100 (positive control) in a 96-well plate. The plate was incubated at room temperature for 1 h and then centrifuged at 500 \times g for 5 min. 50 μ L of the supernatant was transferred to a fresh 96-well plate and absorbance of supernatants was measured at 540 nm. Percent hemolysis was calculated using the following equation: $(A_{540\text{nm}} \text{ of compound treated sample} - A_{540\text{nm}} \text{ of 0.1\% DMSO treated sample}) / (A_{540\text{nm}} \text{ of 1\% Triton X-100 treated sample} - A_{540\text{nm}} \text{ of 0.1\% DMSO treated sample}) \times 100$. These experiments were conducted in triplicate.

Antibiotic-Tolerant Cell Killing

S. aureus VRS1 [32] antibiotic-tolerant cells were acquired by growing liquid cultures >18 h to stationary-phase at 37 °C in 25 mL of TSB [46]. Stationary-phase VRS1 cell tolerance to various antibiotics was previously proven by Kim et al. 2018 [46]. In brief, overnight cultures were washed three times with PBS (pH: 7.4) and diluted to a final concentration of 1.0×10^6 CFU/mL. 500 μ L of washed cells were added to 500 μ L of indicated concentrations of drug in 2 mL deep-dish 96-well plates and incubated at 37 °C

with agitation for 1, 2, 3, and 4 h. In order to wash any residual drug from sample time points, 400 μ L of sample was collected every hour and centrifuged at 15,000 rpm for 3 min and suspended with 400 μ L of fresh PBS. 100 μ L of washed samples were serially diluted and spot-plated on MHB agar plates to measure antibiotic-tolerant cell CFU/mL. These experiments were conducted in triplicate.

SYTOX Green Membrane Permeability Assay

These studies were conducted as previously described in Kim et al. 2018 [19]. In brief, black, clear-bottom, 96-well plates (Corning no. 3904, Corning, NY, USA) were filled with 50 μ L of PBS (pH: 7.4) containing 2 \times the indicated concentration of antibiotics. Stationary-phase VRS1 cells prepared as described in the antibiotic-tolerant cell killing assay were washed 3 times with equal volumes of PBS. Washed cells were then adjusted to OD₆₀₀ 0.4 ($\sim 2 \times 10^7$ CFU/mL) with PBS. SYTOX Green (Molecular Probes, Waltham, MA, USA) was added to 10 mL of the diluted bacterial suspension to a final concentration of 5 μ M and incubated for 30 min at room temperature in the dark. 50 μ L of the bacteria/SYTOX Green mixture was added to each well of the 96-well plates containing antibiotics. Fluorescence was measured at room temperature using a spectrophotometer (SpectraMax M2, Molecular Devices, Sunnyvale, CA, USA), with excitation and emission wavelengths of 485 nm and 525 nm, respectively. All experiments were conducted in triplicate.

Cell Attachment Assay

S. aureus strain VRS1 [32] was grown overnight (> 18 h) in BHI (Sigma, pH: 7.4 \pm 0.2). Absorbance at OD₆₀₀ was measured and adjusted to 0.2 in BHI + 0.1% glucose

medium. 100 μ L of bacteria was added to 2 \times drug concentrations being tested dispensed in polystyrene tissue culture-treated 96-well flat-bottom microplates (Corning no. 353072, Corning, NY, USA) producing a final volume of 200 μ L, OD₆₀₀ of 0.1 ($\sim 8 \times 10^7$ CFU/mL) and 1 \times drug concentration. The plates were then incubated at 37 °C for 1 h. Media were then pipetted out and the wells were washed 3 times with PBS to remove any non-adherent planktonic cells. Biofilm initial cell attachment was measured as described in Biswajit et al. 2016 [58]. In brief, colorimetric quantification of the inhibition of biofilm initial cell attachment was done using XTT [2–3-bis(2-methoxy-4-nitro-5-sulfophenyl)-2H-tertazolium-5-carboxanilide] assay kit following manufacture instructions with minor adjustments (Sigma-Aldrich, MO, USA). 180 μ L of fresh TSB and 20 μ L of XTT solution were added to each well and the plates were again incubated for 2 h at 37 °C. Absorbance at 450 nm was measured and each experimental well was normalized to a non-treatment control. Each biological replicate was done in quadruplicates. One replicate was done in octuplet.

Biofilm Inhibition Assay

S. aureus VRS1 [32] was grown overnight (>18 h) in BHI (Sigma, pH: 7.4 \pm 0.2). Absorbance at OD₆₀₀ was measured and adjusted to 0.1 in BHI + 0.1% glucose medium. 100 μ L of bacteria was added to 2 \times drug concentrations being tested on polystyrene tissue culture-treated 96-well flat-bottom microplates (Corning no. 353072, Corning, NY, USA) producing a final volume of 200 μ L, OD₆₀₀ of 0.05 ($\sim 4 \times 10^7$ CFU/mL) and 1 \times drug concentration. The plates were then incubated at 37 °C for 24 h. Media were then pipetted out and the wells were washed 3 times with PBS to remove any non-adherent planktonic cells. Biofilm inhibition was measured using crystal violet (CV) [59]. In brief, plates were

incubated with 1% CV for 15 min at room temperature. Plates were then washed 3 times with PBS and dissolved with 200 μ L of 30% acetic acid. Absorbance at 550 nm was measured and each experimental well was normalized to a non-treatment control. Each biological replicate was done in octuplet.

Mammalian Cancer Cell Viability Assay

Two-fold concentration drug plates were prepared using Dulbecco's Modified Eagle's medium (DMEM) with 10% FBS . HepG2 or HKC-8 cells were grown in DMEM 10% FBS to confluency and seeded onto 96-well drug plates at 1.0×10^6 cells/mL and 0.4×10^6 cells/mL, respectively. Drug and cell plate were then incubated for 22 h at 37 °C and 5% CO₂. At 22 h, 10 μ L of WST-1 (Roche, Sigma) was added to each well, following manufacturer's directions, and incubated for an additional 2 h. Plate absorbance was read at 450 nm. Samples were normalized to a non-treatment control. All experiments were conducted in triplicate.

Acknowledgements

This research was funded by NIH grant P01 AI083214 to E.M. W.K. is supported by the National Research Foundation of Korea Grants funded by the Korea government (MSIT) (2020R1C1C1008842, 2018R1A5A2025286 and 2017M3A9E4077234). The authors have no other relevant affiliations or financial involvement with any organization or entity with a financial interest in, or financial conflict with, the subject matter or materials discussed in the manuscript, apart from those disclosed. No writing assistance was utilized in the production of this manuscript.

Author Contributions

Conceptualization, E.M. and W.K; methodology, I.E.E. and A.W; formal analysis, I.E.E.; investigation, I.E.E.; data curation, I.E.E.; writing—original draft preparation, I.E.E.; writing—review and editing, I.E.E., E.M. and W.K.; supervision, E.M. and W.K. All authors have read and agreed to the published version of the manuscript.

Conflicts of Interest

The authors declare no conflict of interest.

Figures and Tables

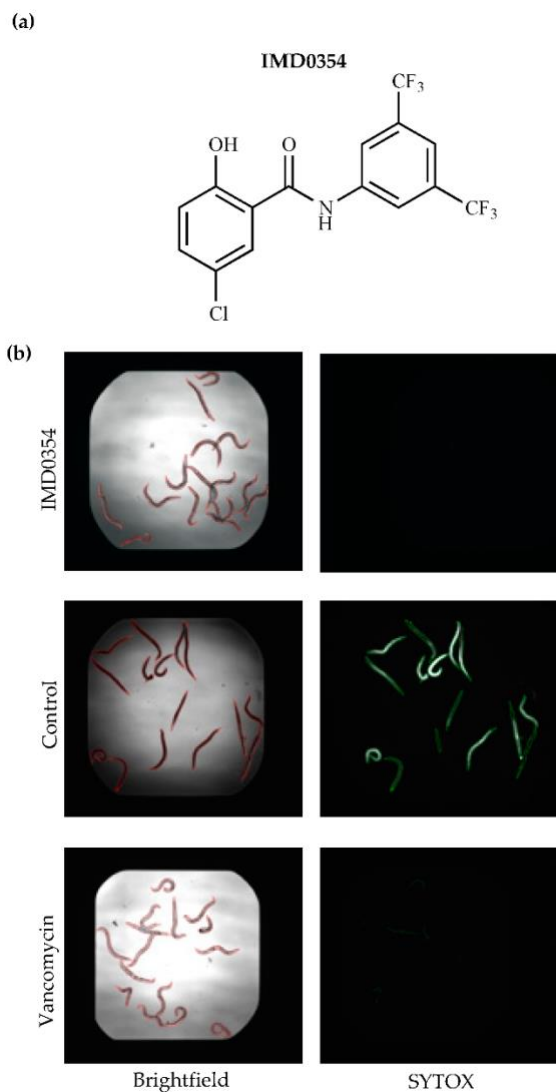


Figure 1. IMD0354 rescues *C. elegans* from MRSA infection.

(a) Chemical structure of IMD0354. (b) Fifteen MRSA-infected *C. elegans* were treated with 7.14 $\mu\text{g}/\text{mL}$ IMD0354, 0.1% dymethyl sulfoxide (DMSO) (control) and 10 $\mu\text{g}/\text{mL}$ vancomycin for 5 days. After staining dead worms with SYTOX Orange, brightfield (left) and fluorescence (right) images were obtained.

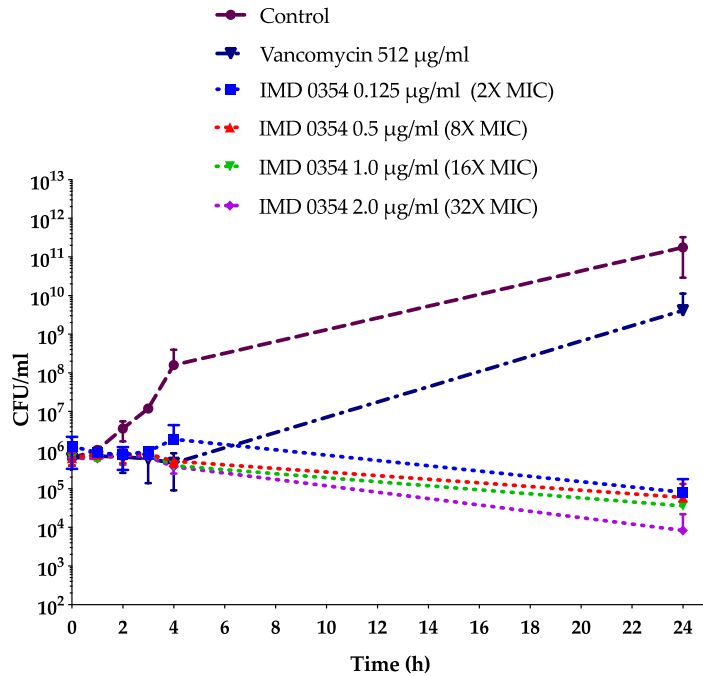


Figure 2. Time-killing curve shows IMD0354 is bacteriostatic against vancomycin-resistant strain VRS1.

In total, 10⁶ CFU/mL of VRS1 overnight culture was treated with various concentrations of vancomycin and IMD0354. At times of 1, 2, 3, 4, and 24 h, samples were collected, serially diluted, and spot-plated in order to enumerate CFU/mL. Each sample was tested in triplicate. ($n = 3, \pm$ S.D.).

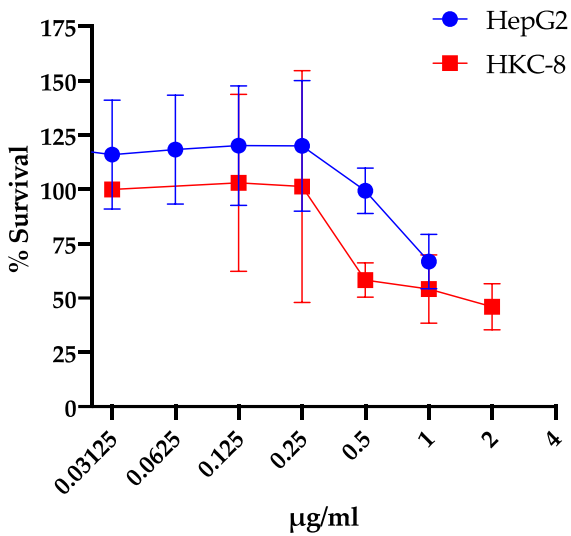


Figure 3. Dose toxicity studies show IMD0354 has cytotoxicity activity above MIC levels.

Cytotoxicity testing of human liver cell line HepG2 and human kidney proximal tubular cell line HKC-8 at various concentrations of IMD0354. LC₅₀ of IMD0354 is 1.1 µg/mL and is 0.94 µg/mL, respectively. Each sample was tested in triplicate. ($n = 3, \pm$ S.D.).

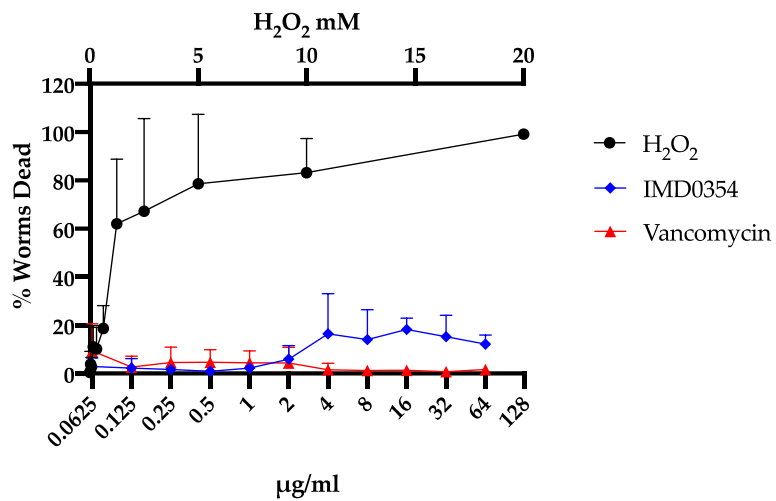


Figure 4. IMD0354 shows minimal toxicity toward *C. elegans*.

Survival of *C. elegans* treated with various concentrations of IMD0354, normalized to *C. elegans* treated with DMSO. H₂O₂ was used as positive control. ($n = 3, \pm$ S.D).

Bottom error bars are omitted for clarity.

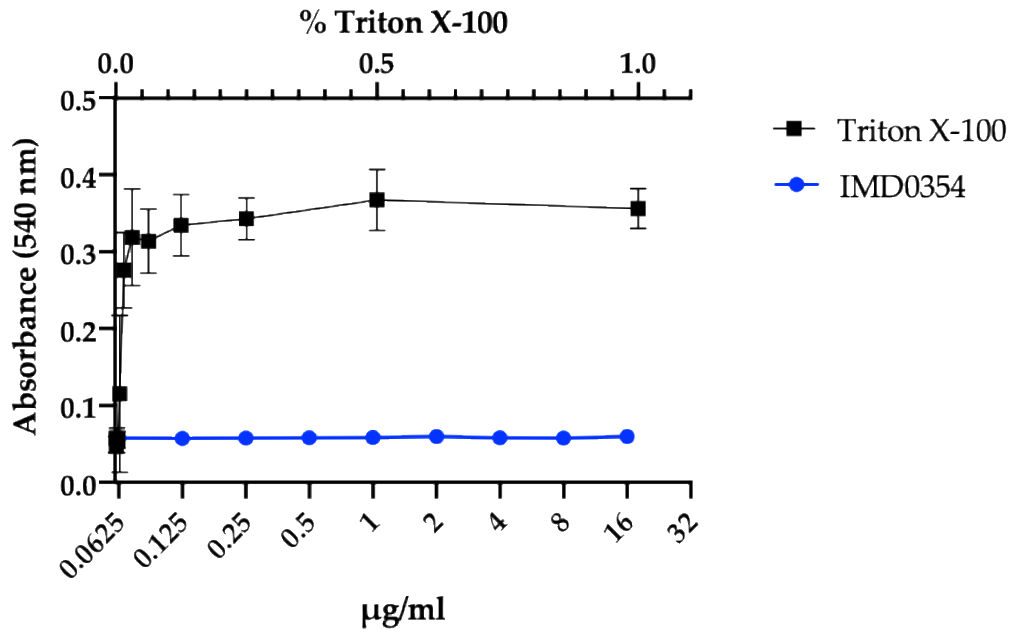


Figure 5. IMD0354 does not show hemolytic activity.

Human red blood cells were incubated with serially diluted IMD0354 (0.0156–16 µg/mL) and normalized to hemolysis of 1% Triton-X 100. Each sample was tested in triplicate ($n = 3, \pm$ S.D).

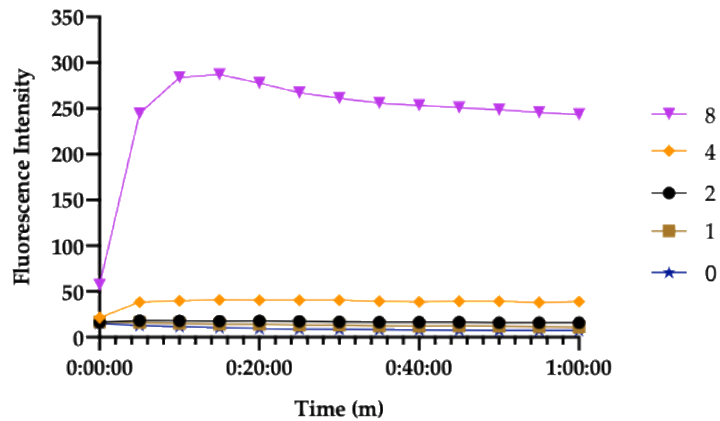


Figure 6. IMD0354 induces membrane permeabilization at high concentrations.

VRS1 membrane permeabilization was measured spectrophotometrically by monitoring the uptake of SYTOX Green (excitation wavelength of 485 nm and an emission wavelength of 525 nm) during treatment with IMD0354 at various concentrations. The legend units are $\mu\text{g/mL}$. Each assay was tested in triplicate. ($n = 3, \pm \text{S.D}$). Error bars are omitted for clarity.

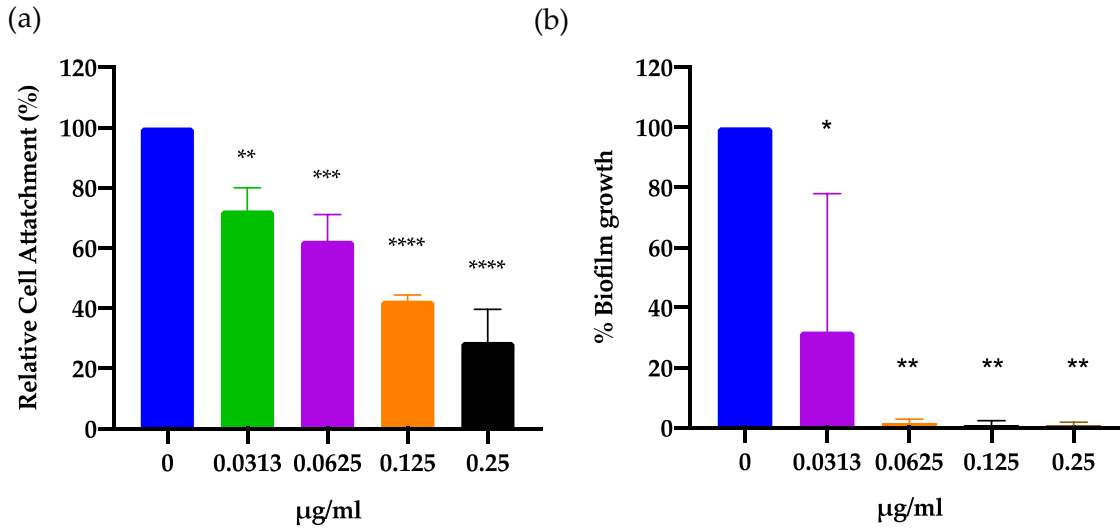


Figure 7. IMD0354 shows dose-dependent inhibition of initial cell attachment and complete inhibition of biofilm formation.

(a) VRS1 cells were incubated in Brain Heart Infusion broth (BHI) 0.5% glucose at an optical density at 600 nm (OD_{600}) of 1.0 for 1 h. Cells were washed three times with phosphate buffered saline (PBS) and then treated with XTT to measure cell attachment. Measurements were normalized to a non-treatment control (0 µg/mL).

(b) VRS1 cells were incubated in BHI 0.5% glucose at an OD_{600} of 0.05 and indicated concentrations of IMD0354 for 24 h. At 24 h biofilm were washed 3 times with PBS. Total biofilm mass was measured using 1% crystal violet . Statistical significance was determined using one-way ANOVA with Sidak's multiple comparisons test. $p < 0.05$; ** $p < 0.01$; *** $p < 0.001$; **** $p < 0.0001$. ($n=3$, \pm S.D.).

Table 1. Minimum inhibitory concentration ($\mu\text{g/mL}$) of IMD0354 to selected ESKAPE pathogens.

Strain	MIC
<i>Pseudomonas aeruginosa</i> PA14	>64
<i>Klebsiella pneumoniae</i> WGLW2	>64
<i>Acinetobacter baumannii</i> ATCC 17978	16
<i>Enterobacter aerogenes</i> EAE 2625	>64
<i>Enterococcus faecalis</i> MMH 594	0.25
<i>Enterococcus faecium</i> E007	0.125

Table 2. Minimum Inhibitory Concentration (MIC) and Minimum Bactericidal Concentration (MBC) ($\mu\text{g/mL}$) of NF- κ B inhibitors IMD0354 against vancomycin-resistant *Staphylococcus aureus* (VISA) and vancomycin-intermediate *Staphylococcus aureus* (VISA) clinical strains.

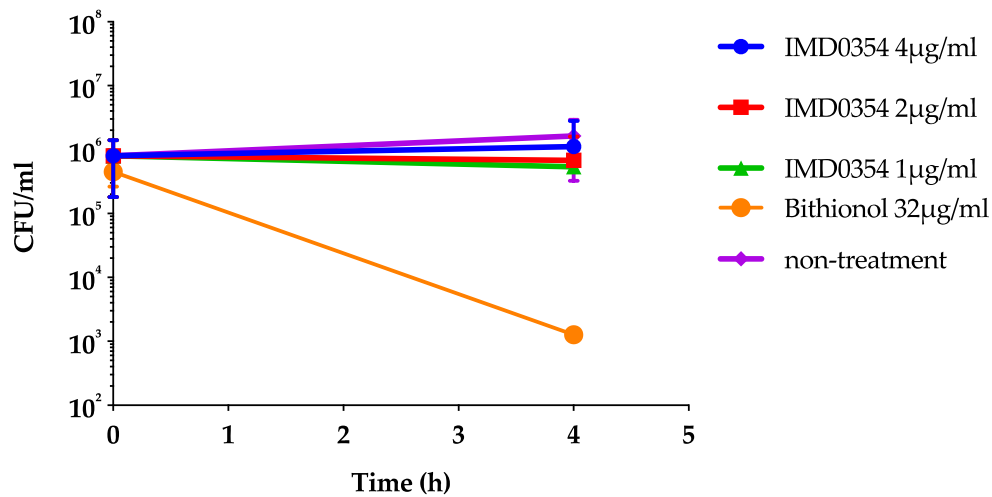
Strain	IMD0354		Vancomycin	
	MIC	MBC	MIC	MBC
VRS1	0.06	2	>64	>64
VISA 215	0.25	0.5	8	8
VISA 216	0.06	2	8	16
VISA 217	0.125	0.5	8	8
VISA 218	0.06	0.5	8	8
VISA 219	0.06	1	8	16
VISA 220	0.25	2.0	8	16
VISA 221	0.06	1.0	8	8
VISA 222	0.125	2.0	8	8
VISA 223	0.125	1.0	4	8
VISA 224	0.25	2	4	16
VISA 225	0.125	0.25	4	8
VISA 226	0.06	0.125	4	4
VISA 227	0.25	0.5	8	8
VISA 228	0.125	0.5	4	8

Table 3. Minimum Inhibitory Concentration (MIC) and Minimum Bactericidal Concentration (MBC) ($\mu\text{g/mL}$) of NF- κ B inhibitors IMD0354 against vancomycin-resistant enterococci (VRE) clinical strains.

Strain	IMD0354		Vancomycin	
	MIC	MBC	MIC	MBC
EM C68 [35]	0.25	8	64	>64
EM D366 [36]	0.25	8	64	>64
EM WB312 [37]	0.25	8	64	>64
EM WC176 [37]	0.25	8	64	>64
EL V583 [38]	0.25	8	64	>64

EM: *Enterococcus faecium*, EL: *Enterococcus faecalis*.

Supplementary Figures and Tables



Supplementary Figure 1. IMD0354 does not kill VRS1 antibiotic-tolerant cells.

An overnight culture of VRS1 was washed twice in PBS. After washing, isolated VRS1 antibiotic-tolerant cells were incubated with 1, 2, or 4µg/ml of IMD0354 for 4 h. Bithionol at 32µg/ml was used as a positive control. At 4 h each sample was additionally washed to remove any excess compound and spot plated on MHB agar plates to enumerate total antibiotic-tolerant cells remaining. Each assay was performed in triplicate. ($n=3$, \pm S.D)

Supplementary Table 1. Fractional Inhibitory Concentration Index of IMD0354 paired in combination with various antibiotics.

	Vancomycin	Gentamicin	Daptomycin	Ciprofloxacin
IMD0354	1	1	1	1

References

1. David, M.Z.; Daum, R.S. Community-Associated Methicillin-Resistant *Staphylococcus aureus*: Epidemiology and Clinical Consequences of an Emerging Epidemic. *Clin. Microbiol. Rev.* **2010**, *23*, 616–687.
2. Lowy, F.D. *Staphylococcus aureus* infections. *N. Engl. J. Med.* **1998**, *339*, 520–532.
3. Lakhundi, S.; Zhang, K. Methicillin-Resistant *Staphylococcus aureus*: Molecular Characterization, Evolution, and Epidemiology. *Clin. Microbiol. Rev.* **2018**, *31*, doi:10.1128/CMR.00020-18.
4. Stogios, P.J.; Savchenko, A. Molecular mechanisms of vancomycin resistance. *Protein Sci.* **2020**, *29*, 654–669.
5. Hiramatsu, K.; Aritaka, N.; Hanaki, H.; Kawasaki, S.; Hosoda, Y.; Hori, S.; Fukuchi, Y.; Kobayashi, I. Dissemination in Japanese hospitals of strains of *Staphylococcus aureus* heterogeneously resistant to vancomycin. *Lancet* **1997**, *350*, 1673–1677.
6. Howe, R.A.; Bowker, K.E.; Walsh, T.R.; Feest, T.G.; MacGowan, A.P. Vancomycin-resistant *Staphylococcus aureus*. *Lancet* **1998**, *351*, 602.
7. Hidayat, L.K.; Hsu, D.I.; Quist, R.; Shriner, K.A.; Wong-Beringer, A. High-dose vancomycin therapy for methicillin-resistant *Staphylococcus aureus* infections: Efficacy and toxicity. *Arch. Intern. Med.* **2006**, *166*, 2006–2144.
8. Leclercq, R.; Derlot, E.; Duval, J.; Courvalin, P. Plasmid-mediated resistance to vancomycin and teicoplanin in *Enterococcus faecium*. *N. Engl. J. Med.* **1988**, *319*, 157–161.
9. Uttley, A.H.; Collins, C.H.; Naidoo, J.; George, R.C. Vancomycin-resistant enterococci. *Lancet* **1988**, *2*, 57–58.
10. Dougherty, T.J.; Pucci, M.J. *Antibiotic Discovery and Development*, Springer Science & Business Media: Boston, MA, USA, 2011.
11. Munita, J.M.; Arias, C.A. Mechanisms of Antibiotic Resistance. *Microbiol. Spectr.* **2016**, *4*, 481–511.
12. Arthur, M.; Molinas, C.; Courvalin, P. The VanS-VanR two-component regulatory system controls synthesis of depsipeptide peptidoglycan precursors in *Enterococcus faecium* BM4147. *J. Bacteriol.* **1992**, *174*, 2582–2591.
13. Meziane-Cherif, D.; Saul, F.A.; Haouz, A.; Courvalin, P. Structural and functional characterization of VanG D-Ala:D-Ser ligase associated with vancomycin resistance in *Enterococcus faecalis*. *J. Biol. Chem.* **2012**, *287*, 37583–37592.
14. Tattevin, P.; Arvieux, C.; Michelet, C. Alternative agents for the treatment of invasive infections due to methicillin-resistant *Staphylococcus aureus* strains with reduced susceptibility to vancomycin. *Arch. Intern. Med.* **2007**, *167*, 1206.
15. Gomes, D.M.; Ward, K.E.; LaPlante, K.L. Clinical implications of vancomycin heteroresistant and intermediately susceptible *Staphylococcus aureus*. *Pharmacotherapy* **2015**, *35*, 424–432.
16. Rybak, M.J.; Hershberger, E.; Moldovan, T.; Grucz, R.G. *In vitro* activities of daptomycin, vancomycin, linezolid, and quinupristin-dalfopristin against *Staphylococci* and Enterococci, including vancomycin-intermediate and -resistant strains. *Antimicrob. Agents Chemother.* **2000**, *44*, 1062–1066.

17. Chen, C.-J.; Huang, Y.-C.; Shie, S.-S. Evolution of Multi-Resistance to Vancomycin, Daptomycin, and Linezolid in Methicillin-Resistant *Staphylococcus aureus* Causing Persistent Bacteremia. *Front. Microbiol.* **2020**, *11*, 1414.
18. Nannini, E.; Murray, B.E.; Arias, C.A. Resistance or decreased susceptibility to glycopeptides, daptomycin, and linezolid in methicillin-resistant *Staphylococcus aureus*. *Curr. Opin. Pharmacol.* **2010**, *10*, 516–521.
19. Kim, W.; Zhu, W.; Hendricks, G.L.; Van Tyne, D.; Steele, A.D.; Keohane, C.E.; Fricke, N.; Conery, A.L.; Shen, S.; Pan, W.; et al. A new class of synthetic retinoid antibiotics effective against bacterial persisters. *Nature* **2018**, *556*, 103–107.
20. Kim, S.M.; Escobar, I.; Lee, K.; Fuchs, B.B.; Mylonakis, E.; Kim, W. Anti-MRSA agent discovery using *Caenorhabditis elegans*-based high-throughput screening. *J. Microbiol.* **2020**, *58*, 431–444.
21. Kim, W.; Steele, A.D.; Zhu, W.; Csatory, E.E.; Fricke, N.; Dekarske, M.M.; Jayamani, E.; Pan, W.; Kwon, B.; Sinitza, I.F.; et al. Discovery and Optimization of nTZDpa as an Antibiotic Effective against Bacterial Persisters. *ACS Infect. Dis.* **2018**, *4*, 1540–1545.
22. Kim, W.; Zou, G.; Hari, T.P.A.; Wilt, I.K.; Zhu, W.; Galle, N.; Faizi, H.A.; Hendricks, G.L.; Tori, K.; Pan, W.; et al. A selective membrane-targeting repurposed antibiotic with activity against persistent methicillin-resistant *Staphylococcus aureus*. *Proc. Natl. Acad. Sci. USA* **2019**, *116*, 16529–16534.
23. Kim, W.; Zou, G.; Pan, W.; Fricke, N.; Faizi, H.A.; Kim, S.M.; Khader, R.; Li, S.; Lee, K.; Escorba, L.; et al. The Neutrally Charged Diarylurea Compound PQ401 Kills Antibiotic-Resistant and Antibiotic-Tolerant *Staphylococcus aureus*. *mBio* **2020**, *11*, 603.
24. Onai, Y.; Suzuki, J.-I.; Kakuta, T.; Maejima, Y.; Haraguchi, G.; Fukasawa, H.; Muto, S.; Itai, A.; Isobe, M. Author Notes Inhibition of I κ B phosphorylation in cardiomyocytes attenuates myocardial ischemia/reperfusion injury. *Cardiovasc. Res.* **2004**, *63*, 51–59.
25. Kim, S.; Ko, D.; Lee, Y.; Jang, S.; Lee, Y.; Lee, I.Y.; Kim, S. Anti-cancer activity of the novel 2-hydroxydiarylamine derivatives IMD-0354 and KRT1853 through suppression of cancer cell invasion, proliferation, and survival mediated by TMPRSS4. *Sci. Rep.* **2019**, *9*, 10003.
26. Kinoshita, Y.; Sawada, K.; Makino, H.; Tomonori, O.; Tomoko, M.; Noriko, S.; Tomoyuki, F.; Eiichi, M.; Koji, N.; Ikuko, S.; Toda, A.; Hashimoto, K.; et al. IKK β Regulates VEGF Expression and Is a Potential Therapeutic Target for Ovarian Cancer as an Antiangiogenic Treatment. *Mol. Cancer Ther.* **2015**, *14*, 909–919.
27. Gomez-Cabrero, A.; Wrasidlo, W.; Reisfeld, R.A. IMD-0354 targets breast cancer stem cells: A novel approach for an adjuvant to chemotherapy to prevent multidrug resistance in a murine model. *PLoS ONE* **2013**, *8*, e73607.
28. Sugita, A.; Ogawa, H.; Azuma, M.; Muto, S.; Honjo, A.; Yanagawa, H.; Nishioka, Y.; Tani, K.; Itai, A.; Sone, S. Antiallergic and anti-inflammatory effects of a novel I κ B kinase beta inhibitor, IMD-0354, in a mouse model of allergic inflammation. *Int. Arch. Allergy Immunol.* **2009**, *148*, 186–198.
29. Barker, W.T.; Nemeth, A.M.; Brackett, S.M.; Basak, A.K.; Chandler, C.E.; Jania, L.A.; Zuercher, W.J.; Melander, R.J.; Koller, B.H.; Ernst, R.K.; et al. Repurposing

- Eukaryotic Kinase Inhibitors as Colistin Adjuvants in Gram-Negative Bacteria. *ACS Infect. Dis.* **2019**, *5*, 1764–1771.
30. Rice, L.B. Federal funding for the study of antimicrobial resistance in nosocomial pathogens: No ESKAPE. *J. Infect. Dis.* **2008**, *197*, 1079–1081.
 31. Pendleton, J.N.; Gorman, S.P.; Gilmore, B.F. Clinical relevance of the ESKAPE pathogens. *Expert Rev. Anti-Infect. Ther.* **2013**, *11*, 297–308.
 32. Weigel, L.M.; Clewell, D.B.; Gill, S.R.; Clark, N.C.; McDougal, L.K.; Flannagan, S.E.; Kolonay, J.F.; Shetty, J.; Killgore, G.E.; Tenover, F.C. Genetic analysis of a high-level vancomycin-resistant isolate of *Staphylococcus aureus*. *Science* **2003**, *302*, 1569–1571.
 33. Centers for Disease Control and Prevention. *CDC & FDA Antibiotic Resistance (AR) Isolate Bank*; CDC: Atlanta, GA, USA, 2019.
 34. Gupta, V.; Singla, N.; Behl, P.; Sahoo, T.; Chander, J. Antimicrobial susceptibility pattern of vancomycin resistant enterococci to newer antimicrobial agents. *Indian J. Med. Res.* **2015**, *141*, 483–486.
 35. Carias, L.L.; Rudin, S.D.; Donskey, C.J.; Rice, L.B. Genetic linkage and cotransfer of a novel, vanB-containing transposon (Tn5382) and a low-affinity penicillin-binding protein 5 gene in a clinical vancomycin-resistant *Enterococcus faecium* isolate. *J. Bacteriol.* **1998**, *180*, 4426–4434.
 36. Williamson, R.; Al-Obeid, S.; Shlaes, J.H.; Goldstein, F.W.; Shlaes, D.M. Inducible resistance to vancomycin in *Enterococcus faecium* D366. *J. Infect. Dis.* **1989**, *159*, 1095–1104.
 37. Thorisdottir, A.S.; Carias, L.L.; Marshall, S.H.; Green, M.; Zervos, M.J.; Giorgio, C.; Mermel, L.A.; Boyce, J.M.; Medeiros, A.A.; Fraimowet, H.; et al. IS6770, an enterococcal insertion-like sequence useful for determining the clonal relationship of clinical *enterococcal* isolates. *J. Infect. Dis.* **1994**, *70*, 1539–1548.
 38. Evers, S.; Sahm, D.F.; Courvalin, P. The vanB gene of vancomycin-resistant *Enterococcus faecalis* V583 is structurally related to genes encoding D-Ala:D-Ala ligases and glycopeptide-resistance proteins VanA and VanC. *Gene* **1993**, *24*, 143–144.
 39. Racusen, L.C.; Monteil, C.; Sgrignoli, A.; Lucskay, M.; Marouillat, S.; Rhim, J.G.; Morin, J.P. Cell lines with extended *in vitro* growth potential from human renal proximal tubule: Characterization, response to inducers, and comparison with established cell lines. *J. Lab. Clin. Med.* **1997**, *129*, 318–329.
 40. Kim, W.; Conery, A.L.; Rajamuthiah, R.; Fuchs, B.B.; Ausubel, F.M.; Mylonakis, E. Identification of an antimicrobial agent effective against methicillin-resistant *Staphylococcus aureus* persists using a fluorescence-based screening strategy. *PLoS ONE* **2015**, *10*, e0127640.
 41. Percival, S.L.; Suleman, L.; Vuotto, C.; Donelli, G. Healthcare-associated infections, medical devices and biofilms: Risk, tolerance and control. *J. Med. Microbiol.* **2015**, *64 Pt 4*, 64323–64334.
 42. Moormeier, D.E.; Bayles, K.W. *Staphylococcus aureus* biofilm: A complex developmental organism. *Mol. Microbiol.* **2017**, *104*, 365–376.
 43. Chung, P.Y.; Toh, Y.S. Anti-biofilm agents: Recent breakthrough against multi-drug resistant *Staphylococcus aureus*. *Pathog. Dis.* **2014**, *70*, 231–239.

44. Bjarnsholt, T.; Ciofu, O.; Molin, S.; Givskov, M.; Høiby, N. Applying insights from biofilm biology to drug development - can a new approach be developed? *Nat. Rev. Drug Discov.* **2013**, *12*, 791–808.
45. Hurdle, J.G.; O'Neill, A.J.; Chopra, I.; Lee, R.E. Targeting bacterial membrane function: An underexploited mechanism for treating persistent infections. *Nat. Rev. Microbiol.* **2010**, *9*, 62–75.
46. Kim, W.; Fricke, N.; Conery, A.L.; Fuchs, B.B.; Rajamuthiah, R.; Jayamani, E.; Vlahovska, P.M.; Ausubel, F.M.; Mylonakis, E. NH125 kills methicillin-resistant *Staphylococcus aureus* persisters by lipid bilayer disruption. *Future Med. Chem.* **2016**, *8*, 257–269.
47. Raetz, C.R.H.; Whitfield, C. Lipopolysaccharide endotoxins. *Annu. Rev. Biochem.* **2002**, *71*, 635–700.
48. Tanaka, A.; Konno, M.; Muto, S.; Kambe, N.; Morii, E.; Nakahata, T.; Itai, A.; Matsuda, H. A novel NF- κ B inhibitor, IMD-0354, suppresses neoplastic proliferation of human mast cells with constitutively activated c-kit receptors. *Blood* **2005**, *105*, 2324–2331.
49. Kwan, B.W.; Chowdhury, N.; Wood, T.K. Combatting bacterial infections by killing persister cells with mitomycin C. *Environ. Microbiol.* **2015**, *17*, 4406–4414.
50. Chowdhury, N.; Wood, T.L.; Martinez-Vazquez, M.; García-Contreras, R. Wood TK. DNA-crosslinker cisplatin eradicates bacterial persister cells. *Biotechnol. Bioeng.* **2016**, *113*, 1984–1992.
51. Yang, E.B.; Tang, W.Y.; Zhang, K.; Cheng, L.Y.; Mack, P.O. Norcantharidin inhibits growth of human HepG2 cell-transplanted tumor in nude mice and prolongs host survival. *Cancer Lett.* **1997**, *117*, 93–98.
52. Li, Y.; Wang, Z.; Ma, X.; Shao, B.; Gao, X.; Zhang, B.; Xu, G.; Wei, Y. Low-dose cisplatin administration to septic mice improves bacterial clearance and programs peritoneal macrophage polarization to M1 phenotype. *Pathog. Dis.* **2014**, *72*, 111–123.
53. CLSI. *M07-A9: Methods for Dilution Antimicrobial Susceptibility Tests for Bacteria That Grow Aerobically*, 9th ed.; Approved Standard; CLSI: Sydney NSW, Australia, 2012; pp. 1–88.
54. Fuchs, S.; Pané-Farré, J.; Kohler, C.; Hecker, M.; Engelmann, S. Anaerobic gene expression in *Staphylococcus aureus*. *J. Bacteriol.* **2007**, *189*, 4275–4289.
55. Yuen, G.J.; Ausubel, F.M. Both live and dead Enterococci activate *Caenorhabditis elegans* host defense via immune and stress pathways. *Virulence* **2018**, *9*, 683–699.
56. Kim, J.; Lee, A.-R.; Kawasaki, I.; Strome, S.; Shim, Y.-H. A mutation of *cdc-25.1* causes defects in germ cells but not in somatic tissues in *C. elegans*. *Mol. Cells* **2009**, *28*, 43–48.
57. Rajamuthiah, R.; Jayamani, E.; Conery, A.L.; Fuchs, B.B.; Kim, W.; Johnston, T.; Vilcinskis, A.; Ausubel, F.M.; Mylonakis, E. A Defensin from the Model Beetle *Tribolium castaneum* Acts Synergistically with Telavancin and Daptomycin against Multidrug Resistant *Staphylococcus aureus*. *PLoS ONE* **2015**, *10*, e0128576.
58. Mishra, B.; Golla, R.M.; Lau, K.; Lushnikova, T.; Wang, G. Anti-Staphylococcal Biofilm Effects of Human Cathelicidin Peptides. *ACS Med. Chem. Lett.* **2016**, *7*, 117–121.
59. O'Toole, G.A. Microtiter dish biofilm formation assay. *J. Vis. Exp.* **2011**, *47*, e2437.

CHAPTER 4: REPURPOSING KINASE INHIBITOR BAY 11-7085 TO COMBAT *STAPHYLOCOCCUS AUREUS* AND *CANDIDA ALBICANS* BIOFILMS

A substantially similar version of this chapter was originally published in *Frontiers in Pharmacology* May 5, 2021, Volume 12, Special Issue: Novel Approaches to The Treatment of Multidrug-Resistant Bacteria

Repurposing kinase inhibitor Bay 11-7085 to combat *Staphylococcus aureus* and *Candida albicans* biofilms

**Iliana E Escobar¹, Fernanda Cristina Possamai Rossatto^{1,2}, Soo Min Kim³,
Min Hee Kang³, Wooseong Kim^{3,*} and Eleftherios Mylonakis^{1,*}**

¹Infectious Diseases Division, Department of Medicine, Warren Alpert Medical School of Brown University, Rhode Island Hospital, Providence, RI 02903, USA;

iliana_escobar@brown.edu (I.E.E.); emylonakis@lifespan.org (E.M.)

²Laboratory of Biofilms and Alternative Models, Federal University of Health Sciences of Porto Alegre, Porto Alegre, Rio Grande do Sul, Brazil; fernandapr@ufcspa.edu.br

(F.P.R)

³College of Pharmacy, Graduate School of Pharmaceutical Sciences, Ewha Womans University, Seoul 03760, Republic of Korea; soominkim14@gmail.com (S.M.K.);

wvhu123@naver.com (M.H.K.); wooseong_kim@ewha.ac.kr (W.K.)

*Correspondence: wooseong_kim@ewha.ac.kr (W.K.); emylonakis@lifespan.org (E.M.);

Tel.: +82-2-3277-3372 (W.K.); +1-401-444-7856 (E.M.)

Abstract

Staphylococcus aureus and *Candida spp.* are commonly linked with topical biofilm-associated infections such as those found associated with chronic wounds. These biofilms are notoriously difficult to treat, highlighting the grave need to discover and study new broad-spectrum agents to combat these infections. Here we report that the kinase inhibitor Bay 11-7085 exhibited bactericidal activity against multidrug-resistant *S. aureus* with a minimum inhibitory concentration (MIC) of 4 µg/ml. In addition, *S. aureus* strain MW2 did not acquire resistance to Bay 11-7085. Furthermore, Bay 11-7085 exhibited potency against *Candida albicans* and the emerging pathogen *Candida auris* with a MIC of 0.5–1 µg/ml. Bay 11-7085 partially inhibited and eradicated biofilm formation of various pathogens, such as VRSA (vancomycin-resistant *S. aureus*), as well as antifungal-resistant *Candida spp.* isolates. Notably, Bay 11-7085 partially inhibited initial cell attachment and formation of a VRSA-*C. albicans* polymicrobial biofilm *in vitro*. In contrast to *C. albicans*, inhibition of VRSA biofilm was linked to initial cell attachment independent of its bactericidal activity. Finally, Bay 11-7085 was effective *in vivo* at increasing the lifespan of *C. elegans* during *S. aureus* or *C. albicans* infections. Our work suggests that kinase inhibitor Bay 11-7085 is a potential compound capable of combating biofilms associated with primary multidrug-resistant bacteria and yeast pathogens associated with wound infections.

Introduction

With the diminished efforts focusing on discovering new antimicrobial agents, antibiotic resistance has been a persistent problem hindering the treatment of bacterial and fungal infections [1]. In addition to spontaneous mutations, antimicrobial resistance is augmented through a pathogen's transition from a planktonic state to a biofilm [2]. Biofilms are an organization of microorganisms adherent to themselves and other surfaces which produce an extracellular matrix (ECM) [3,4] and confer antimicrobial tolerance to their resident microbes through three main mechanisms: adaptive stress, low metabolic rates, and physical blockage of antimicrobial penetration by the ECM [2]. Thus, cells within biofilms are known to have up to 10,000-fold higher tolerance to antimicrobial agents [5].

Although the mechanism of biofilm formation can differ from species to species, most microorganisms share a common scaffold of multiple stages of maturation [3]. The first stage is initial cell attachment, which serves as the microbial network foundation to begin signaling and building the ECM [3,4]. Then, during multiplication and maturation, attached cells start to divide and form colonies that commence interlocking and consequently fortify the ECM [3,4]. Lastly, through detachment and dispersal, biofilms begin to spread by releasing cells from within the ECM and initiating the cycle once again [3,4]. Recent studies have evaluated strategies to combat biofilm-associated infections by targeting different stages of biofilm formation. For example, aryl rhodanines or calcium chelators have shown some success at inhibiting biofilm initial cell attachment [6]. Metallic silver, silver ions, and silver nanoparticles show efficacy as a broad anti-biofilm agent effective

against Gram-negative, Gram- positive, and fungal pathogens [6]. In addition, molecules such a *cis*-2-decenoic acid, the peptide dispersin B, or the quorum-sensing inhibitor RNAIII-inhibiting peptide (RIP) have shown efficacy at disrupting fully mature biofilm *in vivo* [6]. However, only silver is an FDA-approved molecule, further emphasizing the need for new anti-biofilm drug targets.

Clinically, 90% of chronic wounds are associated with biofilms and persistent inflammation [7]. There are multiple stages of wound healing. However, chronic wounds fail to cycle through each phase in less than 3 months or more due to ongoing inflammation and failed antibiotic therapy [8]. Chronic wounds can include venous, diabetic, or pressure ulcers [8]. In addition, chronic wounds pose a significant financial burden to our health care system. In 2014, Nussbaum et al., estimated a total cost burden of \$28–96.8 billion dollars [9]. Furthermore, chronic wounds may lead to a deteriorated quality of life followed by depression and isolation [10]. Other biofilm-associated wounds include those caused by extreme burns or traumatic injury, both of which are difficult to treat and heal [11,12], further highlighting the need for new anti-biofilm drug therapy.

Several human pathogens have the ability to form biofilms. Thus, management of chronic wounds requires compounds effective against antibiotic-tolerant cells housed within biofilms. *Staphylococcus aureus* is a common biofilm-associated pathogen [6,13]. In particular, methicillin-resistant *S. aureus* (MRSA) is responsible for a large percentage of hospital-acquired infections [14]. MRSA can cause systemic and topical infections, one of which is chronic wounds [15]. In addition to bacteria, yeast-like fungi can cause biofilm-associated infections as well.

For example, *Candida* spp. have also been isolated from chronic wound infections, such as diabetic ulcers [16], and similar to *S. aureus*, *Candida* spp. can cause infection both systemically and locally [17]. When associated with biofilm, *Candida* spp. are also more tolerant to antifungal agents than in their planktonic form [4]. More recently, *Candida auris* has rapidly become an emerging antifungal resistant pathogen with threatening infection rates [17–19]. These types of events highlight the need for new lead compounds with the potential to eradicate the planktonic form of a pathogen but also show anti-biofilm potency.

In this study, we investigate the antimicrobial and anti-biofilm properties of Bay 11-7085. This compound was flagged as a hit in our *C. elegans*-MRSA infection high through-put screen [20]. In this screen, we tested over 82,000 small molecules to elucidate compounds that inhibit *C. elegans* MRSA-mediated killing. This approach has become extremely successful, leading to multiple hit compounds, which have been further studied and characterized for their anti-infective capabilities [20–22]. Due to our *C. elegans*-MRSA whole animal screen system, overlooked compounds, such as those with multiple bioactivities, have now been identified as potent antimicrobials [23]. Here we show that the hit compound Bay 11-7085 has antimicrobial and anti-biofilm activity to both *S. aureus* and *Candida* spp. It partially inhibits biofilm initial cell attachment and formation in a polymicrobial co-culture and can partially eradicate mature biofilm. Furthermore, Bay 11-7085 shows activity against *C. albicans* but not *S. aureus* in an *in vitro* multispecies Lubbock chronic wound biofilm model [24]. This model was designed to closer mimic physiological conditions in the body by including blood and serum in the media [24]. Bay 11-7085

exhibits a low probability for resistance development to antibiotic pressure against *S. aureus* strain MW2 and can prolong *C. elegans* life from MRSA or *C. albicans* infections.

Material and Methods

Pathogenic Strains and Growth Conditions

All strains used in these studies are included in Supplementary Table S1. Staphylococcal strains were grown overnight in tryptic soy broth (TSB) at 37°C with shaking at 180–225 rpm. Enterococcal strains were grown overnight in brain heart infusion broth (BHI) at 37°C with shaking at 180–225 rpm. All other bacterial strains were grown overnight in Luria-Bertani broth (LB) at 37°C with shaking at 180–225 rpm. *Candida* spp. isolates were grown overnight in Yeast Peptone Dextrose (YPD) at 37°C with shaking at 225 rpm.

Drugs and Antibiotics

Bay 11-7085 (Tocris 1743), fluconazole, and amphotericin B stocks were dissolved to 10 mg/ml in dimethyl sulfoxide (DMSO). Oxacillin, vancomycin, gentamicin, and ciprofloxacin were dissolved in H₂O to make 10 mg/ml stocks. Kanamycin was dissolved in H₂O to make 100 mg/ml stock.

Minimum Inhibitory Concentration

MIC of bacterial strains were determined by broth microdilution assay according to the Clinical & Laboratory Standards Institute (CLSI) [25]. In brief, strains grown overnight in appropriate media for 20–23 h were diluted to 1×10⁶ CFU/ml in Mueller–Hinton Broth (MHB, BD Difco, pH: 7.3 ± 0.1). In a 96-well plate, 50 µl of diluted culture was added to 50 µl of serial two-fold diluted drug in MHB to a final concentration of 5×10⁵ CFU/ml. All assays were performed in triplicate. Experimental plates were incubated

for 20–22 h at 37°C. Optical density at 600 nm (OD₆₀₀) was quantified using a spectrophotometer (SpectraMax M2, Molecular Devices) as a measure of bacterial growth. MIC was defined as OD₆₀₀ ≤ 0.1 after background subtraction.

The MICs of *Candida* spp. strains were determined by broth microdilution assay according to the CLSI document M27-A using 96-well flat-bottom microtiter plates [26]. Briefly, colonies of each strain were inoculated in 5 ml of YPD overnight. The cells were harvested by centrifugation at 4,300×g for 5 min, washed twice with sterile phosphate-buffered saline (PBS), and adjusted to 1×10³ cells/ml in Roswell Park Memorial Institute (RPMI) 1640 using a hemocytometer. The compound and antifungal agents used as controls were serially diluted to final concentrations ranging from 0.125 to 64 µg/ml. *Candida* spp. cells were subsequently added to wells (final concentration 0.5×10³ cells/ml). Negative controls were performed with RPMI 1640 media only, and positive controls with RPMI 1640 and *Candida* spp. cells only. Microplates were incubated at 37°C without shaking and read after 24 h. The MIC was visually defined as the lowest concentration of compound at which 100% of inhibition was observed, compared with that of the compound-free control. Each assay was performed in triplicate.

C. elegans Infection Assay for Compound Screening

All compounds were screened as previously described in Kim et al. (2018a) [20]. In brief, *glp-4* (bn2);*sek-1*(km4) worm embryos were synchronized by plating 2000 L1 worms on slow-kill (SK) agar plates with HB101 bacteria as a food source at 15°C for four days until they reached gravid adult stage. Eggs were harvested and

hatched in M9 buffer at 15°C for 48 h. L1 stage worms were then transferred onto SK HB101 plates and incubated at 25°C for 52 h to induce sterility. Sterile young adult stage worms were harvested using M9 buffer and sorted into black, clear-bottom, 384-well plates (Corning no. 3712, Corning, NY) containing compounds at 15 worms/well using the Copas Biosort instrument (Union Biometrica, MA, United States). *S. aureus* strain MW2 bacteria were grown overnight in TSB at 37°C with agitation. A static culture was inoculated by seeding 100 µl of overnight culture in 10 ml of fresh TSB, sealed to produce anaerobic conditions, and incubated at 37°C overnight without agitation. We have found that MW2 grown anaerobically elicits a greater infection mortality rate in *C. elegans*. Furthermore, anaerobically grown cells of *S. aureus* strain MW2 express different virulence gene patterns [27]. Static cells of *S. aureus* strain MW2 were added to *C. elegans*-compound 384-well plates at a final concentration of OD₆₀₀ 0.04. The final well composition consisted of 70% M9 buffer, 19% Sheath solution (Union Biometrica Part no. 300-5101-000), 10% TSB, and 1% DMSO or compounds dissolved in DMSO. After a 5-day incubation at 25°C, worms were washed using a multiplate washer and incubated overnight at 37°C with Sytox Orange dissolved in M9 at a final concentration of 0.7 µM. The following day, all plates were imaged using an Image Xpress Micro automated microscope (Molecular Devices, CA, United States), capturing both transmitted light and TRITC (535 nm excitation, 610 nm emission) fluorescent images using a 2× objective.

C. elegans Dose-Dependent Toxicity Assay

In a black, clear-bottom, 96-well plate (Corning, no. 3690 Corning, NY, USA), Bay 11-7085 was serially diluted to a final volume of 50 μ l using M9. N2 worms were sterilized by growing to young adult stage fed on RNAi *cdc 25.1* activated by 1 mM of IPTG [28] for 48 h at 25°C. *cdc 25.1* is an integral part of germ cell mitosis. Mutations of *cdc 25.1* inhibit the germ-line cell division producing *C. elegans* incapable of laying eggs [29]. Young adult worms were washed 3 times with 50 ml of M9 and diluted to an average of 21 worms \pm 7 per 25 μ l using a multichannel pipette. An additional 25 μ l of heat-killed OP50 were added to each well to make a final volume of 100 μ l and OD₆₀₀ of 0.5. All assays were performed in duplicate. Experimental plates were incubated for 24 h at 25°C. Worms were then washed using a 405 LS microplate washer (BioTek, VT, United States) and incubated with 0.7 μ M Sytox Orange for an additional 24 h at 25°C. Each plate was then imaged using an Xpress Micro automated microscope (Molecular Devices, CA, United States), capturing both transmitted light and TRITC (535 nm excitation, 610 nm emission) fluorescent images using a 2x objective. Surviving worms were considered those with no TRITC signal relative to the control.

Bacterial and Fungal Time-Course Killing Assay

An overnight culture *S. aureus* strain MW2 was diluted 1:100 in TSB and grown to log phase (OD₆₀₀ 0.3–0.6). The log phase culture was then diluted 1:100 (2×10^6 CFU/ml) in MHB (BD Difco, pH 7.3 \pm 0.1). 250 μ l of diluted culture was added to 250 μ l of serial two-fold diluted drug in MHB to a final concentration of 1×10^6 CFU/ml. Plates were incubated at 37°C with agitation (225 rpm). At time-points 0, 1, 2, 3, 4, and 24 h, 50- μ l

samples were removed, diluted 5- fold to sub-MIC levels, then serially diluted by 10-fold steps, and lastly spot-plated on TSB agar (BD Difco) plates to enumerate CFU/ ml. These experiments were conducted in triplicate. Experimental plates were incubated for 20–22 h at 37°C.

Log-phase cultures of *C. albicans* were regrown and adjusted to a density of 10^6 cells/ml in RPMI 1640 and added to growth medium alone or specific concentrations of the compound being tested. Plates were incubated at 37°C with agitation (225 rpm). At predetermined time points (0, 6, 12, 24, 48 h), 50 µl aliquots were obtained from each solution, serially diluted in YPD broth, and 5 µl were plated on YPD agar plates for 24 h at 37°C for determination of CFU/ml. Three independent experiments were performed in triplicate.

Human Blood Hemolysis

Hemolytic activity of Bay 11-7085 on human erythrocytes was evaluated using a previously described method with modifications [30]. 10% human erythrocytes were purchased from Rockland Immunochemicals (Limerick, PA, United States). The erythrocytes were diluted to 4% in PBS, and 50 µl were added to 50 µl of two-fold serial dilutions of compound in PBS, 0.2% DMSO (negative control), or 1% Triton-X 100 (positive control) in a 96-well plate. Plates were incubated at 37°C for 1 h and then centrifuged at 500×g for 5 min. 50 µl of the supernatant was transferred to a fresh 96-well plate, and absorbance (A) was measured at 540 nm. Percent hemolysis was calculated using the following equation: $(A_{540 \text{ nm of compound treated sample}} - A_{540 \text{ nm of 0.1\% DMSO treated sample}}) / (A_{540 \text{ nm of 1\% Triton X-100 treated}}$

sample—A540 nm of 0.1% DMSO treated sample) $\times 100$. All experiments were conducted in triplicate.

Mammalian Cell Viability Assay

Human hepatoma cell line HepG2 cells were grown in DMEM 10% FBS to confluency and seeded onto 96-well drug plates at 1×10^6 cells/ml. Human renal proximal tubule epithelial RPTEC cells were grown in Renal Epithelial Cell Basal Medium (ATCC PCS-400-030) with supplements (Renal Epithelial Cell Growth Kit ATCC PCS-400-040) and seeded onto 96-well drug plates at 1×10^6 cells/ml. Two-fold concentration drug plates were prepared using corresponding growth media for each cell. Drug and cell plate were then incubated for 22 h at 37°C and 5% CO₂. At 22 h, 10 μ l of WST-1 (Roche, Sigma-Aldrich, MO, United States) was added to each well, following manufacturer's directions, and incubated for an additional 2 h. Plate absorbance was read at 450 nm. Samples were normalized to a non-treatment control. All experiments were conducted in triplicate.

Biofilm Initial Cell Attachment Assay

Monoculture

Absorbance (OD₆₀₀) of overnight culture *S. aureus* strain VRS1 was measured and adjusted to 0.2 in BHI + 0.1% glucose medium. 100 μ l of bacteria was added to 2 \times drug concentrations being tested (diluted in BHI +0.1% glucose) dispensed in polystyrene tissue culture-treated 96-well flat-bottom microplates (Corning no. 353072, Corning, NY), producing a final volume of 200 μ l, OD₆₀₀ of 0.1 ($\sim 1 \times 10^8$ CFU/ml) and 1 \times drug concentration. The plates were then incubated at 37°C for 1 h. After incubation, the culture was pipetted out, and the wells washed 3 times with PBS

to remove any non-adherent planktonic cells. Biofilm initial cell attachment was measured as described in Mishra et al., 2016 [31]. In brief, colorimetric quantification of the inhibition of biofilm initial cell attachment was done using XTT [2–3-bis(2-methoxy-4-nitro-5-sulphophenyl)-2H-tetrazolium-5-carboxanilide] assay kit following manufacture instructions with minor adjustments (Sigma-Aldrich, Oxoid, St. Louis, MO). 180 µl of fresh BHI and 20 µl of XTT working solution were added to each well, and the plates were again incubated for 2 h at 37°C. Absorbance at 450 nm was measured, and each experimental well was normalized to a non-treatment control. Each biological replicate was done in quadruplicates. One replicate was done in octuplet. Three total biological replicates were conducted in total.

For a *Candida* spp. biofilm assay, 50 µl of RPMI 1640 media containing Bay 11-7085 was serially diluted in a polystyrene tissue culture-treated 96-well flat-bottom microplates (Corning no. 353072, Corning, NY). Overnight cultures of either *Candida* spp. were washed twice with PBS, resuspended in RPMI 1640 (final concentration: 1×10^7 cells/ml), and added to each well to a final volume of 100 µl. Each plate was then statically incubated for 90 min at 37°C. Following incubation, plates were washed twice with PBS, and cell attachment was measured using XTT assay kit following manufactures instructions with minor modification [32]. In brief, a working solution of XTT was prepared where 80 µl of PBS and 20 µl of XTT were added to each well. Plates were then incubated in the dark for 2 h at 37°C, and absorbance was measured at 490 nm using a microtiter plate reader. Experimental wells were normalized to a non-treatment control and background subtraction. Three biological replicates were conducted in octuplet.

Co-culture

Co-culturing of *S. aureus* and *C. albicans* was carried out as previously described [33]. In detail, *S. aureus* strain VRS1 [34] and *C. albicans* strain SC5314 were grown overnight with agitation in BHI or YPD respectively at 37°C with shaking at 225 rpm. Cells were then washed twice with sterile PBS. VRS1 was adjusted to OD₆₀₀ 0.4 (~10⁷ CFU/ml), and *C. albicans* was adjusted to 2×10⁶ CFU/ml by counting cells using a hemocytometer. Washed cells were then diluted in 50% serum-BHI medium at a 1:10 ratio *S. aureus* to *C. albicans*. Drug plates were prepared using 50% serum-BHI medium and 2× concentration of each drug dose tested in a 24-well plate. A Millipore mixed cellulose ester membrane disk (GSWP01300, EMD Millipore, Billerica, MA, United States) was placed in each well containing 500 µl of 2× drug concentration. 500 µl of co-culture mix was added to each well of the drug plate, making a final volume of 1 ml, 10⁵–10⁷ CFU/ml *S. aureus*, and 10⁶ *C. albicans*. Disks were then incubated at 37°C for 90 min, washed 3 times with PBS, and transferred to a 1.5 ml microtube containing equal amounts of PBS. 200 µl were aliquoted in a fresh microtube and stored for later. Microtubes containing disks were sonicated for 10 min using an ultrasonic bath (Fisher Scientific FS 30). Both pre-sonicated and post-sonicated samples were then collected from each tube and serially diluted on selective plates to enumerate total CFU/membrane of *S. aureus* and *C. albicans*. Selective plates used were mannitol salt (BD Difco, pH: 7.4 ± 0.2) incubated at 37°C (for *S. aureus* strain VRS1) and YPD (Research Products International) containing 100 µg/ml of kanamycin incubated at 25°C (for *C. albicans* strain SC5314). Each

sample was normalized to pre-sonicated samples. Three biological replicates were conducted in duplicate.

Biofilm Inhibition and Eradication Assay

Monoculture

Absorbance (OD₆₀₀) of overnight culture *S. aureus* strain VRS1 was measured and adjusted to 0.1 in BHI + 0.1% glucose medium. 100 µl of bacteria was added to 2× drug concentrations (diluted in BHI + 0.1% glucose medium) dispensed in polystyrene tissue culture-treated 96-well flat-bottom microplates (Corning no. 353072, Corning, NY) producing a final volume of 200 µl (~1×10⁷ CFU/ml) and 1× drug concentration. After 24 h of static incubation at 37°C, media was pipetted out, and wells were washed 3 times with PBS to remove any non-adherent planktonic cells. Biofilm formation was measured using crystal violet (CV) [35]. In brief, plates were incubated with 1% CV for 15 min at room temperature. Plates were then washed 3 times with PBS and dissolved with 200 µl of 30% acetic acid. Absorbance at 550 nm was measured and each experimental well was normalized to a non-treatment control. Three biological replicates were conducted in octuplet.

For biofilm eradication, biofilms were prepared as described above, omitting the initial drug dose. After static incubation at 37°C for 24 h, plates were washed 2 times with PBS. Various concentrations of drug tested were diluted in BHI + 0.1% glucose medium and added to each well to a final volume of 200 µl. After an additional incubation of 24 h plates were washed 3 times with PBS and stained with CV as described previously. Three biological replicates were conducted in octuplet.

For *Candida* spp., overnight suspensions were centrifuged (4,000×g for 5 min), washed twice with PBS, and resuspended in RPMI 1640. 50 µl of RPMI 1640 containing Bay 11-7085 were serially diluted in a 96-well polystyrene microtiter plate. 50 µl aliquots of fungal suspensions (final concentration: 1×10^6 cells/ml) were transferred to each well of the microtiter plate and incubated statically for 24 h at 37°C. Unseeded wells (with RPMI 1640 only) acted as the negative background control for the subsequent steps. Following incubation, the biofilm was assessed using XTT [31], as described in the section: Biofilm Initial Cell Attachment Assay, or CV [35]. For CV methodology, cells were fixed with methanol for 15 min and stained with 100 µl of 0.4% CV solution for 15 min. Any excess CV was removed by washing with sterile water before adding 100 µl of absolute ethanol to release the dye from the biofilm. After 30 min, the absorbance was measured at 570 nm using a microtiter plate reader. Three biological replicates were conducted in octuplet.

For biofilm eradication, biofilms were prepared as described above, omitting the initial drug dose. After static incubating at 37°C for 24 h, plates were washed 2 times with PBS, and various drug tested concentrations were added to each well to a final volume of 100 µl. After an additional incubation of 24 h, plates were washed 3 times with PBS and assessed using XTT [31] or stained with CV [35] as described above. Three biological replicates were conducted in octuplet.

Co-culture

Co-culture *S. aureus* and *C. albicans* was carried out as previously described [33]. In detail, *S. aureus* strain VRS1 [34] and *C. albicans* strain SC5314 were grown overnight

with agitation in BHI or YPD, respectively, at 37°C. Cells were then washed twice with sterile PBS. VRS1 was adjusted to OD₆₀₀ 0.4 (~10⁷ CFU/ml), and *C. albicans* was adjusted to 2×10⁶ CFU/ml in PBS by counting cells using a hemocytometer. Washed cells were then diluted in 50% serum-BHI medium (serum: Fetal bovine serum, ThermoFisher, Remel, Waltham, MA) at a 1:10 ratio *S. aureus* to *C. albicans*. Drug plates were prepared by serially diluting 100 µl of 50% serum-BHI medium and 2× concentration of each drug dose tested in a polystyrene tissue culture-treated 96-well flat-bottom microplates (Corning no. 353072, Corning, NY). 100 µl of co-culture mix was added to each well of the drug plate, making a final volume of 200 µl, 10⁵–10⁷ CFU/ml *S. aureus*, and 10⁶ *C. albicans*. After 24 h of static incubation at 37°C, media was pipetted out, and wells were washed 3 times with PBS to remove any non-adherent planktonic cells. Biofilm formation was measured using CV [35]. In brief, plates were incubated with 1% CV for 15 min at room temperature. Plates were then washed 3 times with PBS and dissolved with 200 µl of 30% acetic acid. Absorbance at 550 nm was measured and each experimental well was normalized to a non-treatment control. Each biological replicate was done in octuplet.

For biofilm eradication, biofilms were prepared as described above, omitting the initial drug dose. After static incubating at 37°C for 24 h, plates were washed 2 times with PBS. Various drug concentrations, diluted in BHI + 0.1% glucose medium, were added to each well to a final volume of 200 µl. After an additional incubation of 24 h plates were washed 3 times with PBS and stained with CV as described previously.

In vitro Multispecies Lubbock Chronic Wound Biofilm Model

S. aureus strain VRS1 and *C. albicans* strain SC5314 were co-cultured using the *in vitro* multispecies Lubbock chronic wound biofilm model [24]. Wound like media

(WLM) was composed of 50% Bolton Broth (Sigma-Aldrich, Oxoid, St. Louis, MO), 45% heparinized calf serum (Rockland, Limerick, PA), and 5% haemolyzed horse blood (Thermofisher, Remel, Waltham, MA). In detail, *S. aureus* strain VRS1 [34] and *C. albicans* strain SC5314 were grown overnight with agitation in BHI or YPD, respectively at 37°C. Cells were then washed twice with sterile PBS and diluted into WLM. *S. aureus* was adjusted to OD₆₀₀ 0.04 (~10⁶ CFU/ml), and *C. albicans* was adjusted to 1×10⁷ CFU/ml using a hemocytometer. Drug plates were prepared by serially diluting 50 µl WLM and 2× concentrations of each drug dose tested in a 96-well plate. 50 µl of *S. aureus*-*C. albicans* co-culture mix was added to each well of the drug plate, making a final volume of 100 µl, 10⁵–10⁶ CFU/ml *S. aureus*, and 10⁷ CFU/ml *C. albicans*. *S. aureus* strain VRS1 is coagulase-positive and therefore created a jelly-like substance that served as a scaffold for biofilm formation [36]. After 24 h of static incubation at 37°C, the complete coagulated jelly-mass from each well was transferred to individual 1.5 ml microtubes containing 1 ml of sterile PBS. Tubes were vortexed at the highest setting for 2 min and then sonicated for 10 min to release cells from the jelly mass. 100 µl of each tube was 10-fold serially diluted and spot plated on selective plates in order to enumerate total CFU/ml of *S. aureus* and *C. albicans*. Selective plates used were mannitol salt (BD Difco, pH: 7.4 ± 0.2) incubated at 37°C (*S. aureus*) and YPD (Research Products International) containing 100 µg/ml of kanamycin incubated at 25°C (*C. albicans*). All experiments were conducted in triplicate.

C. elegans-*Candida* spp. Infection Assay

C. elegans strain *glp-4;sek-1* (AU37) was maintained on *Escherichia coli* OP50

spread on nematode growth medium agar plates and incubated at 15°C. For the *C. elegans-Candida* killing assay, worms were synchronized and grown to the young adult stage by incubating 24 h at 15°C and 72 h at 25°C. Worms were collected and washed 3 times with PBS and transferred to a *C. albicans* lawn grown on a BHI plate overnight at 37°C. Worms on *C. albicans*/BHI plates were incubated at 25°C for 4 h and then washed 4 times with PBS. Thirty to seventyfive worms were dispensed into each well of a 6-well plate containing desired drug concentration diluted in 20% BHI and 45 µg/ml kanamycin to a total volume of 2 ml. Worms were incubated at 25°C and scored daily for dead worms for a total of 6 days. Statistical significance was displayed using Kaplan-Meier survival analysis.

Results

Bay 11-7085 Shows Anti-Staphylococcal Activity in vitro and in a Whole Animal C. elegans Infection Model

Through our *C. elegans*-MRSA infection model, we previously identified Bay 11-7085 (Figure 1A) as a hit compound able to rescue *C. elegans* from a lethal MRSA infection [20]. Data from our previous screen showed that Bay 11-7085 saved infected worms at a concentration of 7.14 $\mu\text{g/ml}$ (Figure 1B). Relative to vancomycin, a common Gram-positive antibiotic, Bay 11-7085 showed a distinct antimicrobial profile (Figure 1C) with a MIC of 4 $\mu\text{g/ml}$ (Table 1).

To assess the rate of antimicrobial resistance development to Bay 11-7085, we conducted a serial passage experiment in which *S. aureus* strain MW2 was treated with sub-MIC levels of Bay 11-7085 for 25 days. After 25 serial passages, *S. aureus* strain MW2 was unable to acquire resistance (Figure 1D). However, *S. aureus* MW2 did gain resistance to ciprofloxacin up to 32 \times its original MIC of 0.25 $\mu\text{g/ml}$ (Figure 1D). These results indicate that Bay 11-7085 has a low probability of selecting for antibiotic resistance over an extended period of time.

Bay 11-7085 Shows Antimicrobial Activity to S. aureus and Fungal Candida spp.

To further test Bay 11-7085 antimicrobial capability we tested its activity against a panel of ESKAPE pathogens. The ESKAPE pathogens include two Gram-positive bacteria (*Enterococcus spp.* and *S. aureus*) and four Gram-negative bacteria (*Klebsiella pneumoniae*, *Acinetobacter baumannii*, *Pseudomonas aeruginosa*, and *Enterobacter spp.*) [37,38]. Bay 11-7085 did not show activity toward any of the Gram-negative species

of bacteria with a MIC \geq 64 $\mu\text{g/ml}$ (Table 1) and, unlike *S. aureus* strain MW2, we observed nominal activity toward other Gram-positive pathogens such as *E. faecalis* or *E. faecium* with MICs of 64 $\mu\text{g/ml}$ for both species (Table 1). To further support these findings, we tested a panel of *S. aureus* strains, including vancomycin-resistant *S. aureus* strain VRS1 [34], and found that indeed Bay 11-7085 had a MIC of 2–4 $\mu\text{g/ml}$ against various *S. aureus* strains (Table 1). Interestingly, when we tested Bay 11-7085's bactericidal or bacteriostatic effect, our time-course killing data showed that Bay 11-7085 is bactericidal to log phase *S. aureus* strain MW2 cells at the MIC and higher (Figure 2A). Taken together, these findings suggest that Bay 11-7085 is not a broad bactericidal antibiotic but instead shows specific potency toward *S. aureus* strains.

Next, we tested whether Bay 11-7085 has antifungal activity. As detailed above, *Candida* spp. can cause chronic infection both systemically and topically. To answer this, we measured the MIC of Bay 11-7085 to four *Candida* spp.: *C. albicans*, *Candida glabrata*, *Candida parapsilosis*, and *C. auris* after 24 h of treatment. Strikingly, we found that Bay 11-7085 exhibited a low MIC of 0.5–1 $\mu\text{g/ml}$ for 3 of the 4 species tested (Table 1), while the MIC to *C. parapsilosis* was 8 $\mu\text{g/ml}$ (Table 1). Of particular interest is the activity observed toward *C. auris*. To confirm the activity of Bay 11-7085 toward *C. auris*, we expanded our MIC profiling to 10 total *C. auris* antifungal resistant strains acquired from the Center for Diseases Control and Prevention (CDC) clinical isolate bank. Indeed, we found that Bay 11-7085 had a low MIC of 0.5–1 $\mu\text{g/ml}$ to multiple antifungal resistant *C. auris* clinical strains (Supplementary Table S2).

We then tested whether Bay 11-7085 is fungicidal toward *C. albicans*. To evaluate this, we performed a time-kill kinetics assay using *C. albicans* strain SC5314. In contrast to *S.*

aureus (Figure 2A), Bay 11-7085 is unable to completely kill *C. albicans* (Figure 2B) at 1–2× MIC. However, at a higher concentration such as 4× MIC (4 µg/ml), Bay 11-7085 is fungicidal. Taken in their totality, we conclude that Bay 11-7085 can inhibit fungal growth at a low concentration such as 1–2 µg/ml but is fungicidal at a higher concentration such as 4 µg/ml.

Cytotoxicity of Bay 11-7085 on Human Cells and C. elegans

Next, we assessed the toxicity profile of Bay 11-7085 *in vitro* and *in vivo*. *C. elegans* is widely used as a model organism for toxicology studies [39–41]. Therefore, we first tested toxicity to *C. elegans* at various concentrations of Bay 11-7085 from 1 µg/ml up to 64 µg/ml (Figure 3A). Our data support the conclusion that Bay 11-7085 is minimally toxic to *C. elegans* with greater than 90% survival after 24 h of exposure at the highest concentration tested (Figure 3A). When we subjected human red blood cells to Bay 11-7085, we found no indication of hemolysis at a concentration up to 32 µg/ml (Figure 3B). However, when we examined Bay 11-7085s toxicity to human hepatoma cell line HepG2 and primary human renal proximal tubule epithelial cells (RPTEC), we recorded an IC₅₀ of 4.6 µg/ml and 0.96 µg/ml (Figure 3C), which is nearly equal to or lower than Bay 11-7085's MIC to *S. aureus* strain MW2 (4 µg/ml). Given the toxicity of Bay 11-7085 to primary cells, we conclude that Bay 11-7085 has the most potential as a topical treatment, such as in wound management.

Bay 11-7085 has Anti-Biofilm Activity Toward Three Phases of S. aureus Biofilm Maturation

Given Bay 11-7085's antimicrobial effect on *S. aureus* strains, we wondered if Bay 11-7085 would have any effect on the various stages of *S. aureus* biofilm formation and persistence: initial cell attachment, formation, and mature biofilm. To test this, we first

measured if Bay 11-7085 had any activity on the first stage of *S. aureus* biofilm formation, initial cell attachment [3]. To begin, we first tested the potency of various antibiotic-resistant *S. aureus* strains to form biofilm. Our trials revealed that *S. aureus* strain VRS1 [34], a vancomycin-resistant strain, was able to form a more robust biofilm than other antibiotic-resistant *S. aureus* strains such as MW2 (data not shown). We, therefore, decided to move forward with VRS1 in our biofilm studies. Subsequently, we found that Bay 11-7085 was able to inhibit initial cell attachment by >60% beginning at 8 µg/ml (2× MIC) and as much as >90% at 32 µg/ml (8× MIC) (Figure 4A). Additionally, we also confirmed that this activity was not due to the direct killing of *S. aureus* by Bay 11-7085 (Figure 4B) by measuring total CFU/ml (colony-forming units per ml) before and after treatment.

Next we tested whether Bay 11-7085's activity on initial cell attachment would lead to complete or partial inhibition of *S. aureus* strain VRS1 biofilm formation. We tested this by treating *S. aureus* strain VRS1 cells with various concentration of Bay 11-7085 under biofilm forming condition for 24 h. We found that Bay 11-7085 can significantly begin to inhibit *S. aureus* biofilm formation at concentrations as low as 8 µg/ml with >20% inhibition (Figure 4C). However, at high concentrations such as 32 µg/ml, Bay 11-7085 had an activity of >90% inhibition relative to no-treatment control (Figure 4C). Lastly, we tested if Bay 11-7085 would affect fully mature biofilm of *S. aureus* strain VRS1. Indeed, at concentrations higher than 32 µg/ml, Bay 11-7085 was able to eradicate biofilm >70% (Figure 4D). Given these data we conclude that Bay 11-7085 is a potent anti-biofilm compound with activity on initial cell attachment, biofilm formation, and eradication of mature biofilm.

Bay 11-7085 has Anti-Biofilm Activity Toward Three Phases of C. albicans and C. auris Biofilm Maturation

Next, we questioned whether Bay 11-7085 would also show potency on fungal biofilms. To answer this, we first tested if Bay 11-7085 would inhibit *C. albicans* strain SC5314 and *C. auris* strain #0384 biofilm formation. For our studies, we decided to measure total biofilm mass (including total ECM) using crystal violet (CV) methodology as well as total metabolically active cells using the colorimetric dye XTT [2–3-bis(2-methoxy-4-nitro-5-sulfophenyl)-2H-tetrazolium-5-carboxanilide]. After 24 h of incubation, we found that Bay 11-7085 can inhibit maturation of *C. albicans* total biofilm mass by >50% starting at 4 µg/ml (4× MIC) and as much as >70% at 8–32 µg/ml (8–32× MIC) (Figure 5A). In addition, *C. albicans* biofilm-forming cell viability was significantly decreased >15% starting at 1 µg/ml (1× MIC) and up to >50%, >60%, and >80% at 2, 4–16, and 32 µg/ml, respectively (Figure 5B). In the case of *C. auris*, we found that Bay 11-7085 inhibited total biofilm mass maturation starting at 8 µg/ml with >20% inhibition and as much as >60% at 16–32 µg/ml (Figure 5C). Furthermore, we found that Bay 11-7085 decreased cell metabolic activity by >20% at 16 µg/ml and 45% at 32 µg/ml (Figure 5D). From these data, we conclude that Bay 11-7085 can successfully inhibit the maturation of total biofilm mass, including ECM, comparable to total cell growth.

When we tested the ability of Bay 11-7085 to treat mature biofilm, we found that Bay 11-7085 began to eradicate *C. albicans* total biofilm mass beginning at 16 µg/ml with >30% eradication and >40% eradication at 32 µg/ml (Figure 5E). Surprisingly, after treating mature biofilm with various concentrations of Bay 11-7085 and subsequently incubating with XTT dye, we found that Bay 11-7085 is

ineffective at decreasing cell viability within *C. albicans* mature biofilm (Figure 5F). Moreover, *C. auris* biofilm mass was significantly eradicated beginning at 8 µg/ml at >10% and >30% at 16 µg/ml and >50% at 32 µg/ml, respectively (Figure 5G), while metabolic activity was not changed at 8 µg/ml but significantly decreased >30% at 16 µg/ml and >45% at 32 µg/ml (Figure 5H). We thus conclude that Bay 11-7085 is effective at decreasing the ECM of mature *Candida* spp. biofilm but not potent enough to completely kill biofilm residing cells for both of the species tested.

Lastly, when we looked at initial cell attachment, we found that Bay 11-7085 had greater activity against *C. auris* than *C. albicans* with >40% attachment inhibition at 4 µg/ml for *C. auris* (Figure 6A). At 8 µg/ml and 16–32 µg/ml *C. auris* initial cell attachment was inhibited >40% and >50%, respectively (Figure 6A). While *C. albicans* was inhibited >40% and >60% at 8 µg/ml and 16–32 µg/ml, respectively (Figure 6B). In summary, we conclude that Bay 11-7085 can partially inhibit and eradicate both *C. albicans* and *C. auris* biofilm as well as hinder initial cell attachment.

Given that Bay 11-7085 is fungicidal at high concentrations (Figure 2), concentrations that showed anti-biofilm activity (Figures 5, 6), we hypothesized that Bay 11-7085 would hinder initial cell attachment through direct killing of biofilm-forming cells. To test this, we treated $\sim 10^6$ CFU/ml stationary-phase fungal cells with various concentrations of Bay 11-7085 for 90 min and measured their viability. As expected, our results showed that Bay 11-7085 is able to kill *C. albicans* and *C. auris* cells within 90 min of treatment (Supplementary Figure S1), which we conclude leads to the decrease of initial cell attachment.

Bay 11-7085 has Anti-Biofilm Activity Toward Staphylococcal-Candida Polymicrobial Biofilm

So far, we showed that Bay 11-7085 demonstrates promising activity on both *S. aureus* and *Candida* spp. monoculture biofilms (Figures 4–6). We thus hypothesized that Bay 11-7085 would also have potency on biofilms of a polymicrobial culture of *S. aureus* strain VRS1 and *C. albicans* strain SC5413. To test this hypothesis, we first verified inhibition of initial cell attachment of co-cultured *S. aureus* and *C. albicans* in 50% serum-BHI medium for 90 min on nitrocellulose disks. Disks were washed, sonicated, and plated on selective plates to enumerate the total CFU/membrane of *S. aureus* strain VRS1 and *C. albicans* strain SC5314 cells. Like monoculture experiments, Bay 11-7085 is potent enough to inhibit initial cell attachment of both *S. aureus* and *C. albicans* during polymicrobial co-culture, with *S. aureus* strain VRS1 showing a significant reduction of >55% at 16 µg/ml and >70% at 32 µg/ml (Figure 7A). When we tested *C. albicans*, we found that consistent with our monoculture results, Bay 11-7085 and is more effective on *C. albicans* than *S. aureus*, with *C. albicans* being significantly reduced by >75% at 8 µg/ml and >97% starting at 16–32 µg/ml (Figure 7B).

We then questioned whether Bay 11-7085's effect on initial cell attachment would also hinder the maturation of polymicrobial *S. aureus-C. albicans* biofilm. To investigate this, we treated *S. aureus-C. albicans* co-cultures with Bay 11-7085 at various concentrations and quantified total biomass produced using 1% CV after 24 h of incubation. As expected, Bay 11-7085 was able to inhibit biofilm formation with >45% inhibition at 16 µg/ml and >75% inhibition at 32 µg/ml (Figure 7C).

Lastly, we hypothesized that Bay 11-7085 would have activity on mature *S.*

aureus-*C. albicans* polymicrobial biofilm. We treated fully mature biofilm with various concentrations of Bay 11-7085 and quantified total biofilm remaining, using 1% CV, after a 24 h incubation period. Our findings showed that Bay 11-7085 can significantly eradicate >35% of mature biofilm at concentrations 8–32 µg/ml (Figure 7D). This reduction was greater than with the antibiotic daptomycin (8× MIC) or antifungal amphotericin B (32× MIC) treatment alone and was not significantly different than treatment with a combination of both daptomycin and amphotericin B (Figure 7D). From these studies, we conclude that Bay 11-7085 is not only a potent agent against monoculture biofilms, but is also effective at combating polymicrobial biofilms.

Bay 11-7085 Shows Activity Against C. albicans in an In Vitro Multispecies Lubbock Chronic Wound Model

We then asked whether Bay 11-7085 would have activity on *S. aureus* strain VRS1 or *C. albicans* strain SC5413 co-culture in a more clinically relevant *in vitro* wound-like model. To assess this, we employed the use of the *in vitro* multispecies Lubbock chronic wound biofilm model originally designed by Sun et al. (2008). This model leveraged the use of a unique wound like media (WLM) composed of 50% Bolton Broth, 45% heparinized calf serum, and 5% haemolyzed horse blood to simulate a wound like environment. In WLM, *S. aureus* coagulase-positive strains will form a jelly-like mass of the media. For this reason, we decided to only test Bay 11-7085's activity against biofilm inhibition. Although Bay 11-7085 did not have any effect on *S. aureus* biofilm growth in WLM (Figure 8A), Bay 11-7085 was able to significantly reduce total CFU/ml of *C. albicans* residing within the polymicrobial biofilm by >50%, which was not significantly different than treatment with the combination of

the antibiotic daptomycin and antifungal amphotericin B (Figure 8B). Interestingly, we found that treatment of daptomycin alone abolished *S. aureus* cells completely. However, treatment with daptomycin also allowed *C. albicans* to overgrow >200% more than no treatment control, while treatment with Bay 11-7085 did not allow overgrowth of either organism (Figure 8). We thus conclude that Bay 11-7085 has greater activity on *C. albicans* in an *in vitro* chronic wound biofilm model.

Bay 11-7085 Shows Activity in a C. elegans-C. albicans Infection Model

The data described above shows that Bay 11-7085 is a slightly more potent antimicrobial to *Candida* spp. rather than *S. aureus*. Therefore, to further evaluate Bay 11-7085 as a potential lead anti-infective compound against *Candida* spp., we wanted to test Bay 11-7085s potency in a whole animal infection model system. Accordingly, we tested whether Bay 11-7085 would be able rescue *C. elegans* from *C. albicans*-mediated killing. Worms were first exposed to *C. albicans* strain SC5314 previously grown overnight on BHI agar plates. Worms were then washed and then treated with various concentrations of Bay 11-7085 for a total of 6 days. In the presence of Bay 11-7085, we found a significant increase in the survival of *C. elegans* starting at 8 µg/ml and up to 16 µg/ml. Although there was a significant increase in survival at 32 µg/ml, this was less than at 16 µg/ml (Figure 9). We thus conclude that Bay 11-7085 has potency at combating a *C. albicans* infection in a whole animal system at 8–16 µg/ml. Yet, at higher concentrations such as 32 µg/ml, we theorize a decrease in survival is due to toxicity at long exposure times.

Discussion

In this study, we report a new bioactivity of Bay 11-7085 as an antimicrobial, effective against two biofilm-forming pathogens associated with wound infections: *S. aureus* and *Candida* spp. We show that the MIC of this compound against MRSA and VRSA strains is 4 µg/ml, while the MIC to *C. albicans* and *C. auris* is 0.5–1 µg/ml. Importantly, Bay 11-7085 is also active on both bacterial and fungal biofilm in monoculture and polymicrobial co-culture.

Intriguingly, Bay 11-7085 was originally identified as a potential anti-inflammatory agent by inhibiting the dissociation of IκB-α from NF-κB, thus blocking TNFα-induced phosphorylation of IκB-α [42]. This inhibition of IκB-α phosphorylation by Bay 11-7085 is irreversible and shows a median inhibitory concentration of 10 µM (2.5 µg/ml) [42]. At the dose of 20 mg/kg, Bay 11-7085 also showed *in vivo* anti-inflammatory efficacy in a carrageenan rat paw edema model and a rat adjuvant arthritis model [42]. In addition, Bay 11-7085 can also induce apoptosis of cancerous cells by inhibiting NF-κB signaling. However, previous reports also show that Bay 11-7085 demonstrates anti-cancer activity in an NF-κB-independent manner, all of which indicates that Bay 11-7085 may possess multiple bioactivities [43,44]. Given Bay 11-7085's high level of toxicity to cancer and primary cells *in vitro* (Figure 3C), we theorize that this is mainly due to its multiple mechanisms of eliciting cell apoptosis. Bacteria, on the other hand, do not have NF-κB signaling. Although yeasts have a similar but primitive NF-κB-like signaling pathway, called the retrograde response (RTG) pathway, the inhibition of RTG in yeast does not result in the rapid killing of yeast cells [45]. Like ciprofloxacin, if Bay 11-7085 had only a single target in MRSA, a

resistant mutant would presumably emerge during a 25-day serial passage trial [46]. However, according to our results, this is not the case (Figure 1D). Low rates of resistance development are associated with membrane active compounds [20–22]; however, we observed that Bay 11-7085 did not affect membrane permeability (data not shown). Therefore, it is most likely that Bay 11-7085 may have multiple targets responsible for its antimicrobial activity.

Several reports, especially those concerning immunocompromised patients, have associated antibacterial therapy with subsequent fungal infections [43]. These fungal infections are believed to be caused by antibacterial agents killing microbial competitors of fungi [43] which allow fungi to overgrow and cause infection. The idea of fungal overgrowth is seemed to be supported by our *in vitro* biofilm wound like model data, where we see that treatment of *S. aureus*-*C. albicans* co-culture with daptomycin alone leads to complete killing of *S. aureus* but a 200% increase in *C. albicans* growth (Figure 8B). To prevent this secondary mycoses, antifungal agents are used prophylactically during antibacterial treatments [43]. Therefore, compounds combining narrow-spectrum antibacterial activity and antifungal potency can be clinically beneficial. To date, several agents with dual antibacterial and antifungal potency have been identified and synthesized [44,47–50]. However, except for the synthetic antimicrobial peptide omiganan, none of them are potent against biofilms, and although omiganan shows antibacterial potency against MRSA biofilms, it shows low antifungal activity against *C. albicans* with an MIC >64 µg/ml [48]. Bay 11-7085, however, has strong dual antimicrobial activity with a MIC of 0.5–4 µg/ml against both *S. aureus* and *C. albicans* (Table 1, Supplementary Table S2) and is potent

against biofilms formed by *S. aureus* or *C. albicans* (Figures 4–6). Furthermore, Bay 11-7085 shows narrow spectrum antibacterial activity to *S. aureus* (Table 1). With its low probability of resistance development, Bay 11-7085 is a promising lead compound for prophylactic use.

Biofilms are composed of an ECM which house low metabolically active bacteria, facilitate quorum sensing, and thus creates increased antimicrobial protection to their resident bacteria relative to planktonic state bacteria [4,51,52]. Our studies show that Bay 11-7085 can directly kill cells residing within both *S. aureus* and *Candida* spp. biofilm demonstrating that Bay 11-7085 is able to penetrate the ECM effectively. In addition, we show that *C. albicans* initial cell attachment is inhibited by Bay 11-7085. In the case of *S. aureus*, our data show that Bay 11-7085 cannot directly kill bacteria during the initial cell attachment stage of biofilm formation. Therefore, we theorize Bay 11-7085 may also have anti-virulence activity, possibly targeting adhesion molecules needed for biofilm attachment[3]. Furthermore, our data show that Bay 11-7085 was unable to decrease *C. albicans* cell viability within mature biofilm but was able to decrease total biomass. We hypothesize that this may be due to reduced virulence factors, similar to *S. aureus*, but which may affect the formation of ECM instead of only attachment. Although Bay 11-7085 had some activity on *C. auris* mature biofilm cell viability, our data does show a trend where Bay 11-7085 was more effective at reducing total biomass than direct killing of biofilm residing cells. We therefore conclude that Bay 11-7085 may have dual functionality in which it can kill biofilm residing cells directly but can independently affect virulence factors. All together, these data highlight Bay 11-7085 as a potent anti-biofilm agent capable of combating both

S. aureus and *Candida spp.* biofilm.

As stated previously, *S. aureus* and *C. albicans* are human commensals able to coexist together in various human organs such as the skin [53,54]. However, both can readily turn from commensal to pathogenic when host immunity is compromised [55]. *C. albicans* and *S. aureus* have been co-isolated from a range of biofilm-associated infections, including cystic fibrosis, catheter-associated urinary tract infections, and burn wound infections [53]. These polymicrobial infections caused by *S. aureus* and *C. albicans* are difficult-to-treat due to formation of mixed biofilms and are more virulent due to so-called synergistic pathogen-pathogen interactions [53,55]. While *S. aureus* is a weak biofilm former in the presence of serum, *C. albicans* can readily form biofilms. Once *C. albicans* biofilm matures, *S. aureus* can attach and form biofilms on the surface of *C. albicans* extracellular walls [33]. *C. albicans* hyphae can pierce epithelial layers in this mixed biofilm state, which facilitates *S. aureus* invasion [56]. Moreover, *C. albicans* is known to enhance the production of *S. aureus* virulence factors, such as alpha- and delta-toxins [57]. Consistently, it has been reported that mice co-infected with sub-lethal doses of *S. aureus* and *C. albicans* induce the rapid rise of morbidity and mortality [55,57].

Considering the mechanisms of polymicrobial biofilm formation by *S. aureus* and *C. albicans*, Bay 11–7085 shows promising potential to inhibit the formation of these polymicrobial biofilms. Bay 11-7085 demonstrates relatively higher anti-biofilm activity against *Candida spp.* monoculture biofilms compared to *S. aureus* monoculture biofilms (Figures 4–6) and in addition shows a significant reduction in initial cell attachment, maturation, and eradication in a polymicrobial biofilm culture (Figure 7). It blocks fungal biofilm formation by direct killing of cells and prevents bacterial biofilm formation by

inhibiting initial attachment. In physiological conditions, the key event for developing the polymicrobial biofilms is the maturation of *Candida* spp. Therefore, the fungicidal activity of Bay 11–7085 would effectively block this critical step and thus may impede the following step of *S. aureus* initial cell attachment.

Although we were not able to show a reduction in *S. aureus* cell number in our *in vitro* chronic wound like model, we did find that Bay 11-7085 was able to reduce *C. albicans* cell viability significantly. However, due to our experimental model, we were unable to quantify total biofilm mass. With the reduction of *C. albicans* cell viability, we hypothesize that a Bay 11-7085 may possibly have greater effect on biofilm mass rather than cell viability, which we are unable to test via our model. Further studies would be needed to assess biofilm mass reduction in a wound like model.

Regarding *S. aureus* and the lack of activity by Bay 11-7085 on our *in vitro* WLM model, we speculate this may be partially attributed to coagulation. More specifically, in our model, we used 5% haemolyzed horse blood to mimic a more relevant physiological environment. *S. aureus* strain VRS1 is coagulase-positive (CoP). In the presence of blood, *S. aureus* CoP strains secrete coagulase enzymes, which aid in converting fibrinogen into fibrin. Bacteria begin to interlock and form blood clots. These blood clots are protective to the bacteria and have been shown to increase antimicrobial resistance [58]. However, not all *S. aureus* strains are CoP and it is possible that Bay 11-7085 may have greater efficacy on *S. aureus* coagulase-negative strains, which would also correlate with our polymicrobial anti-biofilm data using blood-negative media (Figures 4, 7). However, additional studies would be needed to confirm the difference between other non-CoP strains.

Although Bay 11-7085 has advantages as an antimicrobial lead compound, it has limitations that need to be resolved. First, Bay 11-7085 shows cytotoxicity to cancer cell lines and primary renal proximal tubule epithelial cells (RPTEC) (Figure 3C). Although Bay 11-7085 induces cancer cell apoptosis by inhibiting NF- κ B signaling, the MOA of its cytotoxicity to RPTEC is unknown. In contrast to our *in vitro* toxicity results (Figure 3C), Bay 11-7085 did not cause observable toxicity in a rat model at a dose of 50 mg/kg (Pierce et al., 1997), consistent with our *C. elegans in vivo* toxicity data (Figure 3A). In any case, the cytotoxicity profile of Bay 11-7085 needs to be further evaluated. Furthermore, to repurpose Bay 11-7085 as an antimicrobial, its NF- κ B inhibitory activity would need to be reduced or nullified. In addition, its antimicrobial mode of action needs to be elucidated for further optimization. Since Bay 11-7085 is expected to have multiple targets, it may be difficult to identify its modes of action. However, current advances in deep learning-based prediction, quantitative imaging, proteomic, genetic, and metabolomic analyses enable elucidating antimicrobial mechanisms having uncommon or multiple modes of action [59].

In conclusion, our studies show that Bay 11-7085 is a potent antimicrobial agent against MRSA, VRSA, and *Candida* spp. Bay 11-7085 shows anti-biofilm activity on both monocultures as well as in mixed cultures and resistant MRSA mutants did not appear after 25 days of serial passaging. We thus find Bay 11-7085 to be a promising lead compound useful for identifying new antimicrobial targets that show low resistance and anti-biofilm activity against pathogens commonly associated with wound biofilms.

Data Availability Statement

The raw data supporting the conclusion of this article will be made available by the authors, without undue reservation.

Author Contributions

All experiments were performed by IE, FP, SK and MK. Data analysis was conducted by IE and FP. The original draft was prepared by IE. Review and editing was done by WK and EM. All authors have read and agreed to the published version of the manuscript.

Funding

This research was funded by NIH grant P01 AI083214 to EM. IE was supported by sub-award 530804. WK is supported by the National Research Foundation of Korea Grants funded by the Korean government (MSIT) (2020R1C1C1008842, 2018R1A5A2025286 and 2017M3A9E4077234). The authors have no other relevant affiliations or financial involvement with any organization or entity with a financial interest in, or financial conflict with, the subject matter or materials discussed in the manuscript, apart from those disclosed. No writing assistance was utilized in the production of this manuscript.

Figures and Tables

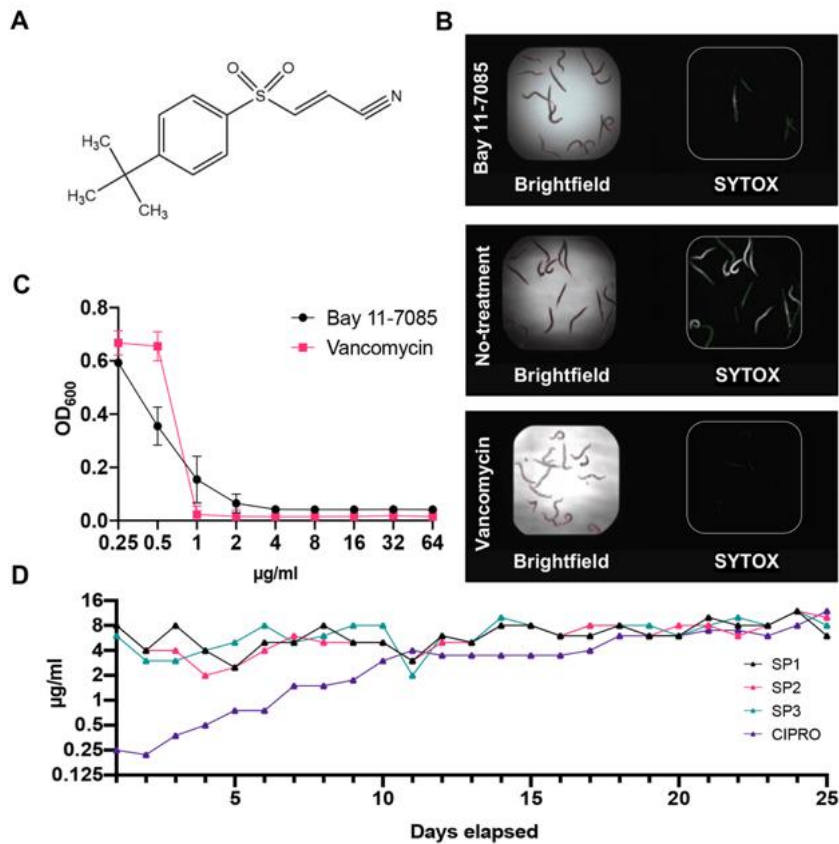


Figure 1. Bay 11-7085 rescues *C. elegans* from a MRSA infection and shows low antibiotic resistance to *S. aureus* strain MW2.

(A) Chemical structure of Bay 11-7085. **(B)** Fifteen MRSA-infected *C. elegans* were treated with 7.14 $\mu\text{g/ml}$ Bay 11-7085, 0.1% dimethyl sulfoxide (DMSO) (no-treatment) or 10 $\mu\text{g/ml}$ vancomycin for 5 days. After staining dead worms with Sytox Orange, brightfield (left) and fluorescence (right) images were obtained. **(C)** *In vitro* activity of Bay 11-7085 and antibiotic control vancomycin against MRSA strain MW2. Bacterial growth is quantified as a measure of OD_{600} . **(D)** Three individual MRSA strain MW2

replicates (SP1-3) were serially passaged in increasing concentrations of Bay 11-7085 for 25 days. Passages with ciprofloxacin (CIPRO) were conducted in parallel as a control.

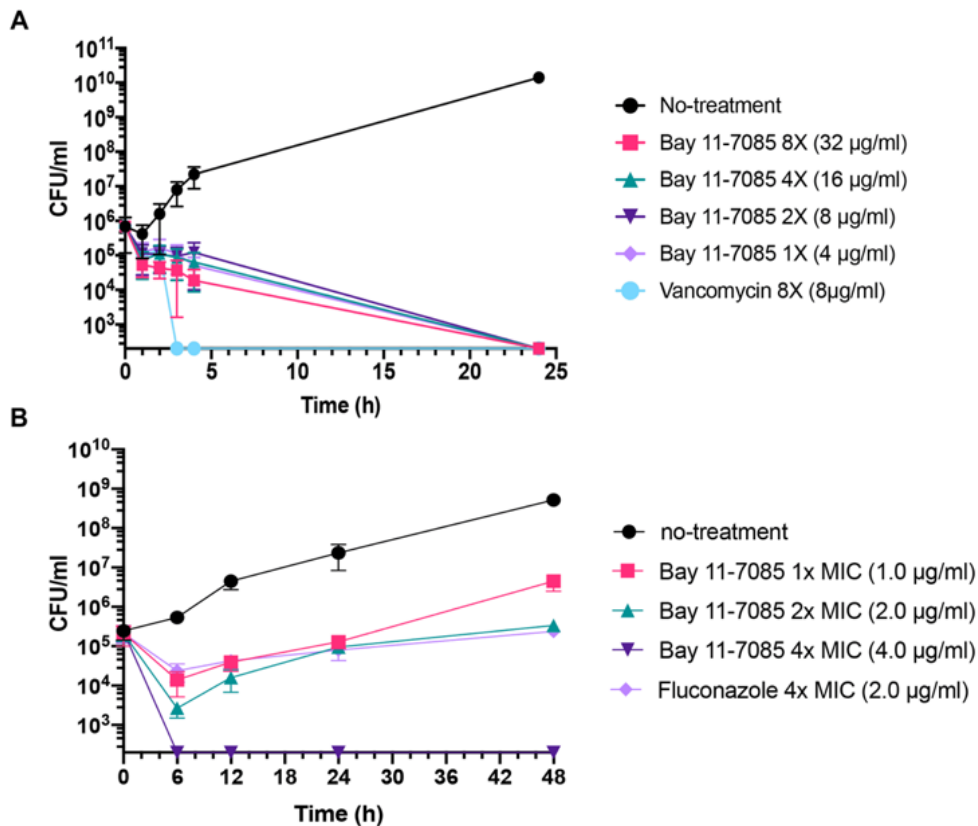


Figure 2. Bay 11-7085 is bactericidal toward MRSA and fungistatic toward *C. albicans*.

(A) MRSA strain MW2 cells were grown to log phase OD₆₀₀ 0.3-0.4 from overnight liquid culture. Log phase cells were diluted to 10⁶ CFU/mL in various concentration of Bay 11-7085 and 8 µg/mL of vancomycin as a positive control. **(B)** Overnight culture of *C. albicans* strain SC5314 was diluted to ~ 10⁶ CFU/mL and added to 1x (1 µg/mL), 2x (2 µg/mL) and 4x (4 µg/mL) MIC of Bay 11-7085. Fluconazole was used a positive control at 4x MIC (2.0 µg/mL). Samples were collected at various time point, serially diluted, and plated to measure total CFU/mL. (*n*=3, ± S.D.).

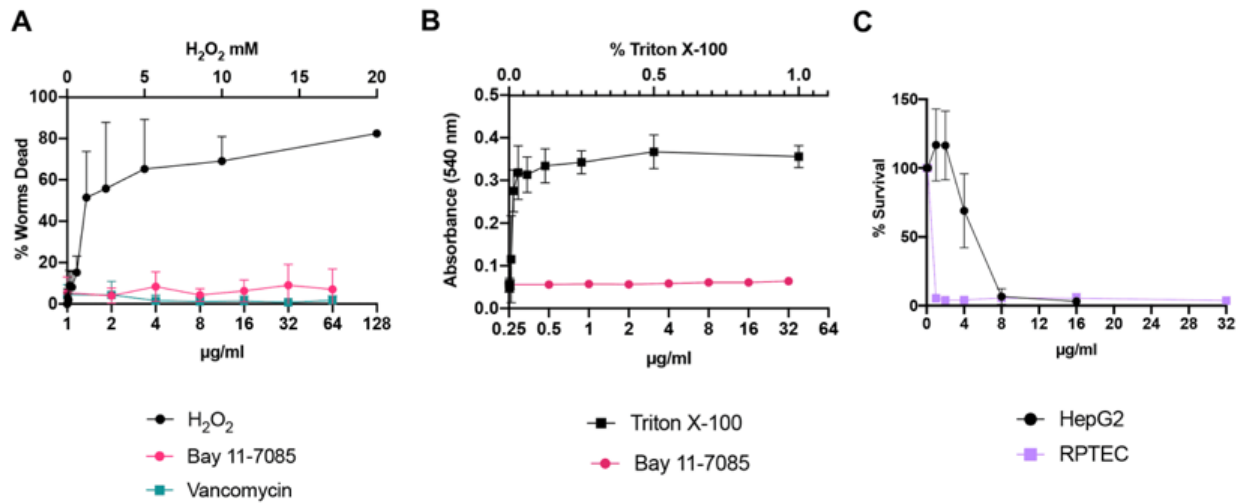


Figure 3. Bay 11-7085 shows varied toxicity to *C. elegans*, human red blood cells, and mammalian cells.

Bay 11-7085s toxicity profile to **(A)** *C. elegans*, **(B)** human red blood cells, and **(C)** mammalian cells at multiple concentrations. X-axis represents concentrations of Bay 11-7085 in µg/mL. Hydrogen peroxide (H₂O₂) was used as a positive control in our *C. elegans* toxicity assay. Triton-X 100 was used as a positive control in our human red blood cell lysis assay. (*n*=3, ± S.D.).

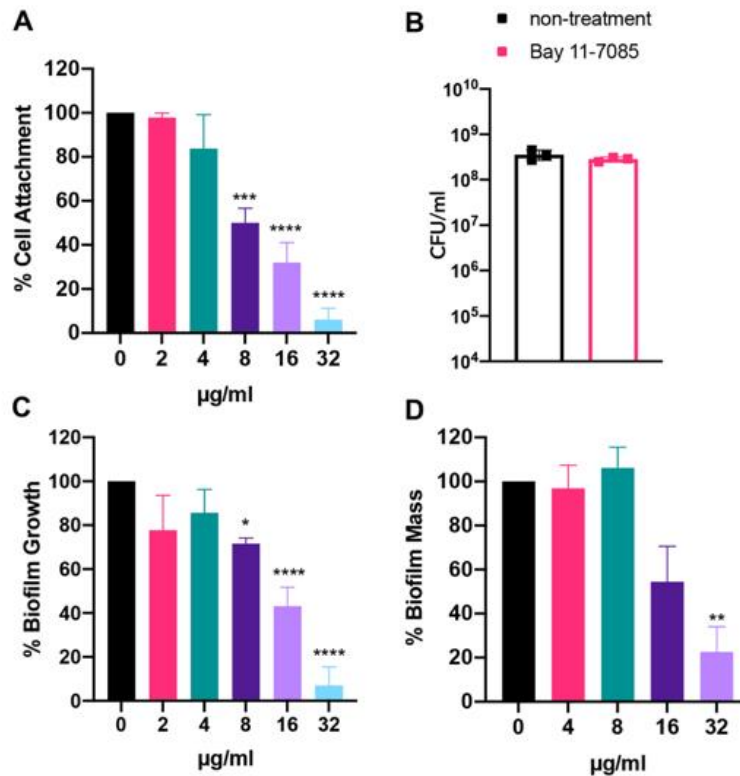


Figure 4. Bay 11-7085 shows anti-biofilm activity toward three phases of *S. aureus* strain VRS1 biofilm maturation.

Efficacy of Bay 11-7085 at various concentrations were tested against *S. aureus* strain VRS1 biofilm (A) initial cell attachment. (B) CFU/mL was measured for treated and untreated conditions after initial cell attachment assay. *S. aureus* strain VRS1 biofilm (C) inhibition and (D) eradication was measured using 1 % crystal violet. X-axis represents concentrations of Bay 11-7085 in µg/mL. Statistical significance was determined using one-way ANOVA with Dunnett's test for multiple comparisons. * $p < 0.05$; ** $p < 0.01$; *** $p < 0.001$; **** $p < 0.0001$. ($n=3$, \pm S.D.).

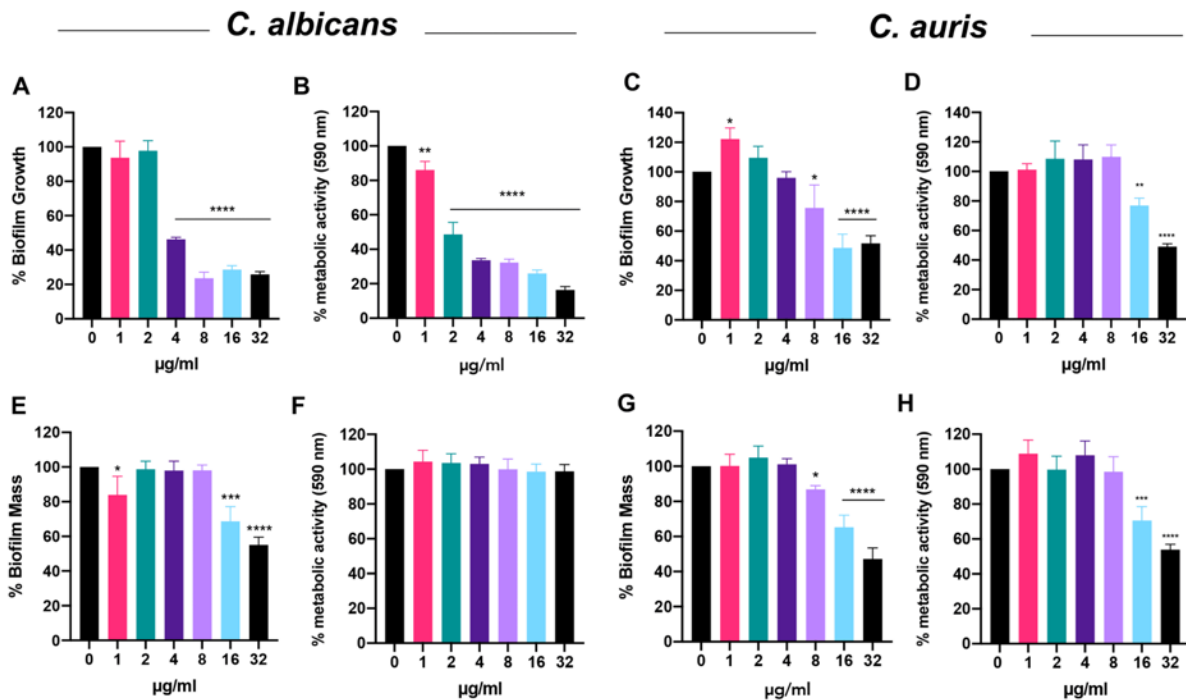


Figure 5. Bay 11-7085 shows anti-biofilm activity toward *C. albicans* and *C. auris* biofilm formation and maturation biofilm.

Efficacy of Bay 11-7085 was measured against *C. albicans* strain SC5314 and *C. auris* strain #0384 biofilm inhibition and eradication. Total biomass was measured using 1 % crystal violet (CV). Metabolic activity was measured using XTT (590 nm). Inhibition of *C. albicans* biofilm formation by various concentrations of Bay 11-7085 as measured by **(A)** 1 % CV and **(B)** XTT dye. Inhibition of *C. auris* biofilm formation by various concentrations of Bay 11-7085 as measured by **(C)** 1 % CV and **(D)** XTT dye. *C. albicans* biofilm eradication as measured by **(E)** 1 % CV, and **(F)** XTT dye. *C. auris* biofilm eradication as measured by **(G)** 1 % CV and **(H)** XTT dye. X-axis represents concentrations of Bay 11-7085 in µg/mL. Statistical significance was determined using

one-way ANOVA with Dunnett's test for multiple comparisons. * $p < 0.05$; ** $p < 0.01$; *** $p < 0.001$; **** $p < 0.0001$. ($n=3$, \pm S.D.).

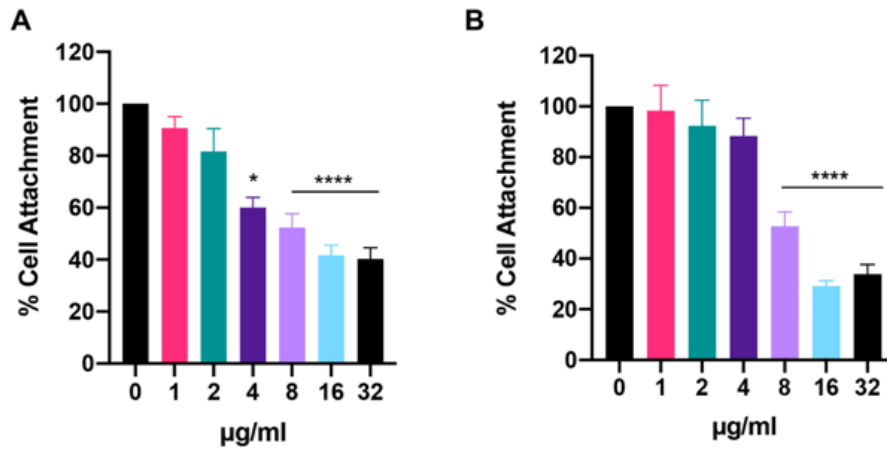


Figure 6. Bay 11-7085 shows anti-biofilm activity against *C. albicans* and *C. auris* initial cell attachment.

(A) *C. auris* strain #0384 and **(B)** *C. albicans* strain SC5314 initial cell attachment was measured using XTT. X-axis represents concentrations of Bay 11-7085 in µg/mL. Statistical significance was determined using one-way ANOVA with Dunnett's test for multiple comparisons. * $p < 0.05$; **** $p < 0.0001$. ($n=3$, \pm S.D.).

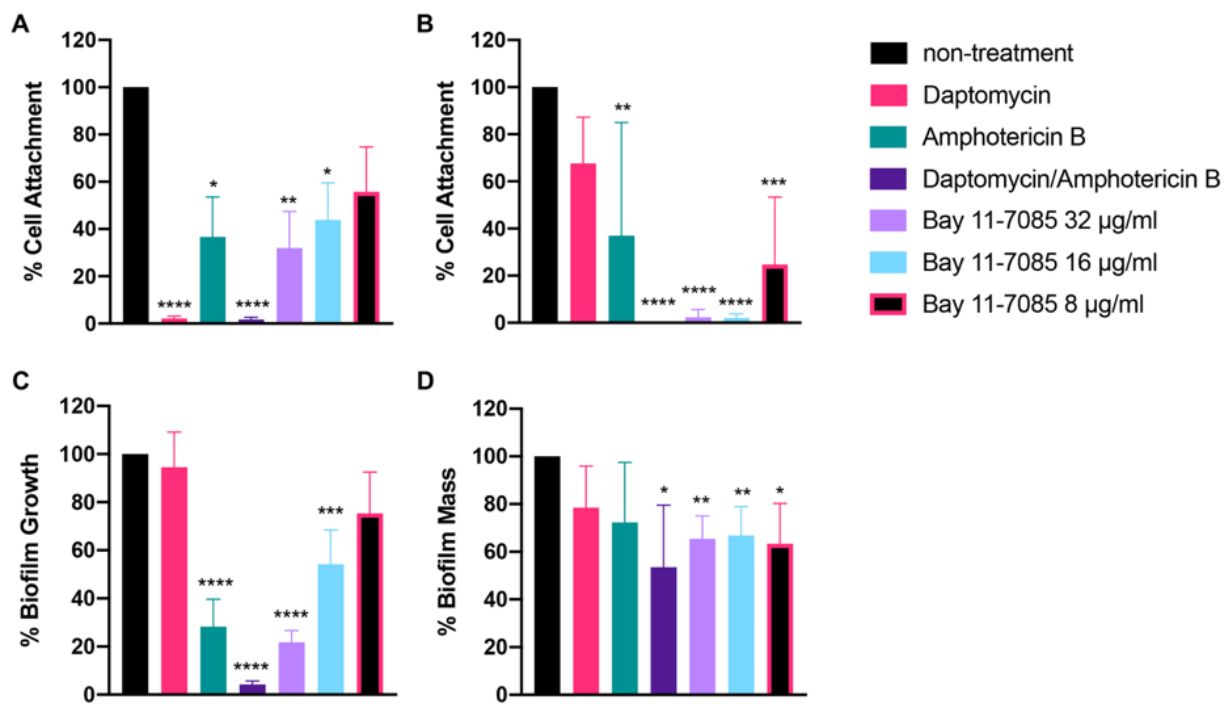


Figure 7. Bay 11-7085 shows anti-biofilm activity towards three phases of *S. aureus*-*C. albicans* polymicrobial biofilm maturation.

Activity of Bay 11-7085 at various concentrations was tested against *S. aureus* VRS1-*C. albicans* SC5314 polymicrobial biofilm initial cell attachment, maturation, and eradication. *S. aureus* strain VRS1 and *C. albicans* strain SC5314 were grown overnight in BHI or YPD medium respectively. Cells were washed and co-cultured at a 1:10 ratio *S. aureus* strain VRS1 to *C. albicans* strain SC5413 under treatment of daptomycin 8x MIC (8 µg/mL), amphotericin B 32x MIC (16 µg/mL), a combination of both daptomycin and amphotericin B and Bay 11-7085 at 36 µg/mL, 16 µg/mL, and 8 µg/mL. Percent cell attachment was normalized to non-treatment control for **(A)** *S. aureus* strain VRS1, and **(B)** *C. albicans* strain SC5413 after treatment. Bay 11-7085s activity on *S. aureus* VRS1-*C. albicans* SC5314 biofilm inhibition **(C)** and eradication **(D)** of mature biofilm

was measured using 1% CV. Statistical significance was determined using one-way ANOVA with Dunnett's test for multiple comparisons (A-C) or Unpaired t-test (D). * $p < 0.05$; ** $p < 0.01$; *** $p < 0.001$; **** $p < 0.0001$. ($n=3$, \pm S.D.)

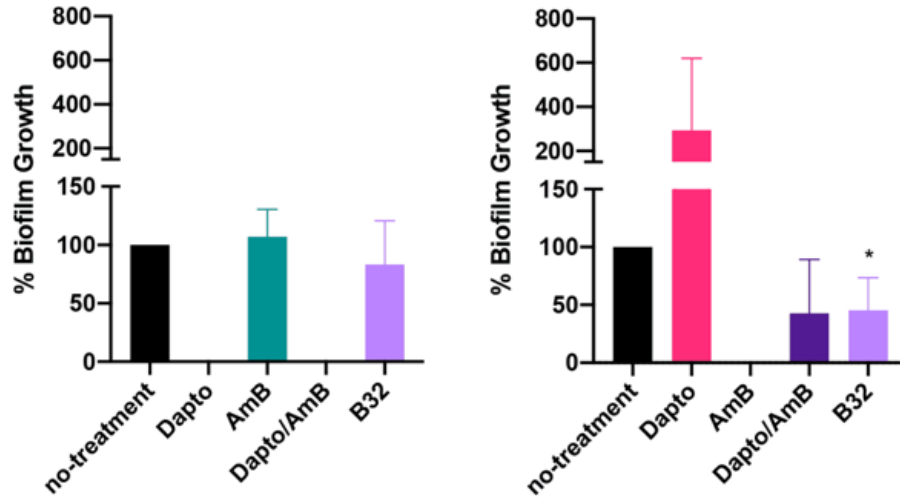


Figure 8. Bay 11-7085 inhibits *C. albicans* but not *S. aureus* growth in an *in vitro* multispecies Lubbock chronic wound model.

(A) *S. aureus* strain VRS1 percent growth after treatment with Bay 11-7085 at 8 µg/mL (B8), 16 µg/mL (B16), or 32 µg/mL (B32) for 24 h. Treatment with 8x daptomycin (8 µg/mL, Dapto), 16x amphotericin B (16 µg/mL, AmB), or a combination of 8x daptomycin and 16x amphotericin B (Dapto/AmB) where used as controls. **(B)** *C. albicans* percent growth after treatment with Bay 11-7085 for 24 h. Statistical significance was determined using Unpaired t-test. * $p < 0.05$. ($n=3$, \pm S.D.).

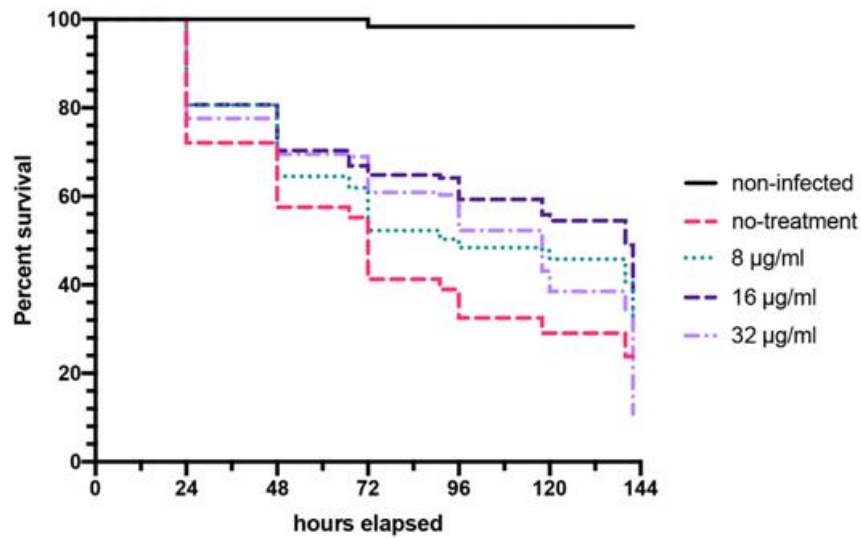


Figure 9. Bay 11-7085 prolongs *C. elegans* survival after *C. albicans* infection.

C. elegans were exposed to *C. albicans* strain SC5314 grown on BHI agar plates, washed, and treated with various concentrations of Bay 11-7085 in liquid medium. Statistical significance was determined using Log-rank (Mantel-Cox). ($n=3$).

Table 1. Minimum inhibitory concentrations ($\mu\text{g/mL}$) of Bay 11-7085 and conventional antibiotics against various pathogenic strains.

Strain	Bay 11-7085	Oxa	Van	Gm	Cipro	FLC
<i>Staphylococcus aureus</i> MW2	4	64	1	0.5	0.25	n.d.
<i>Staphylococcus aureus</i> LAC	2	8	0.5	0.25	8	n.d.
<i>Staphylococcus aureus</i> WKZ-1	4	0.5	1	0.5	1	n.d.
<i>Staphylococcus aureus</i> WKZ-2	2	64	1	0.5	1	n.d.
<i>Staphylococcus aureus</i> ATCC 25923	2	0.25	2	0.25	0.25	n.d.
<i>Staphylococcus aureus</i> ATCC 29213	2	0.25	1	0.5	0.5	n.d.
<i>Staphylococcus aureus</i> ATCC 43300	4	16	1	>64	0.5	n.d.
<i>Staphylococcus aureus</i> VRS1	4	>64	>64	64	64	n.d.
<i>Enterococcus faecium</i> E007	64	16	4	>64	1	n.d.
<i>Enterococcus faecalis</i> MMH 594	64	32	2	>64	0.5	n.d.
<i>Klebsiella pneumoniae</i> KCTC2242	>64	>64	>64	1	<0.06 25	n.d.
<i>Klebsiella pneumoniae</i> WGLW2	>64	>64	>64	1	<0.06 25	n.d.
<i>Pseudomonas aeruginosa</i> ATCC 27853	>64	>64	>64	4	0.5	n.d.
<i>Pseudomonas aeruginosa</i> PA14	>64	>64	>64	2	<0.06 25	n.d.
<i>Enterobacter aerogenes</i> KCTC 2190	>64	>64	>64	1	<0.06 25	n.d.
<i>Candida albicans</i> SC5314	1	n.d.	n.d.	n.d.	n.d.	0.25
<i>Candida glabrata</i> ATCC 90030	1	n.d.	n.d.	n.d.	n.d.	8
<i>Candida parapsilosis</i> ATCC 22019	8	n.d.	n.d.	n.d.	n.d.	1
<i>Candida auris</i> AR-BANK #0381 (CDC)	0.5	n.d.	n.d.	n.d.	n.d.	n.d.

Oxa: oxacillin Van: vancomycin, Gm: gentamicin, Cipro: ciprofloxacin, FLC: fluconazole

Supplementary Figures and Tables

Table S1. Microbial strains used in this study.

Species	Strain	Genotype	Reference
<i>Staphylococcus aureus</i>	MW2	SCCmec Type IV	(Baba et al., 2002)
<i>Staphylococcus aureus</i>	LAC	SCCmec Type IVa	(Kennedy et al., 2008)
<i>Staphylococcus aureus</i>	WKZ-1	<i>SdrC</i> , <i>SdrD</i> , <i>Bbp</i> , SaPI2	(Bloemendaal et al., 2010)
<i>Staphylococcus aureus</i>	WKZ-2	SCCmec, <i>SdrC</i> , <i>SdrD</i> , <i>Bbp</i> , SaPI2	(Bloemendaal et al., 2010)
<i>Staphylococcus aureus</i>	ATCC 25923	Reference strain, SCCmec-like element lacking <i>mecA</i>	(Ito et al., 2001)
<i>Staphylococcus aureus</i>	ATCC 29213	Reference strain, <i>mecA</i> negative	(Ikonomidis et al., 2008), (Soni et al., 2015)
<i>Staphylococcus aureus</i>	ATCC 43300	SCCmec Type II, <i>pvl</i> negative	ATCC® 43300
<i>Staphylococcus aureus</i>	VRS1	SCCmec, <i>vanA</i>	(Bozdogan et al., 2004)
<i>Enterococcus faecium</i>	E007	Clinical Isolate from Massachusetts General Hospital, tetracycline resistant	(Garsin et al., 2001)
<i>Enterococcus faecalis</i>	MMH 594	Clinical isolate from University of Wisconsin and Clinics, resistance to erythromycin and gentamicin	(Huycke et al., 1991)
<i>Klebsiella pneumoniae</i>	KCTC2242	Reference strain	(Shin et al., 2012b)
<i>Klebsiella pneumoniae</i>	WGLW2	Reference strain, Broad Institute	Project accession: AML000000000
<i>Pseudomonas aeruginosa</i>	ATCC 27853	Reference Strain	ATCC® 27853, (Cao et al., 2017)
<i>Pseudomonas</i>	PA14	Reference Strain	(Rahme et al., 1995)

<i>aeruginosa</i>			
<i>Enterobacter aerogenes</i>	KCTC 2190	Reference Strain	(Shin et al., 2012a)
<i>Candida albicans</i>	SC5314	Reference Strain	(Bartelli et al., 2018)
<i>Candida glabrata</i>	ATCC 90030	Reference Strain	ATCC® 90030
<i>Candida parapsilosis</i>	ATCC 22019	Reference Strain	ATCC® 22019
<i>Candida auris</i>	AR-BANK #0381	Clinical isolate, fluconazole resistant	CDC Clinical Isolate Bank, Panel ID: CAU
<i>Candida auris</i>	AR-BANK #0382	Clinical isolate, fluconazole resistant	CDC Clinical Isolate Bank, Panel ID: CAU
<i>Candida auris</i>	AR-BANK #0383	Clinical isolate, fluconazole resistant	CDC Clinical Isolate Bank, Panel ID: CAU
<i>Candida auris</i>	AR-BANK #0384	Clinical isolate, fluconazole resistant	CDC Clinical Isolate Bank, Panel ID: CAU
<i>Candida auris</i>	AR-BANK #0385	Clinical isolate, fluconazole resistant	CDC Clinical Isolate Bank, Panel ID: CAU
<i>Candida auris</i>	AR-BANK #0386	Clinical isolate, fluconazole resistant	CDC Clinical Isolate Bank, Panel ID: CAU
<i>Candida auris</i>	AR-BANK #0387	Clinical isolate, fluconazole resistant	CDC Clinical Isolate Bank, Panel ID: CAU
<i>Candida auris</i>	AR-BANK #0388	Clinical isolate, fluconazole resistant	CDC Clinical Isolate Bank, Panel ID: CAU
<i>Candida auris</i>	AR-BANK #0389	Clinical isolate, fluconazole resistant	CDC Clinical Isolate Bank, Panel ID: CAU
<i>Candida auris</i>	AR-BANK #0390	Clinical isolate, fluconazole resistant	CDC Clinical Isolate Bank, Panel ID: CAU

Table S1 References

Baba, T., Takeuchi, F., Kuroda, M., Yuzawa, H., Aoki, K., Oguchi, A., et al. (2002). Genome and virulence determinants of high virulence community-acquired MRSA. *Lancet* 359, 1819–1827. doi:10.1016/s0140-6736(02)08713-5.

Bartelli, T. F., Bruno, D. do C. F., and Briones, M. R. S. (2018). Whole-Genome Sequences and Annotation of the Opportunistic Pathogen *Candida albicans* Strain SC5314 Grown under Two Different Environmental Conditions. *Genome Announc* 6, e01475-17. doi:10.1128/genomea.01475-17.

- Bloemendaal, A. L. A., Brouwer, E. C., and Fluit, A. C. (2010). Methicillin Resistance Transfer from *Staphylococcus epidermidis* to Methicillin-Susceptible *Staphylococcus aureus* in a Patient during Antibiotic Therapy. *Plos One* 5, e11841. doi:10.1371/journal.pone.0011841.
- Bozdogan, B., Ednie, L., Credito, K., Kosowska, K., and Appelbaum, P. C. (2004). Derivatives of a Vancomycin-Resistant *Staphylococcus aureus* Strain Isolated at Hershey Medical Center. *Antimicrob Agents Ch* 48, 4762–4765. doi:10.1128/aac.48.12.4762-4765.2004.
- Cao, H., Lai, Y., Bougouffa, S., Xu, Z., and Yan, A. (2017). Comparative genome and transcriptome analysis reveals distinctive surface characteristics and unique physiological potentials of *Pseudomonas aeruginosa* ATCC 27853. *Bmc Genomics* 18, 459. doi:10.1186/s12864-017-3842-z.
- Garsin, D. A., Sifri, C. D., Mylonakis, E., Qin, X., Singh, K. V., Murray, B. E., et al. (2001). A simple model host for identifying Gram-positive virulence factors. *Proc National Acad Sci* 98, 10892–10897. doi:10.1073/pnas.191378698.
- Huycke, M. M., Spiegel, C. A., and Gilmore, M. S. (1991). Bacteremia caused by hemolytic, high-level gentamicin-resistant *Enterococcus faecalis*. *Antimicrob Agents Ch* 35, 1626–1634. doi:10.1128/aac.35.8.1626.
- Ikonomidis, A., Michail, G., Vasdeki, A., Labrou, M., Karavasilis, V., Stathopoulos, C., et al. (2008). *In Vitro* and *In Vivo* Evaluations of Oxacillin Efficiency against *mecA*-Positive Oxacillin-Susceptible *Staphylococcus aureus* ∇ . *Antimicrob Agents Ch* 52, 3905–3908. doi:10.1128/aac.00653-08.
- Ito, T., Katayama, Y., Asada, K., Mori, N., Tsutsumimoto, K., Tiensasitorn, C., et al. (2001). Structural Comparison of Three Types of Staphylococcal Cassette Chromosome *mec* Integrated in the Chromosome in Methicillin-Resistant *Staphylococcus aureus*. *Antimicrob Agents Ch* 45, 1323–1336. doi:10.1128/aac.45.5.1323-1336.2001.
- Kennedy, A. D., Otto, M., Braughton, K. R., Whitney, A. R., Chen, L., Mathema, B., et al. (2008). Epidemic community-associated methicillin-resistant *Staphylococcus aureus*: Recent clonal expansion and diversification. *Proc National Acad Sci* 105, 1327–1332. doi:10.1073/pnas.0710217105.
- Rahme, L. G., Stevens, E. J., Wolfort, S. F., Shao, J., Tompkins, R. G., and Ausubel, F. M. (1995). Common virulence factors for bacterial pathogenicity in plants and animals. *Science (New York, N.Y.)* 268, 1899–1902. doi:10.1126/science.7604262.
- Shin, S. H., Kim, S., Kim, J. Y., Lee, S., Um, Y., Oh, M.-K., et al. (2012a). Complete Genome Sequence of *Enterobacter aerogenes* KCTC 2190. *J Bacteriol* 194, 2373–2374. doi:10.1128/jb.00028-12.

Shin, S. H., Kim, S., Kim, J. Y., Lee, S., Um, Y., Oh, M.-K., et al. (2012b). Complete Genome Sequence of the 2,3-Butanediol-Producing *Klebsiella pneumoniae* Strain KCTC 2242. *J Bacteriol* 194, 2736–2737. doi:10.1128/jb.00027-12.

Soni, I., Chakrapani, H., and Chopra, S. (2015). Draft Genome Sequence of Methicillin-Sensitive *Staphylococcus aureus* ATCC 29213. *Genome Announc* 3, e01095-15. doi:10.1128/genomea.01095-15.

Table S2. Minimum inhibitory concentration ($\mu\text{g/ml}$) of Bay 11-7085 against *Candida auris* antifungal-resistant clinical isolates.

Strain	Bay 11-7085	Amphotericin B
<i>C. auris</i> AR-BANK #0382 (CDC)	0.5	0.5
<i>C. auris</i> AR-BANK #0383 (CDC)	1	1
<i>C. auris</i> AR-BANK #0384 (CDC)	1	1
<i>C. auris</i> AR-BANK #0385 (CDC)	1	2
<i>C. auris</i> AR-BANK #0386 (CDC)	1	2
<i>C. auris</i> AR-BANK #0387 (CDC)	1	2
<i>C. auris</i> AR-BANK #0388 (CDC)	1	1
<i>C. auris</i> AR-BANK #0389 (CDC)	0.5	2
<i>C. auris</i> AR-BANK #0390 (CDC)	1	2

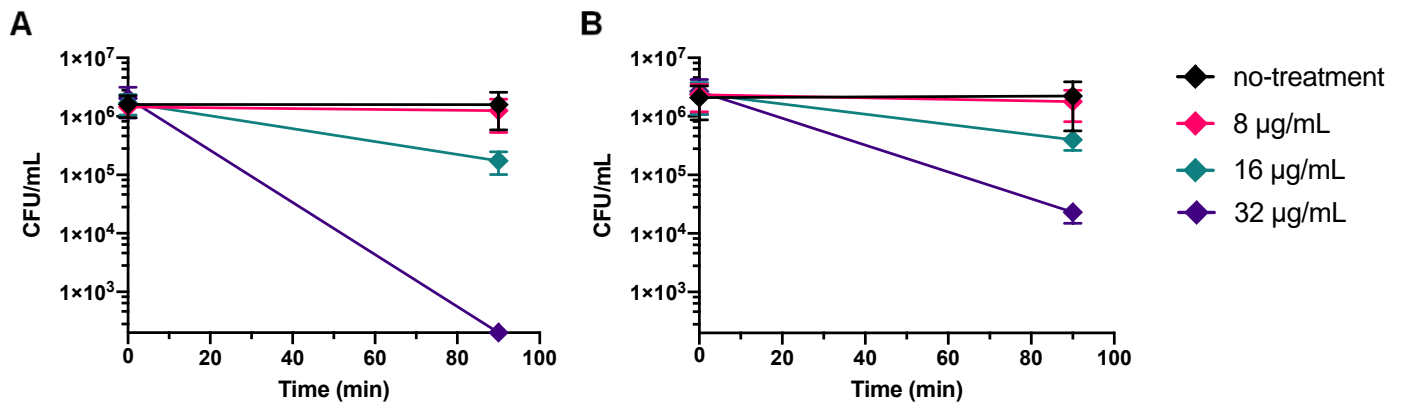


Figure S1. Bay 11-7085 inhibits *C. albicans* and *C. auris* initial cell attachment through direct killing of yeast cells.

CFU/ml of **(A)** *C. albicans* strain SC5314 and **(B)** *C. auris* strain #0834 after 90 min of treatment with multiply concentrations of Bay 11-7085. ($n=3$, \pm S.D.)

References

1. Munita, J.M.; Arias, C.A. Mechanisms of Antibiotic Resistance. *Microbiology spectrum* **2016**, *4*, doi:10.1128/microbiolspec.vmbf-0016-2015.
2. Stewart, P.S. Mechanisms of Antibiotic Resistance in Bacterial Biofilms. *International journal of medical microbiology : IJMM* **2002**, *292*, 107–113, doi:10.1078/1438-4221-00196.
3. Moormeier, D.E.; Bayles, K.W. Staphylococcus Aureus Biofilm: A Complex Developmental Organism. *Molecular microbiology* **2017**, *104*, 365–376, doi:10.1111/mmi.13634.
4. Cavalheiro, M.; Teixeira, M.C. Candida Biofilms: Threats, Challenges, and Promising Strategies. *Frontiers in medicine* **2018**, *5*, 28, doi:10.3389/fmed.2018.00028.
5. Sharma, D.; Misba, L.; Khan, A.U. Antibiotics versus Biofilm: An Emerging Battleground in Microbial Communities. *Antimicrobial resistance and infection control* **2019**, *8*, 76–10, doi:10.1186/s13756-019-0533-3.
6. Chung, P.Y.; Toh, Y.S. Anti-Biofilm Agents: Recent Breakthrough against Multi-Drug Resistant Staphylococcus Aureus. *Pathogens and disease* **2014**, *70*, 231–239, doi:10.1111/2049-632x.12141.
7. Attinger, C.; Wolcott, R. Clinically Addressing Biofilm in Chronic Wounds. *Advances in wound care* **2012**, *1*, 127–132, doi:10.1089/wound.2011.0333.
8. Bowers, S.; Franco, E. Chronic Wounds: Evaluation and Management. *American family physician* **2020**, *101*, 159–166.
9. Nussbaum, S.R.; Carter, M.J.; Fife, C.E.; DaVanzo, J.; Haught, R.; Nusgart, M.; Cartwright, D. An Economic Evaluation of the Impact, Cost, and Medicare Policy Implications of Chronic Nonhealing Wounds. *Value in health : the journal of the International Society for Pharmacoeconomics and Outcomes Research* **2018**, *21*, 27–32, doi:10.1016/j.jval.2017.07.007.
10. Beitz, J.M.; Goldberg, E. The Lived Experience of Having a Chronic Wound: A Phenomenologic Study. *Medsurg nursing : official journal of the Academy of Medical-Surgical Nurses* **2005**, *14*, 51-62–82.
11. Kennedy, P.; Brammah, S.; Wills, E. Burns, Biofilm and a New Appraisal of Burn Wound Sepsis. *Burns : journal of the International Society for Burn Injuries* **2010**, *36*, 49–56, doi:10.1016/j.burns.2009.02.017.
12. Akers, K.S.; Mende, K.; Cheatle, K.A.; Zera, W.C.; Yu, X.; Beckius, M.L.; Aggarwal, D.; Li, P.; Sanchez, C.J.; Wenke, J.C.; et al. Biofilms and Persistent Wound Infections in United States Military Trauma Patients: A Case-Control Analysis. *BMC infectious diseases* **2014**, *14*, 190–11, doi:10.1186/1471-2334-14-190.
13. Percival, S.L.; Suleman, L.; Vuotto, C.; Donelli, G. Healthcare-Associated Infections, Medical Devices and Biofilms: Risk, Tolerance and Control. *Journal of Medical Microbiology* **2015**, *64*, 323–334, doi:10.1099/jmm.0.000032.
14. Lakhundi, S.; Zhang, K. Methicillin-Resistant Staphylococcus Aureus: Molecular Characterization, Evolution, and Epidemiology. *Clinical Microbiology Reviews* **2018**, *31*, 5, doi:10.1128/cmr.00020-18.
15. Bhattacharya, S.; Bir, R.; Majumdar, T. Evaluation of Multidrug Resistant Staphylococcus Aureus and Their Association with Biofilm Production in a Tertiary

- Care Hospital, Tripura, Northeast India. *Journal of clinical and diagnostic research : JCDR* **2015**, 9, DC01-4, doi:10.7860/jcdr/2015/13965.6417.
16. Heald, A.H.; O'Halloran, D.J.; Richards, K.; Webb, F.; Jenkins, S.; Hollis, S.; Denning, D.W.; Young, R.J. Fungal Infection of the Diabetic Foot: Two Distinct Syndromes. *Diabetic medicine : a journal of the British Diabetic Association* **2001**, 18, 567–572, doi:10.1046/j.1464-5491.2001.00523.x.
 17. Lockhart, S.R. Candida Auris and Multidrug Resistance: Defining the New Normal. *Fungal genetics and biology: FG & B* **2019**, 131, 103243, doi:10.1016/j.fgb.2019.103243.
 18. Chowdhary, A.; Sharma, C.; Meis, J.F. Candida Auris: A Rapidly Emerging Cause of Hospital-Acquired Multidrug-Resistant Fungal Infections Globally. *PLOS Pathogens* **2017**, 13, e1006290, doi:10.1371/journal.ppat.1006290.
 19. Jeffery-Smith, A.; Taori, S.K.; Schelenz, S.; Jeffery, K.; Johnson, E.M.; Borman, A.; Team, C. auris I.M.; Manuel, R.; Brown, C.S. Candida Auris: A Review of the Literature. *Clinical Microbiology Reviews* **2018**, 31, 41, doi:10.1128/cmr.00029-17.
 20. Kim, W.; Zhu, W.; Hendricks, G.L.; Tyne, D.V.; Steele, A.D.; Keohane, C.E.; Fricke, N.; Conery, A.L.; Shen, S.; Pan, W.; et al. A New Class of Synthetic Retinoid Antibiotics Effective against Bacterial Persisters. *Nature* **2018**, 556, 103–107, doi:10.1038/nature26157.
 21. Kim, W.; Steele, A.D.; Zhu, W.; Csatory, E.E.; Fricke, N.; Dekarske, M.M.; Jayamani, E.; Pan, W.; Kwon, B.; Sinitsa, I.F.; et al. Discovery and Optimization of NTZDpa as an Antibiotic Effective Against Bacterial Persisters. *ACS infectious diseases* **2018**, 4, 1540–1545, doi:10.1021/acsinfecdis.8b00161.
 22. Kim, W.; Zou, G.; Pan, W.; Fricke, N.; Faizi, H.A.; Kim, S.M.; Khader, R.; Li, S.; Lee, K.; Escorba, I.; et al. The Neutrally Charged Diarylurea Compound PQ401 Kills Antibiotic-Resistant and Antibiotic-Tolerant Staphylococcus Aureus. *mBio* **2020**, 11, 603, doi:10.1128/mbio.01140-20.
 23. Escobar, I.E.; White, A.; Kim, W.; Mylonakis, E. New Antimicrobial Bioactivity against Multidrug-Resistant Gram-Positive Bacteria of Kinase Inhibitor IMD0354. *Antibiotics (Basel, Switzerland)* **2020**, 9, 665, doi:10.3390/antibiotics9100665.
 24. Sun, Y.; Dowd, S.E.; Smith, E.; Rhoads, D.D.; Wolcott, R.D. In Vitro Multispecies Lubbock Chronic Wound Biofilm Model. *Wound Repair and Regeneration* **2008**, 16, 805–813, doi:10.1111/j.1524-475x.2008.00434.x.
 25. CLSI M07-A9: Methods for Dilution Antimicrobial Susceptibility Tests for Bacteria That Grow Aerobically; Approved Standard—Ninth Edition. **2012**, 1–88.
 26. Rex, J.H. *Reference Method for Broth Dilution Antifungal Susceptibility Testing of Yeasts*; Clinical & Laboratory Standards Institute; Clinical & Laboratory Standards Institute, 2008; ISBN 9781562386665.
 27. Fuchs, S.; Pané-Farré, J.; Kohler, C.; Hecker, M.; Engelmann, S. Anaerobic Gene Expression in Staphylococcus Aureus. *Journal of Bacteriology* **2007**, 189, 4275–4289, doi:10.1128/jb.00081-07.
 28. Yuen, G.J.; Ausubel, F.M. Both Live and Dead Enterococci Activate Caenorhabditis Elegans Host Defense via Immune and Stress Pathways. *Virulence* **2018**, 9, 683–699, doi:10.1080/21505594.2018.1438025.

29. Kim, J.; Lee, A.-R.; Kawasaki, I.; Strome, S.; Shim, Y.-H. A Mutation of Cdc-25.1 Causes Defects in Germ Cells but Not in Somatic Tissues in *C. Elegans*. *Molecules and cells* **2009**, *28*, 43–48, doi:10.1007/s10059-009-0098-8.
30. Rajamuthiah, R.; Jayamani, E.; Conery, A.L.; Fuchs, B.B.; Kim, W.; Johnston, T.; Vilcinskis, A.; Ausubel, F.M.; Mylonakis, E. A Defensin from the Model Beetle *Tribolium Castaneum* Acts Synergistically with Telavancin and Daptomycin against Multidrug Resistant *Staphylococcus Aureus*. *PloS one* **2015**, *10*, e0128576, doi:10.1371/journal.pone.0128576.
31. Mishra, B.; Golla, R.M.; Lau, K.; Lushnikova, T.; Wang, G. Anti-Staphylococcal Biofilm Effects of Human Cathelicidin Peptides. *ACS medicinal chemistry letters* **2016**, *7*, 117–121, doi:10.1021/acsmchemlett.5b00433.
32. Khan, S.N.; Khan, S.; Iqbal, J.; Khan, R.; Khan, A.U. Enhanced Killing and Antibiofilm Activity of Encapsulated Cinnamaldehyde against *Candida Albicans*. *Frontiers in microbiology* **2017**, *8*, 1641, doi:10.3389/fmicb.2017.01641.
33. Harriott, M.M.; Noverr, M.C. *Candida Albicans* and *Staphylococcus Aureus* Form Polymicrobial Biofilms: Effects on Antimicrobial Resistance. *Antimicrobial Agents and Chemotherapy* **2009**, *53*, 3914–3922, doi:10.1128/aac.00657-09.
34. Weigel, L.M.; Clewell, D.B.; Gill, S.R.; Clark, N.C.; McDougal, L.K.; Flannagan, S.E.; Kolonay, J.F.; Shetty, J.; Killgore, G.E.; Tenover, F.C. Genetic Analysis of a High-Level Vancomycin-Resistant Isolate of *Staphylococcus Aureus*. *Science (New York, N.Y.)* **2003**, *302*, 1569–1571, doi:10.1126/science.1090956.
35. O'Toole, G.A. Microtiter Dish Biofilm Formation Assay. *Journal of visualized experiments : JoVE* **2011**, e2437, doi:10.3791/2437.
36. DeLeon, S.; Clinton, A.; Fowler, H.; Everett, J.; Horswill, A.R.; Rumbaugh, K.P. Synergistic Interactions of *Pseudomonas Aeruginosa* and *Staphylococcus Aureus* in an In Vitro Wound Model. *Infect Immun* **2014**, *82*, 4718–4728, doi:10.1128/iai.02198-14.
37. Pendleton, J.N.; Gorman, S.P.; Gilmore, B.F. Clinical Relevance of the ESKAPE Pathogens. *Expert review of anti-infective therapy* **2013**, *11*, 297–308, doi:10.1586/eri.13.12.
38. Rice, L.B. Federal Funding for the Study of Antimicrobial Resistance in Nosocomial Pathogens: No ESKAPE. *The Journal of infectious diseases* **2008**, *197*, 1079–1081, doi:10.1086/533452.
39. Uring-Lambert, B.; Vegnaduzzi, N.; Carroll, M.C.; Tongio, M.M.; Goetz, J.; Hauptmann, G. Heterogeneity in the Structural Basis of the Human Complement C4A Null Allele (C4A Q0) as Revealed by HindIII Restriction Fragment Length Polymorphism Analysis. *FEBS letters* **1987**, *217*, 65–68, doi:10.1016/0014-5793(87)81244-9.
40. Hunt, P.R.; Olejnik, N.; Bailey, K.D.; Vaught, C.A.; Sprando, R.L. *C. Elegans* Development and Activity Test Detects Mammalian Developmental Neurotoxins. *Food and chemical toxicology: an international journal published for the British Industrial Biological Research Association* **2018**, *121*, 583–592, doi:10.1016/j.fct.2018.09.061.
41. Wittkowski, P.; Marx-Stoelting, P.; Violet, N.; Fetz, V.; Schwarz, F.; Oelgeschläger, M.; Schönfelder, G.; Vogl, S. *Caenorhabditis Elegans* As a Promising Alternative Model for Environmental Chemical Mixture Effect Assessment-A Comparative Study.

- Environmental science & technology* **2019**, *53*, 12725–12733, doi:10.1021/acs.est.9b03266.
42. Pierce, J.W.; Schoenleber, R.; Jesmok, G.; Best, J.; Moore, S.A.; Collins, T.; Gerritsen, M.E. Novel Inhibitors of Cytokine-Induced I κ B α Phosphorylation and Endothelial Cell Adhesion Molecule Expression Show Anti-Inflammatory Effects in Vivo. *Journal of Biological Chemistry* **1997**, *272*, 21096–21103, doi:10.1074/jbc.272.34.21096.
 43. Azevedo, M.M.; Teixeira-Santos, R.; Silva, A.P.; Cruz, L.; Ricardo, E.; Pina-Vaz, C.; Rodrigues, A.G. The Effect of Antibacterial and Non-Antibacterial Compounds Alone or Associated with Antifungals upon Fungi. *Frontiers in microbiology* **2015**, *6*, 669, doi:10.3389/fmicb.2015.00669.
 44. Reddy, P.V.G.; Kiran, Y.B.R.; Reddy, C.S.; Reddy, C.D. Synthesis and Antimicrobial Activity of Novel Phosphorus Heterocycles with Exocyclic P-C Link. *Chemical & pharmaceutical bulletin* **2004**, *52*, 307–310, doi:10.1248/cpb.52.307.
 45. Srinivasan, V.; Kriete, A.; Sacan, A.; Jazwinski, S.M. Comparing the Yeast Retrograde Response and NF- κ B Stress Responses: Implications for Aging. *Aging Cell* **2010**, *9*, 933–941, doi:10.1111/j.1474-9726.2010.00622.x.
 46. Friedman, L.; Alder, J.D.; Silverman, J.A. Genetic Changes That Correlate with Reduced Susceptibility to Daptomycin in Staphylococcus Aureus. *Antimicrobial Agents and Chemotherapy* **2006**, *50*, 2137–2145, doi:10.1128/aac.00039-06.
 47. Ezabadi, I.R.; Camoutsis, C.; Zoumpoulakis, P.; Geronikaki, A.; Soković, M.; Glamocilija, J.; Cirić, A. Sulfonamide-1,2,4-Triazole Derivatives as Antifungal and Antibacterial Agents: Synthesis, Biological Evaluation, Lipophilicity, and Conformational Studies. *Bioorganic & medicinal chemistry* **2008**, *16*, 1150–1161, doi:10.1016/j.bmc.2007.10.082.
 48. Rubinchik, E.; Dugourd, D.; Algara, T.; Pasetka, C.; Friedland, H.D. Antimicrobial and Antifungal Activities of a Novel Cationic Antimicrobial Peptide, Omiganan, in Experimental Skin Colonisation Models. *International journal of antimicrobial agents* **2009**, *34*, 457–461, doi:10.1016/j.ijantimicag.2009.05.003.
 49. Zhang, Y.-Y.; Zhou, C.-H. Synthesis and Activities of Naphthalimide Azoles as a New Type of Antibacterial and Antifungal Agents. *Bioorganic & medicinal chemistry letters* **2011**, *21*, 4349–4352, doi:10.1016/j.bmcl.2011.05.042.
 50. Vestergaard, M.; Ingmer, H. Antibacterial and Antifungal Properties of Resveratrol. *International journal of antimicrobial agents* **2019**, *53*, 716–723, doi:10.1016/j.ijantimicag.2019.02.015.
 51. Kruppa, M. Quorum Sensing and Candida Albicans. *Mycoses* **2009**, *52*, 1–10, doi:10.1111/j.1439-0507.2008.01626.x.
 52. Nobile, C.J.; Johnson, A.D. Candida Albicans Biofilms and Human Disease. *Annual review of microbiology* **2015**, *69*, 71–92, doi:10.1146/annurev-micro-091014-104330.
 53. Peleg, A.Y.; Hogan, D.A.; Mylonakis, E. Medically Important Bacterial-Fungal Interactions. *Nature reviews. Microbiology* **2010**, *8*, 340–349, doi:10.1038/nrmicro2313.
 54. Kühbacher, A.; Burger-Kentischer, A.; Rupp, S. Interaction of Candida Species with the Skin. *Microorganisms* **2017**, *5*, 32, doi:10.3390/microorganisms5020032.

55. Carolus, H.; Dyck, K.V.; Dijck, P.V. Candida Albicans and Staphylococcus Species: A Threatening Twosome. *Frontiers in microbiology* **2019**, *10*, 2162, doi:10.3389/fmicb.2019.02162.
56. Peters, B.M.; Jabra-Rizk, M.A.; Scheper, M.A.; Leid, J.G.; Costerton, J.W.; Shirtliff, M.E. Microbial Interactions and Differential Protein Expression in Staphylococcus Aureus -Candida Albicans Dual-Species Biofilms. *FEMS immunology and medical microbiology* **2010**, *59*, 493–503, doi:10.1111/j.1574-695x.2010.00710.x.
57. Todd, O.A.; Peters, B.M. Candida Albicans and Staphylococcus Aureus Pathogenicity and Polymicrobial Interactions: Lessons beyond Koch's Postulates. *Journal of fungi (Basel, Switzerland)* **2019**, *5*, 81, doi:10.3390/jof5030081.
58. Giedrys-Kalemba, S.; Czernomysy-Furowicz, D.; Fijałkowski, K.; Jursa-Kulesza, J. Pet-To-Man Travelling Staphylococci. **2018**, 253–264, doi:10.1016/b978-0-12-813547-1.00019-4.
59. Martin, J.K.; Sheehan, J.P.; Bratton, B.P.; Moore, G.M.; Mateus, A.; Li, S.H.-J.; Kim, H.; Rabinowitz, J.D.; Typas, A.; Savitski, M.M.; et al. A Dual-Mechanism Antibiotic Kills Gram-Negative Bacteria and Avoids Drug Resistance. *Cell* **2020**, *181*, 1518-1532.e14, doi:10.1016/j.cell.2020.05.005.

CHAPTER 5: SUMMARY AND FUTURE DIRECTIONS

The *C. elegans*-infection platform is a novel means of gaining insight and foundational clarity on drug development in light of the complexity of host-microbe interactions. It resides at the crossroads of basic and translational research and helps bridge the gap between high-throughput screening and lead compound or drug target identification. Therefore, we stress the importance of studying the host equally to the pathogen. Understanding the host allows investigators to probe the effect of hit compounds on host immunity and overall physiology, while studying the pathogen facilitates discovering traditional antimicrobial and atypical anti-virulent compounds.

Throughout this thesis, I have provided examples of how the *C. elegans*-infection model is a powerful tool to study host-microbe interactions. Chapter 2 of this thesis demonstrated how this model system has furthered our understanding of the role S1P and its transporters play on *C. elegans* immunity. When wild-type *C. elegans* are supplemented with extracellular S1P, we see an increase in their lifespan when challenged with *P. aeruginosa* or *E. faecalis*. By mutating the S1P transporters *spin-2* and *spin-3*, we found that S1P can no longer rescue the worms from pathogen-mediated killing, whereas mutating a third S1P transporter, *spin-1*, does not affect the immune-enhancing activity of S1P. Regardless of S1P supplementation, mutating S1P transporter genes *spin-2* or *spin-3* and the sphingosine kinase gene (*sphk-1*) decreased nematode survival following infection, whereas mutating transporter gene *spin-1* lead to increased resistance. We also discovered that SIP signaling is dependent on the evolutionarily conserved *C. elegans* p38 MAPK immunity signaling pathway. By mutating *C. elegans* *sek-1* and *pmk-1* genes, both critical for p38 MAPK signaling, the mediated immunomodulatory effects of S1P were diminished. Therefore, our working model is that

***spin-2* and *spin-3* import S1P intracellularly** and activate the immune response, while on the one hand, ***spin-1*, exports S1P extracellularly**. This suggests an evolutionarily conserved function for S1P, but a non-canonical role for S1P transporters in the *C. elegans* immune response to Gram-negative and Gram-positive bacteria.

Although the role of S1P in the *C. elegans* immune response is relatively clear, there are still many limitations to this work. For one, understanding the exact mechanism by which S1P activates the immune response is still up for debate. We currently hypothesize that the intestinal mitochondrial unfolded protein response (UPR^{mt}) is responsible for immune gene activation, which we addressed in detail in the Discussion of Chapter 1. We propose additional studies that would measure *C. elegans* survivability during pathogen infection with and without S1P supplementation and UPR^{mt} worm mutants. Based on this understanding, we speculate that UPR^{mt} mutants will have increased susceptibility to infection even under S1P supplementation. As for S1P transporters *spin-2* and *spin-3*, we suspect a decrease in UPR^{mt} activation, which we may be tested using genetically modified worms, which increase in fluorescence during UPR^{mt} activation [1].

Lastly, we acknowledge that measuring S1P directly intra- or extracellularly would be the most definitive way to support our hypothesis. One way of doing this is via radiolabeling techniques and mass spectrometry [2]. These techniques have been attempted in *C. elegans* previously but were unsuccessful [3]. Alternatively, there is a fluorochrome-coupled sphingosine that is commercially available [4]. However, it would be nearly impossible to distinguish intracellular vs. extracellular fluorescence in a tiny animal such as *C. elegans*. Furthermore, there are no *C. elegans* cell lines available to perform *in vitro* studies. The suggested experiments to measure S1P's direct transport

are essential; however, we must first wait for novel approaches and the advancement of technology.

The study of the *C. elegans* response to pathogen attack has helped establish ancestral immunity pathways activated by infection [5]. Through this model, researchers have identified vital immune regulatory genes, such as the transcription factor *hlh-30*, relevant to my work, which was first shown to regulate immune gene activation toward *S. aureus* and then found to work similarly in mammalian cells [6,7]. Here we continue to add to this narrative by clarifying the role of S1P and its transporters in *C. elegans* innate immunity. Although the function of intracellular S1P in mammalian cells is still up for debate [8], our work helps build a foundation to study S1P signaling activity and its transporters in the future.

As mentioned at the beginning of this chapter, elucidating immune signaling pathways in *C. elegans* led to the development of tools to study traditional antimicrobials in addition to novel immunomodulatory compounds [9]. Aside from the synthetic compound RPW-24, not many other *C. elegans* immunomodulatory drugs are known [10], leaving this area of research desperate for follow-up studies. In addition, *C. elegans* immunity research gives us an understanding of potential new drug immunotherapy targets such as S1P. In totality, we find that this research is advancing our knowledge of the host response to pathogens, thereby highlighting the *C. elegans*-infection model as a powerful tool in drug discovery.

In Chapter 3 and 4 of this thesis, I gave examples of how the *C. elegans*-infection model is used to identify compounds that target the *pathogen side* of host-microbe interactions. I discussed how a high-throughput *C. elegans* infection screen identified two

compounds with uncharacterized antimicrobial activity to antibiotic-resistant *S. aureus*, which were studied in detail in chapters 3 and 4. Kinase IMD0354 is a known NF- κ B inhibitor that exhibits an unusually low minimum inhibitory concentration (MIC) level of 0.06 μ g/ml to various vancomycin-resistant strains. IMD0354 inhibited multiple stages of *S. aureus* biofilm maturation at sub-MIC levels. In addition, we demonstrated that IMD0354's mechanism of action (MOA) at high concentrations (≥ 4 μ g/ml) is membrane permeabilization. However, we are still unclear what the MOA is at low concentrations.

Moving forward, we believe that further development of IMD0354 has merit, in particular, resolving its MOA at low concentrations. Future experiments may include the development of IMD0354-resistant mutants through serial passaging under antibiotic pressure. In this case, we would culture *S. aureus* at sub-MIC levels of IMD0354 daily over 25 days in an attempt to generate a resistant strain. Genomic sequencing and RNA seq analysis of these resistant lines could identify critical gene targets required for the efficacy of IMD0354 on Gram-positive bacteria [11].

As our second hit compound, we reported our findings on Bay 11-7085 in Chapter 4, another kinase inhibitor that can target inflammation through NF- κ B and additionally display anti-cancer activity. Our data confirmed the bactericidal activity of Bay 11-7085 against multidrug-resistant *S. aureus* with a MIC of 4 μ g/ml. Importantly, Bay 11-7085 was active against *C. albicans* and the emerging pathogen *C. auris* with a MIC of 0.5–1 μ g/ml. Bay 11-7085 partially inhibited and eradicated biofilm formation of various pathogens, including VRSA (vancomycin-resistant *S. aureus*), as well as antifungal-resistant *Candida* spp. isolates. Bay 11-7085 increased the lifespan of *C. elegans* infected with either *S. aureus* or *C. albicans*, and showed an extremely low rate of resistance

development in *S. aureus* strain MW2. We suspect Bay 11-7085 to have multiple targets. Therefore, it may be challenging to find its modes of action. However, current advances in deep learning-based prediction, quantitative imaging, proteomic, genetic, and metabolomic analyses enable us to elucidate antimicrobial mechanisms possessing uncommon or multiple modes of action [12].

A common strategy to study the MOA of lead antimicrobial compounds is developing a resistant mutant strain through serial passaging under antibiotic pressure, as explained previously in regards to IMD0354. This method has successfully identified mutated genes that may play an essential role in the MOA of resistance to various compounds [13–15]. However, we have already shown that Bay 11-7085 does not acquire resistance to MRSA strain MW2 after 25-days of serial passage (Chapter 4, Figure 1); thus this method would be inadequate.

The next most reasonable solution would be to attempt chemical proteomics. Recently, Le et al. presented the MOA of another kinase inhibitor effective on MRSA persister using this technique [16]. In short, this method would involve biotinylation of Bay 11-7085, mixing Bay 11-7085 with *S. aureus* lysates and then extracting out biotinylated Bay 11-7085 via avidin enrichment [16]. In theory, the protein(s) or molecule(s) that Bay 11-7085 is interacting with would be filtered out when extracting Bay 11-7085. This extract would then be analyzed via mass spectrometry to identify potential proteins or molecules Bay 11-7085 binds with. These proteins may be critical for the MOA of Bay 11-7085 against *S. aureus* and thus be a promising target to study further.

Furthermore, we cannot entirely exclude that Bay 11-7085 or IMD0354 may also have other MOA's in addition to antimicrobial that aid in its anti-infective properties. This possibility is due to the unique qualities of the *in vivo* *C. elegans* infection whole animal assay. Although we can definitively say that Bay 11-7085 and IMD0354 have an antimicrobial effect on *S. aureus*, there is still the possibility that this is not the full reason for worm survival. For instance, it may be possible that either compound is acting as an adjuvant to an upregulated antimicrobial peptide or possibly synergizing with one or more immune effector genes. Both Bay 11-7085 and IMD0354 are NF- κ B inhibitors, and NF- κ B is a crucial transcription factor regulating many immune response genes in mammals [17]. However, *C. elegans* do not have an NF- κ B homolog [18]. Therefore, Bay 11-7085 or IMD0354 would not be expected to inhibit an immune response through this bioactivity.

Nonetheless, if resistant mutant strain development or chemical proteomics fail, my next attempt to elucidate a MOA would be to leverage an *S. aureus* transposon mutant library [19]. A mutant transposon library is a collective of bacterial strains which have transposon insertions in all non-essential genes. Using this library, I would conduct an *in vitro* screen measuring Bay 11-7085's or IMD0354's MIC against each mutant strain. I would be looking for a change in MIC of either compound to a mutant strain which would indicate a possible lead target for further study concerning MOA. This strategy has been used previously on other antibiotics such as daptomycin. Mutant library screening identified lipoteichoic acid (LTA) anchor, diglucosyl-diacylglycerol (Glc2DAG) which exhibit reduced growth and attenuated pathogenicity [20].

Aside from deciphering their MOAs, in order to further develop IMD0354 or Bay 11-7085 as a lead compound, common limitations associated with new drugs must be overcome. Compounds have consistently failed due to low *in vivo* efficacy and high levels of toxicity [21,22]. In the case of IMD0354 and Bay 11-7085, extensive analog development is needed to eliminate toxicity and fine-tune dose efficacy. In addition, pathogen specificity is an essential factor to consider. Somewhat unexpectedly, our data show that Bay 11-7085 has an unusually limited host range, exhibiting efficacy against *S. aureus* but not *E. faecalis* or *E. faecium*. Although we tested multiple *S. aureus* strains in-house, further screening on clinical isolates will generate valuable knowledge when pushing these compounds forward. Once these factors are analyzed and addressed, mammalian studies using rat or mouse models would be an appropriate next step.

There is a paradox in the field of antimicrobial discovery. As antibiotic resistance rises, large pharmaceutical companies continue to end their research on antibiotic development [23,24]. It takes an estimated \$1.5 billion to develop an antibiotic, while industry analysts predict a yearly average revenue of only \$46 million for a newly introduced antibiotic [23]. As a result, companies such as Novartis, Sanofi, and AstraZeneca have ended their antibiotic development efforts and decided on investing in more lucrative drug targets, such as in cancer [23]. Antibiotic discovery is often described as a “difficult field” [23]. Not only is it highly expensive, but new genomic *in vitro* high-throughput screening methods have constantly failed to yield effective and safe drugs *in vivo* [21,22]. With larger companies winding down their antibiotic research, and smaller companies filing for bankruptcy[23,24], much of the responsibility to address the antibiotic-resistance crisis has landed on the shoulders of academics like ourselves.

Therefore we are now tasked with the responsibility to develop new or innovative methods to identify new or different types of anti-infectives.

Due to the nature of the *C. elegans* whole animal screen, it is possible to identify not only traditional antimicrobials but also potential immunomodulatory or anti-virulent compounds [14,25–27]. For example, using this *C. elegans*-MRSA platform, the Mylonakis lab was able to screen over 80,000 small synthetic molecules against MRSA infection in *C. elegans* of which 168 were scored as positive hits as measured by worm survival [14]. Interestingly a subgroup of these compounds was able to rescue worms from MRSA infection yet had little to no antimicrobial effect as measured by Clinical and Laboratory Standards Institute (CLSI) [28] protocols (data not shown), suggesting that they affected host immunity or possible bacterial virulence.

In addition, the *C. elegans* whole animal screen is unique and versatile enough to identify lead compounds that would otherwise be excluded by traditional *in vitro* screens due to toxicity such as kinase inhibitors Bay 11-7085 and IMD0354. Both of these compounds inhibit NF- κ B function. NF- κ B activation is toxic to standard laboratory strain lines (which are artificially immortalized) due to their anti-cancer activity. Therefore, these compounds would have automatically been excluded from old *in vitro* methods of screening. However, the *C. elegans in vivo* assay allows us to identify these hits because *C. elegans* do not have a conserved NF- κ B and thus, both Bay 11-7085 and IMD0354 are not toxic to *C. elegans*. These findings are relevant because, although Bay 11-7085 and IMD0354 are toxic to monoculture cell lines, they are safe to use *in vivo* in various rat models [29,30].

In chapter one, I stated that *the focus of this thesis was to study basic innate immunity and antimicrobial discovery using Caenorhabditis elegans as a whole-animal infection model.* Thus far, we have provided numerous data to validate the *C. elegans*-infection model as dynamic enough to study both ends of host-microbe interactions. We find this platform to be an effective stepping stone between basic and translational research capable of advancing drug discovery and development amidst the antibiotic resistance crisis.

References

1. Kim, S.; Sieburth, D. Sphingosine Kinase Activates the Mitochondrial Unfolded Protein Response and Is Targeted to Mitochondria by Stress. *Cell Reports* **2018**, *24*, 2932-2945.e4, doi:10.1016/j.celrep.2018.08.037.
2. Meacci, E.; Bini, F.; Battistini, C. Sphingosine-1-Phosphate Signaling in Skeletal Muscle Cells. In: Sphingosine-1-Phosphate; Humana Press, **2012**; Vol. 874, pp. 155–165 ISBN 978-1-61779-799-6.
3. Chan, J.P.; Brown, J.; Hark, B.; Nolan, A.; Servello, D.; Hrobuchak, H.; Staab, T.A. Loss of Sphingosine Kinase Alters Life History Traits and Locomotor Function in *Caenorhabditis Elegans*. *Frontiers in genetics* **2017**, *8*, 132, doi:10.3389/fgene.2017.00132.
4. Kobayashi, N.; Otsuka, M.; Yamaguchi, A.; Nishi, T. Fluorescence-Based Rapid Measurement of Sphingosine-1-Phosphate Transport Activity in Erythrocytes. *Journal of lipid research* **2016**, *57*, 2088–2094, doi:10.1194/jlr.d071068.
5. Ermolaeva, M.A.; Schumacher, B. Insights from the Worm: The *C. Elegans* Model for Innate Immunity. *Seminars in immunology* **2014**, *26*, 303–309, doi:10.1016/j.smim.2014.04.005.
6. Apfeld, J.; Alper, S. Disease Gene Identification, Methods and Protocols. *Methods Mol Biology* **2018**, *1706*, 53–75, doi:10.1007/978-1-4939-7471-9_4.
7. Irazoqui, J.E.; Troemel, E.R.; Feinbaum, R.L.; Luhachack, L.G.; Cezairliyan, B.O.; Ausubel, F.M. Distinct Pathogenesis and Host Responses during Infection of *C. Elegans* by *P. Aeruginosa* and *S. Aureus*. *PLOS Pathogens* **2010**, *6*, e1000982, doi:10.1371/journal.ppat.1000982.
8. Hisano, Y.; Nishi, T.; Kawahara, A. The Functional Roles of S1P in Immunity. *J Biochem* **2012**, *152*, 305–311, doi:10.1093/jb/mvs090.
9. Kim, W.; Hendricks, G.L.; Lee, K.; Mylonakis, E. An Update on the Use of *C. Elegans* for Preclinical Drug Discovery: Screening and Identifying Anti-Infective Drugs. *Expert Opinion on Drug Discovery* **2017**, *00*, 1–9, doi:10.1080/17460441.2017.1319358.
10. Pukkila-Worley, R.; Feinbaum, R.; Kirienko, N.V.; Larkins-Ford, J.; Conery, A.L.; Ausubel, F.M. Stimulation of Host Immune Defenses by a Small Molecule Protects *C. Elegans* from Bacterial Infection. *PLoS genetics* **2012**, *8*, e1002733, doi:10.1371/journal.pgen.1002733.
11. Silverman, J.A.; Oliver, N.; Andrew, T.; Li, T. Resistance Studies with Daptomycin. *Antimicrob Agents Ch* **2001**, *45*, 1799–1802, doi:10.1128/aac.45.6.1799-1802.2001.
12. Martin, J.K.; Sheehan, J.P.; Bratton, B.P.; Moore, G.M.; Mateus, A.; Li, S.H.-J.; Kim, H.; Rabinowitz, J.D.; Typas, A.; Savitski, M.M.; et al. A Dual-Mechanism Antibiotic Kills Gram-Negative Bacteria and Avoids Drug Resistance. *Cell* **2020**, *181*, 1518-1532.e14, doi:10.1016/j.cell.2020.05.005.
13. Friedman, L.; Alder, J.D.; Silverman, J.A. Genetic Changes That Correlate with Reduced Susceptibility to Daptomycin in *Staphylococcus Aureus*. *Antimicrobial Agents and Chemotherapy* **2006**, *50*, 2137–2145, doi:10.1128/aac.00039-06.
14. Kim, W.; Zhu, W.; Hendricks, G.L.; Tyne, D.V.; Steele, A.D.; Keohane, C.E.; Fricke, N.; Conery, A.L.; Shen, S.; Pan, W.; et al. A New Class of Synthetic Retinoid

- Antibiotics Effective against Bacterial Persisters. *Nature* **2018**, *556*, 103–107, doi:10.1038/nature26157.
15. Man, N.Y.T.; Knight, D.R.; Stewart, S.G.; McKinley, A.J.; Riley, T.V.; Hammer, K.A. Spectrum of Antibacterial Activity and Mode of Action of a Novel Tris-Stilbene Bacteriostatic Compound. *Sci Rep-uk* **2018**, *8*, 6912, doi:10.1038/s41598-018-25080-w.
 16. Le, P.; Kunold, E.; Macsics, R.; Rox, K.; Jennings, M.C.; Ugur, I.; Reinecke, M.; Chaves-Moreno, D.; Hackl, M.W.; Fetzer, C.; et al. Repurposing Human Kinase Inhibitors to Create an Antibiotic Active against Drug-Resistant Staphylococcus Aureus, Persisters and Biofilms. *Nature chemistry* **2019**, *19*, 56–14, doi:10.1038/s41557-019-0378-7.
 17. Hayden, M.S.; West, A.P.; Ghosh, S. NF-KB and the Immune Response. *Oncogene* **2006**, *25*, 6758–6780, doi:10.1038/sj.onc.1209943.
 18. Irazoqui, J.E.; Urbach, J.M.; Ausubel, F.M. Evolution of Host Innate Defence: Insights from Caenorhabditis Elegans and Primitive Invertebrates. *Nature reviews. Immunology* **2010**, *10*, 47–58, doi:10.1038/nri2689.
 19. Yajjala, V.K.; Widhelm, T.J.; Endres, J.L.; Fey, P.D.; Bayles, K.W. The Genetic Manipulation of Staphylococci, Methods and Protocols. *Methods Mol Biology* **2015**, *1373*, 103–110, doi:10.1007/7651_2014_189.
 20. Sargison, F.A.; Fitzgerald, J.R. Advances in Transposon Mutagenesis of Staphylococcus Aureus: Insights into Pathogenesis and Antimicrobial Resistance. *Trends Microbiol* **2020**, *29*, 282–285, doi:10.1016/j.tim.2020.11.003.
 21. Brown, E.D.; Wright, G.D. Antibacterial Drug Discovery in the Resistance Era. *Nature* **2016**, *529*, 336–343, doi:10.1038/nature17042.
 22. Silver, L.L. Challenges of Antibacterial Discovery. *Clin Microbiol Rev* **2011**, *24*, 71–109, doi:10.1128/cmr.00030-10.
 23. Plackett, B. Why Big Pharma Has Abandoned Antibiotics. *Nature* **2020**, *586*, S50–S52, doi:10.1038/d41586-020-02884-3.
 24. McKenna, M. The Antibiotic Paradox: Why Companies Can't Afford to Create Life-Saving Drugs. *Nature* **2020**, *584*, 338–341, doi:10.1038/d41586-020-02418-x.
 25. Kim, W.; Steele, A.D.; Zhu, W.; Csatory, E.E.; Fricke, N.; Dekarske, M.M.; Jayamani, E.; Pan, W.; Kwon, B.; Sinitsa, I.F.; et al. Discovery and Optimization of NTZDpa as an Antibiotic Effective Against Bacterial Persisters. *ACS infectious diseases* **2018**, *4*, 1540–1545, doi:10.1021/acsinfecdis.8b00161.
 26. Kim, W.; Fricke, N.; Conery, A.L.; Fuchs, B.B.; Rajamuthiah, R.; Jayamani, E.; Vlahovska, P.M.; Ausubel, F.M.; Mylonakis, E. NH125 Kills Methicillin-Resistant Staphylococcus Aureuspersisters by Lipid Bilayer Disruption. *Future medicinal chemistry* **2016**, *8*, 257–269, doi:10.4155/fmc.15.189.
 27. Tharmalingam, N.; Jayamani, E.; Rajamuthiah, R.; Castillo, D.; Fuchs, B.B.; Kelso, M.J.; Mylonakis, E. Activity of a Novel Protonophore against Methicillin-Resistant Staphylococcus Aureus. *Future medicinal chemistry* **2017**, *9*, 1401–1411, doi:10.4155/fmc-2017-0047.
 28. CLSI M07-A9: Methods for Dilution Antimicrobial Susceptibility Tests for Bacteria That Grow Aerobically; Approved Standard—Ninth Edition. 2012, 1–88.
 29. Pierce, J.W.; Schoenleber, R.; Jesmok, G.; Best, J.; Moore, S.A.; Collins, T.; Gerritsen, M.E. Novel Inhibitors of Cytokine-Induced I kappa Balpha Phosphorylation

and Endothelial Cell Adhesion Molecule Expression Show Anti-Inflammatory Effects in Vivo. *Journal of Biological Chemistry* **1997**, *272*, 21096–21103, doi:10.1074/jbc.272.34.21096.30.

30. Onai, Y.; Suzuki, J.-I.; Kakuta, T.; Maejima, Y.; Haraguchi, G.; Fukasawa, H.; Muto, S.; Itai, A.; Isobe, M. Inhibition of IkappaB Phosphorylation in Cardiomyocytes Attenuates Myocardial Ischemia/Reperfusion Injury. *Cardiovascular research* **2004**, *63*, 51–59, doi:10.1016/j.cardiores.2004.03.002.